



# LUND UNIVERSITY

## Ventricular Depolarization in Ischemic Heart Disease. Value of Electrocardiography in Assessment of Severity and Extent of Acute Myocardial Ischemia.

Ringborn, Michael

2013

[Link to publication](#)

*Citation for published version (APA):*

Ringborn, M. (2013). *Ventricular Depolarization in Ischemic Heart Disease. Value of Electrocardiography in Assessment of Severity and Extent of Acute Myocardial Ischemia*. [Doctoral Thesis (compilation), Cardiology]. Cardiology.

*Total number of authors:*

1

### General rights

Unless other specific re-use rights are stated the following general rights apply:

Copyright and moral rights for the publications made accessible in the public portal are retained by the authors and/or other copyright owners and it is a condition of accessing publications that users recognise and abide by the legal requirements associated with these rights.

- Users may download and print one copy of any publication from the public portal for the purpose of private study or research.
- You may not further distribute the material or use it for any profit-making activity or commercial gain
- You may freely distribute the URL identifying the publication in the public portal

Read more about Creative commons licenses: <https://creativecommons.org/licenses/>

### Take down policy

If you believe that this document breaches copyright please contact us providing details, and we will remove access to the work immediately and investigate your claim.

LUND UNIVERSITY

PO Box 117  
221 00 Lund  
+46 46-222 00 00



# Ventricular Depolarization in Ischemic Heart Disease

Value of Electrocardiography in Assessment of  
Severity and Extent of Acute Myocardial Ischemia

Michael Ringborn, MD



**LUND**  
UNIVERSITY

Doctoral Thesis

2013

Department of Cardiology  
Clinical Sciences, Lund  
Faculty of Medicine  
Lund University  
Sweden

The public defense of this thesis will, with due permission from the Faculty of Medicine at Lund University, take place at Segerfalksalen, Wallenberg Neurocentrum, BMC, on Friday 5 April 2013, at 9:30 a.m.

Cover:

Myocardial perfusion single photon emission computed tomography (SPECT) images from patients in the *STAFF III* population representing occlusion of right coronary artery (RCA), left anterior descending artery (LAD) and left circumflex coronary artery (LCX), respectively (from left to right). Examples of ECG-analysis methods applied in this thesis; high-frequency QRS components (HF-QRS), QRS-slopes as well as standard ECG.

ISSN 1652-8220

ISBN 978-91-87449-10-9

Lund University, Faculty of Medicine Doctoral Dissertation Series 2013:40

Department of Cardiology, Skåne University Hospital, Lund  
SE-221 85 LUND, Sweden

Clinical Sciences, Lund University, Center for Integrative Electrophysiology at  
Lund University (CIEL), LUND, Sweden  
Thoracic Center, KARLSKRONA, Sweden

Printed by: Printfabriken, KARLSKRONA, Sweden

**Copyright © Michael Ringborn 2013**

michaelringborn@yahoo.com

This thesis is dedicated to my dear wife Helena and our wonderful children William, Hugo and Ella.





# Table of contents

<b>List of original publications .....</b>	<b>viii</b>
<b>Abstract.....</b>	<b>ix</b>
<b>Sammanfattning på svenska .....</b>	<b>xi</b>
<b>Abbreviations .....</b>	<b>xiv</b>
<b>1 Introduction.....</b>	<b>1</b>
<b>1.1 Ischemic heart disease.....</b>	<b>1</b>
1.1.1 Epidemiology .....	1
1.1.2 Pathophysiology .....	2
1.1.2.1 Coronary arteriosclerotic plaque formation .....	2
1.1.2.2 Ischemia on the myocardial cell level .....	2
1.1.3 Clinical manifestations and classification of ischemic heart disease ..	3
1.1.4 Diagnosis of acute MI .....	4
1.1.5 Acute management and treatment of STEMI.....	5
1.1.6 Determinants of final infarct size .....	6
1.1.6.1 Myocardium at risk (MaR).....	6
1.1.6.2 Myocardial protection and severity of ischemia .....	6
<b>1.2 Anatomy, electrophysiology and myocardial ischemia.....</b>	<b>8</b>
1.2.1 Basic electrophysiological principles.....	8
1.2.1.1 Electrophysiology at the cellular level: the action potential .....	8
1.2.1.2 Ventricular propagation of the depolarization wavefront .....	10
1.2.2 Electrocardiography (ECG).....	12
1.2.3 ECG changes during acute ischemia.....	14
<b>1.3 Depolarization changes during ischemia.....</b>	<b>18</b>
1.3.1 Standard, 12-lead ECG.....	19
1.3.1.1 QRS amplitude changes .....	19
1.3.1.2 The Sclarovsky-Birnbaum ischemia grading .....	20
1.3.1.3 QRS prolongation.....	23
1.3.1.4 QRS changes and myocardial infarction .....	23
1.3.1.5 Selvester QRS score .....	25
1.3.2 High frequency QRS analysis based on the 12-lead ECG system ....	26
1.3.3 QRS slope analysis based on 12-lead ECG system.....	27
1.3.4 QRS evaluation by vectorcardiography (VCG) .....	28



<b>1.4 Myocardial Single Photon Emission Computed Tomography (SPECT) .....</b>	<b>29</b>
1.4.1 Radioactive tracers: Tc-99m Sestamibi.....	29
1.4.2 Tomographic imaging acquisition.....	30
<b>2 Aims of the thesis.....</b>	<b>31</b>
<b>3 Materials and methods .....</b>	<b>33</b>
<b>3.1 Study populations.....</b>	<b>33</b>
3.1.1 “STAFF III” population .....	33
3.1.2 “STRESS” population.....	34
3.1.3 “MONAMI” population .....	34
<b>3.2 Ethical considerations .....</b>	<b>34</b>
<b>3.3 ECG analysis and processing .....</b>	<b>35</b>
3.3.1 ECG acquisition .....	35
3.3.2 Standard 12-lead ECG analysis.....	36
3.3.2.1 Selvester QRS scoring (Study I) .....	38
3.3.2.2 Sclarovsky-Birnbaum ischemia grading (Study IV) .....	40
3.3.3 QRS slope analysis (Study III).....	40
3.3.4 High-Frequency QRS (HF-QRS) analysis (Studies I, II).....	43
3.3.4.1 Preprocessing .....	44
3.3.4.2 Signal averaging-noise reduction .....	44
3.3.4.3 Band-pass filtering .....	45
3.3.4.4 HF-QRS quantification .....	45
<b>3.4 Myocardial SPECT perfusion imaging .....</b>	<b>46</b>
3.4.1 Studies II and III.....	46
3.4.1.1 Acquisition .....	46
3.4.1.2 Image analysis.....	47
3.4.2 Study IV .....	48
3.4.2.1 Acquisition .....	48
3.4.2.2 Image analysis.....	48
<b>3.5 Statistical methods .....</b>	<b>49</b>
<b>4 Results and Discussion.....</b>	<b>51</b>
<b>4.1 Results .....</b>	<b>51</b>
4.1.1 HF-QRS in patients with and without old MI (Study I).....	51
4.1.2 HF-QRS to quantify acute ischemia (Study II) .....	53
4.1.3 QRS slope analysis to quantify acute ischemia (Study III).....	56
4.1.4 Ischemia severity grading in STEMI patients (Study IV).....	59
<b>4.2 Discussion.....</b>	<b>64</b>

4.2.1	General clinical considerations .....	64
4.2.2	Depolarization changes in relation to extent (MaR) and severity of ischemia by SPECT .....	64
4.2.3	Ischemia grades and “terminal QRS distortion” in relation to MaR, severity and evolving infarct in acute STEMI.....	69
4.2.4	Depolarization changes by HF-QRS and standard ECG in relation to prior MI .....	72
<b>5</b>	<b>Conclusions .....</b>	<b>75</b>
<b>6</b>	<b>Acknowledgements.....</b>	<b>77</b>
<b>7</b>	<b>References .....</b>	<b>79</b>
	<b>Appendix.....</b>	<b>95</b>
	Study I	
	Study II	
	Study III	
	Study IV	
	Supplementary Technical Study	

# List of original publications

- I. **Ringborn M**, Pahlm O, Wagner GS, Warren SG, Pettersson J. The absence of high-frequency QRS changes in the presence of standard electrocardiographic QRS changes of old myocardial infarction. *Am Heart J* 2001; 141(4):573-579.
- II. **Ringborn M**, Pettersson J, Persson E, Warren SG, Platonov P, Pahlm O, Wagner GS. Comparison of high-frequency QRS components and ST-segment elevation to detect and quantify acute myocardial ischemia. *J Electrocardiol* 2010; 43(2):113-120.
- III. **Ringborn M**, Romero D, Pueyo E, Pahlm O, Wagner GS, Laguna P, Platonov PG. Evaluation of depolarization changes during acute myocardial ischemia by analysis of QRS slopes. *J Electrocardiol* 2011; 44(4):416-424.
- IV. **Ringborn M**, Birnbaum Y, Nielsen SS, Kaltoft AK, Bøtker HE, Pahlm O, Wagner GS, Platonov PG, Terkelsen CJ. Pre-hospital evaluation of electrocardiographic grade 3 ischemia predicts infarct progression and final infarct size in ST elevation myocardial infarction patients treated with primary percutaneous coronary intervention. *In manuscript*.

## Supplementary Technical Publication

- I. Romero D, **Ringborn M**, Laguna P, Pahlm O, Pueyo E. Depolarization changes during acute myocardial ischemia by evaluation of QRS slopes: standard lead and vectorial approach. *IEEE Trans Biomed Eng* 2011; 58(1):110-120.

*Studies I, II and III*, as well as *Supplementary Technical Study*, are reprinted with kind permission from the publishers.

# Abstract

## Background

In patients with symptoms compatible with acute myocardial infarction (MI), early triage by ECG in the pre-hospital phase by ST-segment elevation myocardial infarction (STEMI) criteria is important for direct transport of these patients to a regional center for primary percutaneous coronary intervention (pPCI). The time from first medical contact to pPCI should, due to present guidelines, be no longer than two hours. One main determinant of final infarct size (IS), in addition to myocardium at risk (MaR) and time to treatment, is the *severity* of ischemia, which relates to the rate of progression of the infarction wavefront. Presently, no assessment of severity is made. Patients with severe ischemia may have changes within the QRS complex in addition to ST-T changes, making it possible to identify these high-risk patients. QRS changes are, however more difficult to determine and to quantify correctly as compared to the changes within the ST segment.

## Aims and methods

The overall objective was to increase the understanding of depolarization changes during myocardial ischemia and to evaluate whether these changes have possible clinical implications in patients with acute MI. Different QRS methods are applied in patients during ischemia produced by elective, prolonged PCI as well as during STEMI, and comparisons are made with conventional ECG parameters as well as single-photon emission computed tomography (SPECT) images.

## Results and conclusions

*Study I* compared the computer-derived high-frequency QRS components (HF-QRS) in patients with and without standard ECG changes indicative of old MI. In contrast to previous findings we found that HF-QRS cannot differentiate between patients with and without old MI.

*Study II* tested the ability of HF-QRS versus conventional ST-segment measurements to detect and quantify myocardial ischemia, as determined by SPECT, in a group of patients undergoing elective balloon PCI. We showed that HF-QRS can provide valuable information both for detecting acute ischemia and for quantifying MaR and its severity.

*Study III* evaluated a potentially more readily available (compared with HF-QRS) new marker of ventricular depolarization distortion, which is based on calculation of up- and downslope within the QRS complex, in patients undergoing

coronary intervention that includes temporary occlusion of a coronary artery. We found that in particular the downward slope between R and S waves better correlates with ischemia than conventional QRS parameters, as quantified by SPECT, and thus can be of value in risk stratification of patients with ischemia in addition to conventional ST-segment analysis.

*Study IV*, in a large cohort of STEMI patients, assessed the value of the conventional Sclarovsky-Birnbaum ischemia grading system that includes terminal QRS distortion in addition to ST elevation, on pre-hospital ECG and its dynamic behavior during transport time to the PCI center for prediction of final infarct size and salvage, as estimated by SPECT imaging. The study explored the temporal behavior of the ischemia grading and showed the strong association of ischemia grade assessed from pre-hospital ECG, as well as the dynamic patterns, with infarct size, independent of ST-segment analysis. It also demonstrated the importance of early intervention, which was found to be particularly important in patients who had advanced, QRS-based ischemia grade.

# Sammanfattning på svenska

## Bakgrund

Den medicinska utvecklingen har varit stark under de senaste åren vad gäller akut omhändertagande av patienter med misstänkt hjärtinfarkt. Snabb teknisk utveckling inom området för kateterburen koronarkärlsintervention (PCI) och framsteg inom farmakologisk behandling har bidragit till allt bättre vårdresultat. Omedelbar och korrekt beslutsprocess har kommit att bli alltmer avgörande för att rädda hotad hjärtmuskelvävnad, och därmed avsevärt påverka patientens framtida liv. Beslut bör tas redan prehospitalt, för triagering av patienterna antingen till lokalt sjukhus eller till regionalt PCI-center. Detta ställer mycket höga krav på tillförlitlig diagnostik.

Den undersökning som ger mest information i den akuta situationen är 12-avlednings EKG, som är ett enkelt, lättillgängligt och icke-invasivt diagnosredskap vid sidan om patientens sjukdomshistoria och aktuella symtom. I den akuta situationen ses vanligen ingen diagnostiskt värdefull information i hjärtspecifika blodprover. Den förhärskande metoden att upptäcka akut hjärtinfarkt är att studera förändringar under repolarisationen (ST-T-sträckan) på EKG. Om vissa EKG-kriterier uppfylls för ST-sträckan (sk STEMI-kriterier), bör patienten helst så snart som möjligt behandlas med primär PCI. Detta kan ofta innebära lång transport av patienten till ett sjukhus där PCI kan utföras. I enlighet med både amerikanska och europeiska riktlinjer bör man eftersträva att patienterna får sådan behandling inom 2 timmar från första EKG där STEMI-kriterier verifierats. Telemedicin med digital överföring av akuta EKG tagna i patientens hem, i ambulansen alternativt på lokalt sjukhus underlättar för att effektivisera denna process.

Idag ges alla patienter liknande avlastande behandling under transporten. Vissa patienter har emellertid mera allvarlig syrebrist (ischemi) i hjärtat än andra, vilket får till följd att en större andel av hjärtmuskelvävnaden utsatt för syrebrist kommer att gå under (infarcera) per tidsenhet innan man kommer till PCI-behandlingen. Genom att även analysera andra delar av hjärtcykeln med EKG (depolarisationen, dvs QRS komplexet), finns det möjligheter att identifiera dessa högriskpatienter och i framtiden eventuellt kunna skräddarsy mera intensiv, kompletterande behandling redan under transporten. Denna kunskap skulle kunna nyttjas i stor omfattning och adderas till utvecklingen av akut hjärtinfarktbehandling globalt.

## Övergripande syfte och ingående patientgrupper

Avhandlingens övergripande mål var att utvärdera metoder för att extrahera mer information från EKG-signalen under depolarisationen (QRS-komplexet), som

additivt diagnostiskt hjälpmedel till dagens repolarisationsanalys (ST-T sträckan). I de olika delarbetena studerades patienter med olika typer av akut ischemi, dels i en mindre population under planerad och kontrollerad ballongvidgning av ett kranskärl (*Studie II* och *III*), dels i en betydligt större patientgrupp med akut pågående hjärtinfarkt (STEMI) i *Studie IV*. I dessa populationer fanns multipla kliniska variabler liksom kvantifiering av graden av ischemi med myokardscintigrafi (SPECT). I *Studie I* analyserades patienter dessutom under vilobetingelser avseende olika typer av QRS-förändringar som tyder på äldre hjärtinfarkt.

Generellt sett är QRS-förändringar svårare att karakterisera och mäta än de som ses under ST-sträckan. Inom QRS-komplexet i ett standard-EKG kan man mäta skillnader i amplitud av ingående komponenter samt deras durationer. Båda, men i synnerhet den sistnämnda har felkällor, varför det finns behov av ett mera övergripande och tillförlitligt QRS-mått. I denna avhandling har QRS-komplexet analyserats utifrån både konventionellt, standard-EKG, samt de två mer tekniskt avancerade analysmetoderna högfrekvens-EKG (HF-QRS) och QRS-slope metoden. Dessa metoder värderades under akut ischemi, pågående och tidigare infarkt. Den förstnämnda, standard-EKG baserade metoden, sk Sclarovsky-Birnbaum (S-B) graderingen av ischemi, värderar allvarlighetsgraden av ischemi under ett akut hjärtinfarktskede. Denna metod är sedan tidigare beskriven, men har ännu inte kommit att användas i klinisk praxis.

## Specifika mål

*Delarbete I:* Studera om man med hjälp av HF-QRS metoden kan differentiera mellan patienter med en tidigare genomgången hjärtinfarkt och de som inte haft någon infarkt, där själva infarktdiagnosen verifierats med vanligt standard-EKG.

*Delarbete II:* Värdera om förändringar av HF-QRS vid akut ischemi är associerade till dess utbredning och allvarlighetsgrad.

*Delarbete III:* Studera hur den, jämfört med HF-QRS- metoden, mindre bruskänsliga och mera kliniskt lättillgängliga QRS-slope- metoden, kan användas för att värdera utbredning och allvarlighetsgrad av akut ischemi.

*Delarbete IV:* Undersöka hur depolarisationförändringarna som ingår i S-B graderingen av ischemi varierar över tid (från ambulans-EKG till EKG taget senare på mottagande sjukhus just innan PCI behandlingen). Vidare studera det kliniska värdet av tidig hjärtinfarktgradering, dels utifrån ambulans-EKG, men även värdet av själva dynamiken under transporten fram till PCI behandlingen. Testa om denna EKG-information relaterar till faktisk allvarlighetsgrad, dvs hastighet av infarktutveckling och behandlingsresultatet av akut PCI inklusive slutlig infarktstorlek.

## Fynd och sammanfattning

*Studie I* visade att vid värdering av en större patientpopulation och med fler EKG-avledningar jämfört med tidigare, liknande studier, kunde vi, till skillnad från tidigare resultat, med hjälp av HF-QRS inte differentiera mellan patienter med och utan tecken till tidigare hjärtinfarkt.

I *Studie II* fann vi att högfrekvenskomponenter inom QRS komplexet sjunker vid ischemi. Graden av förändringen visar signifikant korrelation med både utbredning och svårighetsgrad av ischemin kvantifierad med SPECT med högre korrelationskoefficient än konventionella ST-förändringar.

Med den betydligt mera bruståliga och därmed mera kliniskt lättillgängliga QRS-slope metoden, kunde vi i *Studie III* konstatera att förändringar i synnerhet vad gäller nedåtgående lutningen av R vågen uppvisar signifikant korrelation med både utbredning och svårighetsgrad av ischemin kvantifierad med SPECT, som är starkare än för övriga, konventionella QRS parametrar i standard-EKG och adderar information till ST-analys.

*Studie IV* visade att "QRS distortion", som ingår i den allvarligaste grad 3 i S-B ischemigradering, uppvisar en dynamik mellan ambulans-EKG och EKG precis innan PCI-behandlingen. Patienter med grad 3-ischemi redan vid tidig EKG värdering i ambulansen, liksom de som uppvisade en dynamik där de bibehöll eller utvecklade denna grad under transporten, utvecklade större infarkter än de som inte hade dessa EKG-förändringar. Detta trots motsvarande storlek av det ischemiska området och samma tid från symtomdebut till PCI behandling. Vidare kunde vi konstatera att det är avhängigt graden av ischemi hur snabbt infarkten utvecklar sig, och hur stor del av det hotade hjärtmuskelområdet man därigenom kan rädda med hjälp av att öppna det stängda kranskärlet med PCI. Patienter som behandlades inom 2.5 timmar från symtomdebut uppvisade samma behandlingseffekt av PCI oavsett ischemigrad. Vid behandling senare än 2.5 timmar såg vi däremot sämre resultat för den grupp av patienter som hade grad 3 ischemi på ambulans EKG jämfört med patienter som hade grad 2 ischemi.

Avhandlingen visar att uttalad akut ischemi ger förändringar under själva depolarisationen som kan kvantifieras. Då analysmetoden för HF-QRS är relativt bruskänslig och därmed kräver avancerad medelvärdesberäkning, testades en nyutvecklad QRS-slopetmetod, som vi bedömer kunna ge likvärdig information på ett mera lättillgängligt och tillförlitligt sätt. Den lämpar sig främst för att följa förändringar under pågående EKG-monitorering, men kan även nyttjas i bedömning av ett enskilt EKG om det finns ett tidigare, jämförande EKG. Resultaten från *Studie IV* indikerar att grad 3-ischemi som noteras tidigt kan indikera allvarlig ischemi med snabb infarktutveckling. Fler studier behövs både för att vidare applicera QRS-slope metoden i ett mera kliniskt sammanhang och för att få ytterligare förståelse för hur förändringar i den senare delen av QRS-komplexet bäst kan nyttjas för riskvärdering av patienter med akut hjärtinfarkt.



# Abbreviations

ACC	American College of Cardiology
ACS	Acute Coronary Syndrome
AHA	American Heart Association
AMI	Acute Myocardial Infarction
ATP	Adenosine Triphosphate
BBB	Bundle Branch Block
BMI	Body Mass Index
CABG	Coronary Artery By-pass Graft surgery
DS	Down-Slope of the R wave
ECG	Electrocardiogram
ESC	European Society of Cardiology
HF-QRS	High-Frequency QRS components
IS	Infarct Size
LAD	Left Anterior Descending coronary artery
LBBB	Left Bundle Branch Block
LCX	Left Circumflex coronary artery
LV	Left Ventricle
LVEF	Left Ventricular Ejection Fraction
LVH	Left Ventricular Hypertrophy
MaR	Myocardium at Risk
MI	Myocardial Infarct
MPI	Myocardial Perfusion Imaging
MONAMI	The ST-MONitoring in AMI patients registry
MRI	Magnetic Resonance Imaging
NSTEMI	Non ST-Elevation Myocardial Infarction
PCI	Percutaneous Coronary Intervention
pPCI	Primary Percutaneous Coronary Intervention
RBBB	Right Bundle Branch Block
RCA	Right Coronary Artery
RMS	Root-Mean-Square
S-B grade	Sclarovsky-Birnbaum ischemia grade
SD	Standard Deviation
SPECT	Single Photon Emission Computed Tomography
Spont STR	Spontaneous ST- segment Resolution before PCI

STEMI	ST-Elevation Myocardial Infarction
STM	ST level at J+1/16 of the average RR interval
STR	ST- segment Resolution
<sup>99m</sup> Tc	Technetium-99m
TIMI	Thrombolysis In Myocardial Infarction
TMVG	Trans Membrane Voltage Gradient
TnT	Troponin T
TS	Terminal Slope
US	Up-Slope of the R wave
VCG	Vectorcardiography



# 1 Introduction

## 1.1 Ischemic heart disease

### 1.1.1 *Epidemiology*

Ischemic heart disease (IHD) is the number one cause of death in low-, middle- and high income countries<sup>1</sup>. According to WHO more than seven million people die worldwide each year from IHD, about 12.8% of all deaths<sup>2</sup>. The 2012 European Cardiovascular Disease statistics reports IHD to account for 1.8 million deaths per year in Europe, and is the single most common cause of death. It is estimated that 22% of women and 20% of men will die from this disease<sup>3</sup>. From the 2010 Heart Disease and Stroke Statistics update of the American Heart Association it was reported that IHD is responsible for about one-third of all deaths in individuals over 35 years of age in the US<sup>4</sup>.

The mortality rate due to IHD has declined in countries with developed economies and health care systems during the last few decades, mainly due to improvements in therapy, including acute initial medical treatment for acute coronary syndromes (ACS), acute reperfusion management of acute myocardial infarction (AMI), secondary preventive measures after AMI, therapy for heart failure, and revascularization for chronic, stable angina pectoris. Other reasons are increased attention to risk factors like cholesterol levels, systolic blood pressure, smoking prevalence and physical inactivity<sup>5</sup>. The overall decline in IHD-caused mortality during the last decades in the US has been estimated at about 60-65%, whereas in Europe approximately 30%<sup>6</sup>.

Despite decreased mortality rates in some regions, it is however, expected to increase in other, developing countries. Furthermore, in many developed countries many risk factors have increased, and in the US the increase in body-mass index (BMI) and prevalence of diabetes, hypertension and hypercholesterolemia are challenging the positive trend<sup>7</sup>. Furthermore, because of the changing demographic situation worldwide with a growing proportion of elderly people we will probably encounter great challenges managing an increasing total number of people with IHD.

### *1.1.2 Pathophysiology*

#### *1.1.2.1 Coronary arteriosclerotic plaque formation*

The underlying pathophysiologic process consists of arteriosclerosis development in the coronary artery wall. It is a complicated process mediated through both lipid accumulation and complex inflammatory activity<sup>8</sup>, involving many different cell types including monocytes, T lymphocytes, endothelial and smooth muscle cells.

The arteriosclerotic process takes decades to develop and probably starts early in life. Initially, fatty acids accumulate into the intima layer of the vessel, building up fatty streaks. This is mediated through monocytes and T lymphocytes passing through the inner endothelial layer of the vessel, into the intima, where they transform into macrophages. Through this process these cells become “foam cells”, making up the fatty streaks. Parallel to the growth of these lipid storages, complex inflammatory activities take place, leading to a necrotic inner core, which may further enlarge due to hemorrhage from vasa vasorum. On the outer border of the necrotic lipid formation it is a thin fibrous cap composed of type I collagen, macrophages, lymphocytes and smooth muscle cells, thus forming a fibroatheroma that is more or less prone to rupture<sup>9</sup>.

During the process of establishing these intimal arteriosclerotic fibroatheromas, or plaques, the lumen of the coronary vessels may become narrow, causing decreased blood flow. At some point in this process, the blood flow will not be sufficient for meeting the metabolic demand of the myocardium, thereby leading to lack of oxygen, myocardial ischemia and angina. This is the reason for stress-induced angina pectoris.

Due to structural changes and remodeling within the necrotic central lipid core, inflammatory action to the fibrous cap, thinning of the capsule as well as neovascularization, the plaque can suddenly become “vulnerable”. Such plaques are especially sensitive to mechanical stress and/or inflammatory-mediated further weakening of the collagen capsule, leading to sudden rupture<sup>10</sup>. This initiates a complex cascade with sudden activation of platelets in the blood, leading to rapid thrombus formation and compromised coronary blood flow, thus an acute coronary syndrome (ACS). The process may also include vasospasm of the affected artery, further compromising myocardial perfusion.

#### *1.1.2.2 Ischemia on the myocardial cell level*

In order to maintain the highly energy-demanding contraction process and ion pump function the myocardial cells need an adequate supply of oxygen as well as fuel such as fatty acids, glucose and lactate. In the normal situation, with adequate coronary blood flow, 60–90% of the energy used for the myocardial cells in

synthesizing ATP from ADP comes from fatty acids supplied from the plasma. The rest comes from glucose and lactate.

Breakdown of ATP then releases energy to be used for the contractile process and ion pumps that handle the relaxation process and the ion homeostasis necessary for the electrophysiological guidance of the pumping process<sup>11</sup>.

With sudden coronary artery occlusion, oxygen delivery to the myocardial cells becomes insufficient in relation to the demand, thus slowing or inhibiting the aerobic, oxidative phosphorylation process of ATP in the mitochondria. This stimulates glycolysis, by which storages of glycogen in the cells are used and an accelerated anaerobic metabolism is triggered. This leads to high intracellular lactate levels and acidosis. The myocardial cells can quickly adapt to anaerobic metabolism, however with persistent lack of oxygen they gradually progress from reversible ischemia to an irreversible status, where mitochondrial function is irreversibly damaged, as well as the structure of the cell membranes, leading to cell death<sup>12</sup>.

In the mid 1970s Jennings et al.<sup>12</sup> described a gradually increasing metabolic, and thus ischemic, severity gradient that arises within the myocardial wall from the outermost epicardial to the inner subendocardial layer. Thus the subendocardium is the portion of the myocardium wall most vulnerable to ischemia, due to: a) a generally lesser degree of contribution to this layer from the coronary vascular bed, b) ischemia-induced vasodilatation in the better perfused layers, and c) increased intra-cavitary and intramural pressure, that further hampers subendocardial perfusion.

### ***1.1.3 Clinical manifestations and classification of ischemic heart disease***

The main clinical manifestation of ischemic heart disease is chest pain, often located centrally, but can be located at various sites in the thoracic region, neck, chin or upper abdomen. The symptoms can vary from very light, uncomfortable pressure to very intense pain, with or without radiation to either or both arms, neck or back. Systemic, vegetative symptoms like nausea, sweating or dizziness often occur. Atypical symptoms such as shortness of breath can also be caused by myocardial ischemia.

The classification of IHD is based on stability:

1. **Stable angina pectoris:** Symptoms evoked by physical or emotional stress. Reversible symptoms upon rest or short-term nitrates.
2. **Acute coronary syndrome (ACS):**
  - a. **Unstable angina pectoris:** Either very intense, newly developed angina pectoris, or worsened and/or more easily evoked symptoms by either physical, emotional stress or at rest during the last 4 weeks.

- b. **Acute myocardial infarction (AMI):** Symptoms at rest for more than 20 minutes not alleviated by short-term nitrates. Due to the appearance on ECG patients are further stratified into two types of AMI: ST elevation myocardial infarction (STEMI) and non-ST elevation myocardial infarction (NSTEMI).

ACS is an unstable coronary process in which a patient quickly can transition from unstable angina to acute MI.

#### *1.1.4 Diagnosis of acute MI*

The three cornerstones for the clinical diagnosis of acute MI are: clinical symptoms, ECG findings and cardiac biochemical markers. The definitions of acute MI have been gradually updated from the traditional WHO criteria, originally published in 1979<sup>13</sup>, to the more clinically based definition by the European Society of Cardiology (ESC) and the American College of Cardiology (ACC) in 2000<sup>14</sup>. The latter has been further updated to the present “Third universal definition of acute MI” published in 2012<sup>15</sup>.

In this clinical definition, the assumed cause of the MI is the basis for classification into five different types:

- **Type 1:** Spontaneous MI due to a pathologic process in the coronary artery wall resulting in an intracoronary thrombus formation (most often plaque erosion/rupture).
- **Type 2:** Ischemic imbalance secondary to various conditions such as anemia, tachy-/brady-arrhythmias, respiratory failure, etc .
- **Type 3:** MI resulting in death, without available biochemical markers.
- **Type 4:** Procedure-related MI after percutaneous coronary intervention (PCI), or stent thrombosis.
- **Type 5:** Associated with coronary artery by-pass graft surgery (CABG).

In this thesis only Type 1 is considered. The criteria are as follows:

Significant rise of cardiac biochemical markers and at least one of the following:

1. Symptoms of ischemia (see above).
2. ECG-findings:
  - a. Development of pathologic Q waves in the ECG.

- b. New or presumably new ST-segment-T wave (ST-T) changes or new left bundle branch block (LBBB)
- 3. Coronary angiographic, or autopsy-identified intracoronary thrombus.
- 4. Imaging evidence of new loss of viable myocardium, or regional wall motion abnormality.

Early differentiation between unstable angina, NSTEMI and STEMI is important. Immediate recognition of STEMI patients is of particular importance, since treatment is directed towards immediate revascularization (see below).

Despite improved sensitivity and specificity of cardiac biochemical markers, possibilities for early detection are limited by their delayed appearance in the blood (3-9 hours for Troponin)<sup>15</sup>. Thus, this diagnostic modality can only differentiate between unstable angina and NSTEMI. Consequently, ECG is the only immediately available diagnostic tool to identify patients with an acute need for coronary revascularization.

### *1.1.5 Acute management and treatment of STEMI*

The most important aim is to restore coronary blood flow as soon as possible to optimize myocardial salvage and patient outcome<sup>16</sup>. This is particularly important during the first few hours after symptom onset<sup>17, 18</sup>. The revascularization modalities are by either pharmaceutical, iv thrombolytic administration, or primary percutaneous coronary intervention (pPCI). In the 2009 ACC/AHA focused update<sup>19</sup> each geographic community was recommended to develop systems to ensure prompt STEMI management, including logistical algorithms from early, pre-hospital ECG evaluation, through referral and transfer for revascularization at a high-quality pPCI-center. Increasing evidence from multiple randomized trials have shown that pPCI performed in a timely fashion is a better reperfusion strategy compared with thrombolysis in most patients. However, the complexity of factors such as patient delay (time from symptom onset to first medical contact) as well as different reasons for system delay due to both different door-to-needle, or door-to-balloon time (delay for administration of thrombolytics or applying mechanic (pPCI) revascularization), effectiveness of the treatment given (fast reperfusion by pPCI, slower by thrombolysis), logistics of patient transfer between hospitals etc., have resulted in the recommendation by the ACC/AHA and ESC that pPCI is the preferred reperfusion treatment for any STEMI patient if the procedure can be made within 120 minutes from first medical contact<sup>2, 19-22</sup>. If there is longer delay for pPCI, thrombolytic therapy could be preferred.

Until proper reperfusion treatment is achieved all patients receive administration of antiplatelet agents, beta blockers, nitrates, oxygen, morphine etc., as



appropriate, to optimize myocardial perfusion and reduce the metabolic demand of the myocardial cells.

### ***1.1.6 Determinants of final infarct size***

The most central determinants of final infarct size (IS), besides the time elapsed from coronary occlusion to reperfusion, are the size of the myocardium at risk (MaR) and the severity of ischemia within the MaR. The latter will determine the rate of progression of infarction development within the MaR, i.e. the more severe ischemia the more rapid progression of the wavefront of necrosis.

#### ***1.1.6.1 Myocardium at risk (MaR)***

MaR is mainly related to the area supplied by the occluded, infarct-related coronary artery, distal to the occlusion. Thus, both the size of the coronary artery and site of occlusion along the vessel (proximal or more distal) will determine the oxygen-deprived myocardial territory at risk for infarct development.

During the phase of an acute MI, the activated thrombotic system may result in a dynamic antegrade coronary flow where spontaneous recanalization with or without distal embolization and thrombotic re-occlusion might occur, changing the risk area. Furthermore, recruitment of collaterals may play a role in reducing the risk area, as seen below.

#### ***1.1.6.2 Myocardial protection and severity of ischemia***

The myocardium has an inherent ability for physiologic adaptation to ischemia that renders it more resistant to serious ischemic events and significantly delays the progression of infarct evolution. There are two main mechanisms for this adaptation process; long-term *collateral development* and *ischemic preconditioning*.

### **Coronary collateral formation**

As an adaptation to repeated episodes of myocardial ischemia collateral vessels can develop from other territories in order to improve blood flow. The mechanisms by which this is mediated are still not fully elucidated, however factors such as fibroblasts and vascular endothelial growth factors<sup>23, 24</sup>, as well as nitric oxide<sup>25</sup> appear to be involved.

Two kinds of collateral vessels have been identified:

- Epicardially located, muscular collaterals, developed from preexisting arterioles.
- Capillary-size collaterals, without smooth muscle cells, which can be distributed throughout the myocardial wall<sup>26</sup>.

In humans, the presence of collaterals and/or their recruitment during a sudden, acute MI has been shown to reduce the severity of ischemia, thus resulting in limitation of final infarct size, improved post-infarction left ventricular ejection fraction (LVEF) as well as reducing mortality<sup>27-29</sup>.

### Ischemic preconditioning

This phenomenon was already reported by Murry et al. in 1986, as an observed delayed effect on infarction development upon experimental coronary occlusion in a canine preparation preceded by short, repetitive episodes of ischemia separated by periods of reperfusion<sup>30</sup>. Compared to a control group, this precondition protocol of four repetitive, 5-minute episodes of regional ischemia, each followed by 5 minutes reperfusion, resulted in a 75 percent reduction in final infarct size. These findings have been reproduced and further confirmed by several other animal experiments, in different species<sup>31-34</sup>.

In humans this phenomenon has been evaluated both in vitro<sup>35</sup> and in vivo models from various clinical situations, as exercise stress test<sup>36, 37</sup>, elective PCI<sup>38, 39</sup> and CABG<sup>40</sup>.

The underlying mechanisms for ischemia preconditioning are still not completely known. However, growing evidence supports the notion that this protection is not due to recruitment of collaterals<sup>30-32</sup>. Cells in the preconditioned myocardium have slower metabolism, demanding less ATP, and producing less lactate than the non-preconditioned myocardial cells<sup>41, 42</sup>. One hypothesis is attenuation of intracellular acidosis during the critical ischemia as an effect of lower intracellular glycogen levels due to its depletion in the previous, shorter ischemia episodes. However there are some conflicting results<sup>43</sup>. Most likely this intrinsic cardioprotective process is mediated through several complex pathways, also including endogenous mediators released during the brief periods of ischemia, acting on local receptors and channels. Some tentative mediators have been proposed, such as: adenosine, bradykinin, protein kinase C, reactive oxygen radicals, ATP-dependent potassium channels, etc<sup>32, 34, 44, 45</sup>.

Clinically, ischemia preconditioning is probably the cause of “warm-up angina”, i.e. improvement of stable stress-induced angina symptoms during the day due to repetitive ischemia episodes<sup>37</sup>.

However, the most important role of ischemia preconditioning is played during the acute MI situation. In numerous clinical studies, pre-infarction angina (repetitive short episodes of unstable angina within hours to days before the acute MI) has been reported to be associated with smaller infarct size, improved left ventricular function and regional wall motion, less malignant ventricular arrhythmias as well as lower both short- and long-term mortality<sup>46-48</sup>. The timing of previous angina symptoms in relation to the acute MI episode is important,

since the protective effect has especially been reported in patients suffering from angina within 24-48 hours prior to the acute MI<sup>49, 50</sup>.

Methods for early identification of acute MI patients without this kind of myocardial protection, who thus have an extremely high risk for rapid evolution of necrosis within the MaR, would be of great clinical importance. This sort of risk stratification could lead to individual tailoring of the acute management, for example during transfer to pPCI. However, there are no such clinically used methods today.

## Evaluation of myocardial protection/ischemia severity by ECG

The effects of experimental ischemic preconditioning protocols have been evaluated by changes in the ECG. Several studies have reported changes in the repolarization phase (ST-T) with reduced ST elevation when inducing ischemia after a preconditioning protocol compared to the ones with non-preconditioned myocardium<sup>39, 51-53</sup>.

However, another, presumably more useful electrophysiological determinant of the level of protection (or severity of ischemia) is found within the depolarization phase (QRS complex). This has been reported in both experimental animal studies<sup>54</sup> and in several human studies on STEMI patients<sup>55-58</sup> and will be dealt with in greater detail further on.

## 1.2 Anatomy, electrophysiology and myocardial ischemia

### 1.2.1 Basic electrophysiological principles

#### 1.2.1.1 Electrophysiology at the cellular level: the action potential

The basis of myocardial electrophysiology is the inborn excitability of both the specially designed cardiac conduction system and the myocytes, as mediated by the ionic currents in the different phases of the action potential (AP) throughout the cardiac cell cycle (Figure 1.1).

In the normal situation of adequate coronary blood flow, the resting potential of the myocardial cell is between -80 and -95 mV, with the cell interior having negative charge in relation to the extracellular space. This negative potential is created by an energy demanding procedure of pumping potassium ( $K^+$ ) into and sodium ( $Na^+$ ) out of the cell (the  $Na^+/K^+$ -ATPase pump), fueled by the continuous production of ATP by aerobic cell metabolism. By this process, different ion concentration levels inside and outside the cell are created, with high

concentration of intracellular  $K^+$  and lower concentration of  $Na^+$  in relation to the extracellular space. The equilibrium potential across the cell membrane is different for these ions. For  $K^+$  it is between -80 and -95mV. Thus, excess of intracellular  $K^+$  will be balanced by a passive outflow of this ion down its current in the resting phase to maintain a stable, negative intracellular potential.

The depolarization phase (*Phase 0*) of the AP is initiated by the sudden opening of fast, voltage-dependent  $Na^+$  channels, leading to a rapid inflow of  $Na^+$  into the cell, thus shifting (depolarizing) the interior of the cell from its negative to positive (about +45 mV) potential, which is the equilibrium potential for this specific ion. Meanwhile also slower calcium ( $Ca^{2+}$ ) channels open, producing a slight inward  $Ca^{2+}$  flow. Then, *Phase 1* creates a small “notch”, caused by an initial outward  $K^+$  flow and a decay of the  $Na^+$  current. This is followed by the plateau comprising *Phase 2*, where an outward  $K^+$  flow (to passively regain its negative equilibrium potential), and inward  $Ca^{2+}$  and to a small degree  $Na^+$  ion-flow balance each other to a stable potential. In the following, *Phase 3*, a fast repolarization is taking place, thus regaining the negative, resting membrane potential, by decay of the remaining  $Ca^{2+}$  in-flow and, most importantly, a fast outflow of  $K^+$ .

In *Phase 4* the negative resting potential is maintained, again created by the  $Na^+/K^+$ -ATPase pump and balanced by a slow, passive outflow of  $K^+$ .

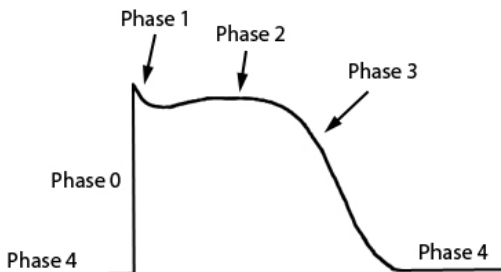


FIGURE 1.1 Different phases of the myocardial AP.

### Ischemic effect on the action potential

Sudden coronary occlusion and lack of oxygen quickly affects this balanced process:

- The ATP dependent  $Na^+/K^+$  ATPase- pump cannot maintain the normal, negative resting potential.
- Lactate acid accumulates and acidosis develops both within the cell and in the extracellular space.
- $K^+$  accumulates in the extracellular space.

By these processes the AP will change in the following ways within the ischemic region<sup>59-62</sup>:

1. Reduced resting membrane potential. Thus, the extracellular space within the ischemic region becomes more negative in comparison to surroundings in this phase.
2. At a reduced membrane potential of about  $-50$  mV, the fast  $\text{Na}^+$  channels are inactivated. Instead, the AP is elicited by an inward current of  $\text{Ca}^{2+}$  ions by slow inward channels, causing a delayed and slower upstroke of the AP (*Phase 0*).
3. Lower maximal AP amplitude.
4. Shortened duration of the AP, thus earlier repolarization.

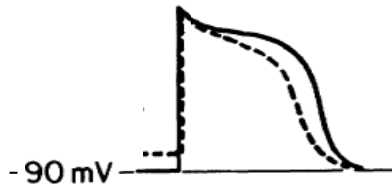


FIGURE 1.2 Illustration of ischemia-induced changes of the different phases of the AP. Solid line represents normal AP and dashed line the situation during ischemia with reduced resting membrane potential, slower upstroke, lower amplitude and earlier repolarization. Reprinted and modified from Vincent et al.<sup>63</sup>, with permission.

These changes, illustrated in Figure 1.2, cause a voltage gradient between the ischemic area and the normal myocardium during different phases of the cardiac electrical cycle that leads to current flow between these regions.

These “currents of injury” are represented on the surface ECG by deviation of the ST segment and also have secondary effects on the QRS complex.

#### *1.2.1.2 Ventricular propagation of the depolarization wavefront*

Conduction of the electrical signal is mediated by cell-to-cell propagation through gap junctions. All myocytes are capable of conduction. However, the specialized conduction system ensures an efficient propagation of the signal. The signal originating from the atria is conducted through the AV node, and rapidly through the ventricles in this specialized conduction system involving the bundle of His, the right and left bundle branches and the Purkinje network, which branches into a fine network terminating in the ventricular endocardium. The electrical and metabolic properties of these structures are slightly different from those of the

myocytes, e.g. by being more resistant to ischemia<sup>64-66</sup>. This has implications for the changes in the activation wavefront during severe ischemia.

Human ventricular excitation was first described in detail by Durrer et al. in the early 1970s<sup>67</sup>, and further verified by animal studies, by epicardial mapping during open heart surgery and by computer simulation by Selvester, Solomon et al<sup>68, 69</sup>. The normal ventricular activation is a rapid, balanced process that results in the normal synchronous contraction of the right and left ventricles. This normal sequence is determined by the anatomical and physiological features of the rapidly conducting Purkinje network that inserts in the endocardium at 5 major sites<sup>70</sup>, 3 of which are positioned within the left ventricle as illustrated in Figure 1.3, and the other 2 insertion sites are at the right side of the septum and the free lateral wall in the right ventricle. Activation propagates more slowly from the endocardial to the epicardial myocardial wall by the myocytes. Depolarization can be viewed as an activation wavefront that excites the myocardial wall from endo- to epicardium as well as different regions of the ventricles at specific time instants, as illustrated in Figure 1.3. First, the intraventricular septum is depolarized from left to right. Then the right and left ventricles are depolarized simultaneously, however, due to the larger mass of the LV the main vector in this phase is left oriented, mainly towards the apex. Subsequently the activation vector, at about 40 ms depolarizes the anterior free wall, thus the main vector shifts more leftward. Finally the last area to be depolarized is the basal parts of the heart.

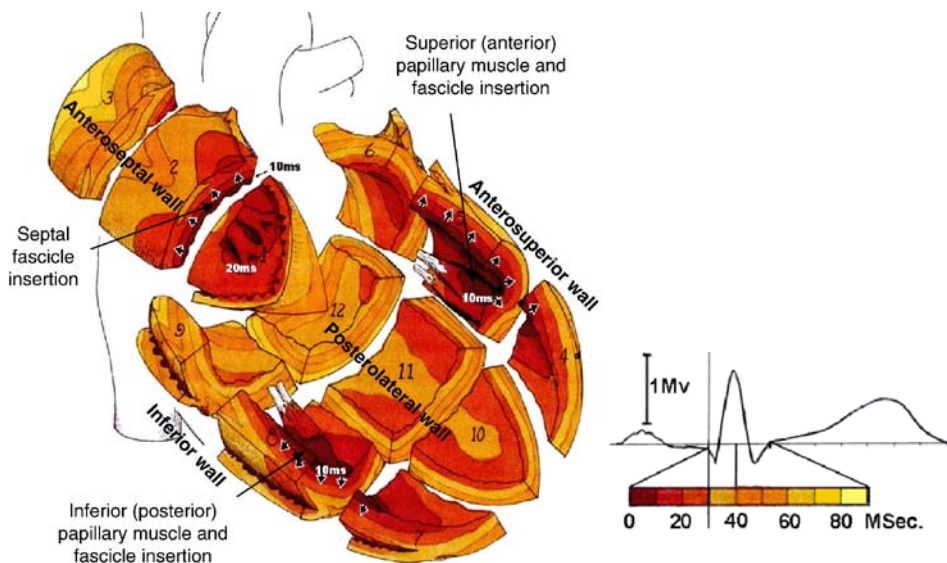


FIGURE 1.3 Three-dimensional illustration of the left ventricular (LV) activation with respect to its timing in different layers of the myocardial wall and different segments. Modified from Selvester et al.<sup>71</sup> with permission.

### 1.2.2 Electrocardiography (ECG)

Despite advances of cardiac biochemical marker analysis and cardiac imaging techniques in recent years, the standard 12-lead ECG is still the most important and valuable tool in the acute clinical situation evaluating a patient with ongoing symptoms compatible with acute MI. With the advanced technical, digital development of telemedicine, an ECG recording can be made already in the pre-hospital phase, in the patient's home or in the ambulance. The ECG can be directly transmitted to the attending emergency physician or cardiologist for instant evaluation and clinical decision-making.

The electrical activity of the myocardium, as described in previous sections, produces an electrical field with a 1) *magnitude* and 2) *direction* that change during the cardiac cycle. The standard ECG provides a graphical representation of this electrical field at every instant where each specific lead registers this field from its specific location on the body surface.

There are different lead systems available, however the one most often used clinically, and considered in this thesis, is the standard, 12-lead ECG with six limb leads in the frontal plane and six precordial leads in the transverse plane, organized as in Figure 1.4. This display of the limb leads (the Cabrera format) is recommended in the 2000 European Society of Cardiology (ESC)/American College of Cardiology (ACC) guidelines for universal adoption in 12-lead ECG and has been used in Sweden for many years<sup>72</sup>.

Each lead is bipolar and records the difference between the exploring electrode and either an opposite (as for leads I, II and III), or a reference electrode (the Wilson's central terminal) as for the "augmented leads" aVR, aVL, aVF and V1-V6. Electrical impulses moving toward the exploring electrode is registered as a positive deflection and vice versa.

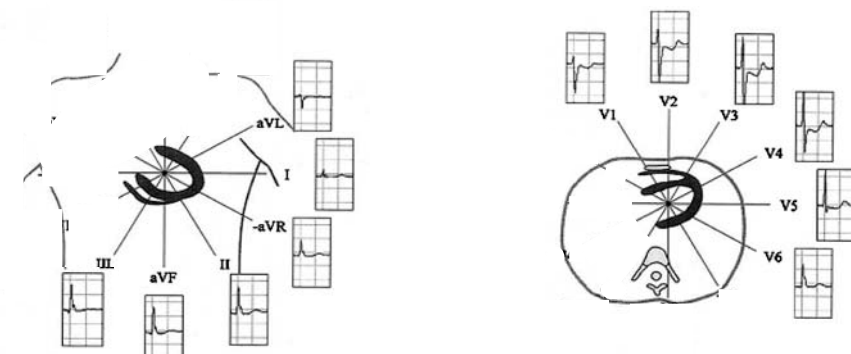


FIGURE 1.4 The standard 12-lead ECG displayed in the Cabrera format. Reprinted and adapted from Pahlm-Webb et al.<sup>73</sup> with permission.

In Figures 1.5 and 1.6 the same lead display is shown including the time-sequence of the ventricular depolarization.

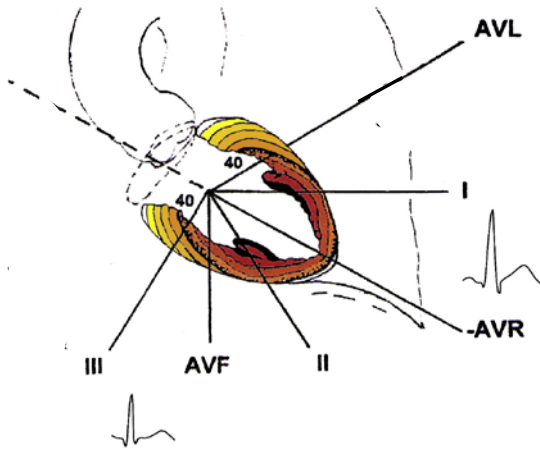


FIGURE 1.5 Showing the limb leads in the frontal plane in the Cabrera lead configuration as well as the timing of the LV activation sequence. The colored lines represent areas of myocardium activated within the same 10-millisecond period. Modified from Strauss, Selvester et al.<sup>74</sup> with permission.

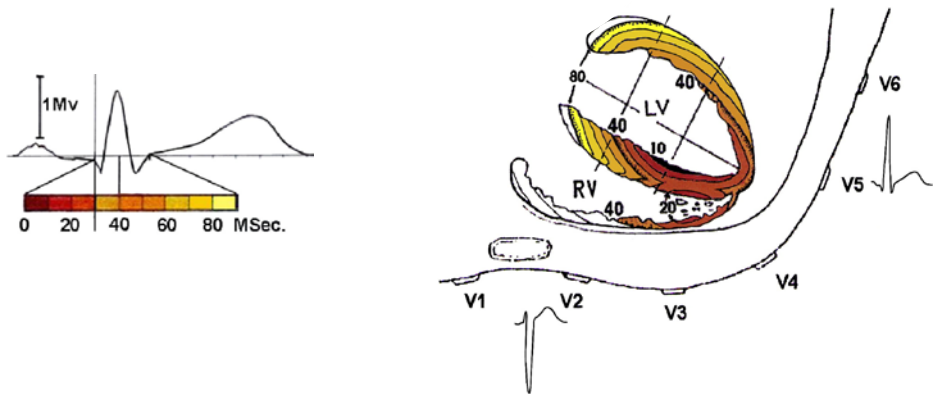


FIGURE 1.6 Transverse plane showing both left and right ventricles (LV and RV) within the thorax cavity in reference to the precordial leads V1-V6. Adjusted from Strauss, Selvester et al.<sup>74</sup> with permission.



### 1.2.3 ECG changes during acute ischemia

Due to ischemia-induced effects on the cardiac cell cycle, changes in both the repolarization and depolarization phases can be registered by the ECG.

#### T-wave change

As an early sign of ischemia tall, hyperacute T waves, as suggested due to the local reduction of the AP duration<sup>75</sup>, may be seen. As an isolated finding, such early changes are, however, rarely seen in clinical practice, since they develop very rapidly and are shortly followed also by ST-segment deviation.

#### ST-segment deviation

ST-segment change is the most commonly used ECG marker of ischemia. The changes in the AP described above explain the ST changes seen during acute ischemia. Both the changed resting membrane potential and earlier repolarization within the ischemic region results in ST-segment elevation seen on the ECG:

1. **Diastolic injury current:** The ischemic cells remain relatively depolarized during *phase 4* of the AP, thus creating a relative negative extracellular charge compared to the surrounding, normal myocardium. Therefore, during the electrical diastole, current (diastolic current of injury) will flow between ischemic and normal myocardium. ECG-leads overlying the ischemic zone will record a negative deflection during electrical diastole and produce depression of the TQ segment. However, the ECG recorders in clinical practice automatically “compensate” for any negative shift in the TQ segment, thus it appears as ST-segment elevation on the ECG. This is illustrated in Figure 1.7A.
2. **Systolic injury current:** In systole the other three ischemia-induced changes on the AP described above makes ischemic myocardium relatively positive in comparison to the normal surroundings. This creates a voltage gradient between normal and ischemic zones during the systolic phase such that the current-of-injury vector will be directed toward the ischemic region resulting in primary ST elevation, as demonstrated in Figure 1.7B.

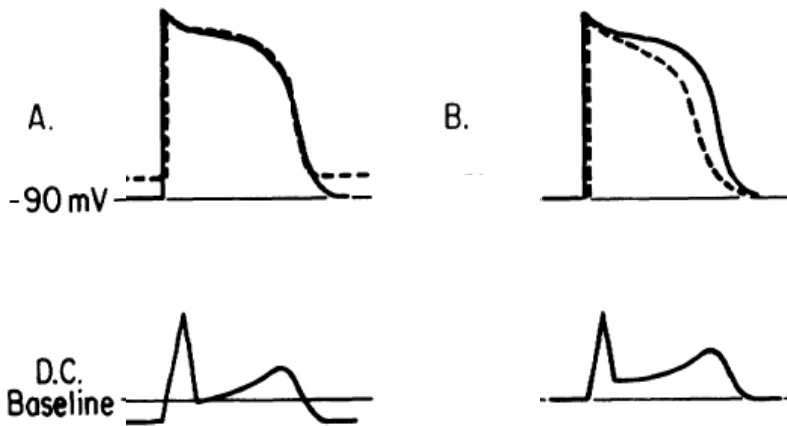


FIGURE 1.7 In the upper panel AP changes due to ischemia (dashed line) are shown. In the lower panel the corresponding changes on the overlying ECG lead is demonstrated. In A) the diastolic injury current with downward displacement of the TQ segment is illustrated. In B) the early repolarization of the ischemic area, causing a systolic injury current directed toward the ischemic region is demonstrated, giving rise to a primary ST-segment elevation. Adjusted from Vincent et al.<sup>63</sup> with permission.

In transmural ischemia the overall ST vector is usually directed toward the epicardium, thus exhibiting ST-segment elevation in leads whose positive poles are overlying the ischemic region, and reciprocal ST depression in leads whose positive poles are directed opposite to (i.e. approximately 180° away from) these leads. In ischemia mainly restricted to the subendocardial layer, on the other hand, the overall ST vector is directed toward the inner layer of the ventricular wall or cavity, displayed as ST-segment depression in the overlying ECG lead. The latter is more often present in demand ischemia, such as stress-induced ischemia or unstable angina, whereas the former is often related to supply ischemia, due to sudden coronary artery occlusion. However, the picture may vary considerably, and at many times total coronary occlusion is displayed as ST-segment depression, or no significant ST-segment changes at all. This is because the 12-lead ECG is not equally distributed around the thorax, covering all parts of the myocardium, and because of cancellation effects that may arise between two ischemic regions opposite to each other.

ST-segment elevation, as in the STEMI-guidelines, is used to identify those with acute MI who should be referred for immediate revascularization<sup>20</sup>.

A mathematical model of explanation regarding the *amount* of ST-segment elevation observed on a surface ECG lead with a certain location in relation to the ischemic area, is the solid angle theory<sup>76</sup>. This is illustrated in Figure 1.8.

Basically, this model contains both spatial factors (solid angle,  $\Omega$ ) and nonspatial factors. The solid angle is subtending a spherical surface area about the recording electrode. The nonspatial factors include the transmembrane voltage gradient (TMVG) across the ischemic boundary, thus the current flow between the ischemic ( $V_{m1}$ ) and nonischemic, normal myocardial cells ( $V_{m2}$ ) during the electrical cardiac cycle (systole and diastole).  $K$  is the conductivity factor. Conductivity is determined by many factors affected by acute myocardial ischemia, such as the volume of intra- and extra-cellular space, acidosis, effects on gap-junctions, etc. Thus, the ST-segment displacement is related to the shape and the size of the ischemic area, level of TMVG in the boundary between ischemic and normal cells, and the conductivity.

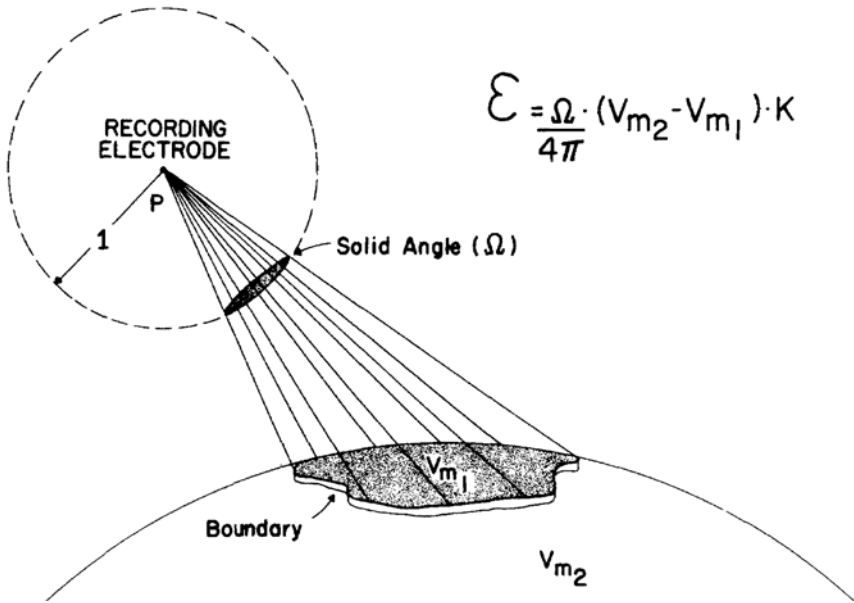


FIGURE 1.8. Mathematical and pictorial characterization of the solid angle theory. The solid angle ( $\Omega$ ) is defined as the area of spherical surface cut off a unit sphere (inscribed about the recording electrode) by a cone formed by drawing lines from the recording electrode to every point at the boundary of interest. The ischemic boundary is a source of current flow established by portions of the heart having different transmembrane voltages between the ischemic ( $V_{m1}$ ) and normal myocardial cells ( $V_{m2}$ ) during the electrical cardiac cycle (systole and diastole).  $K$  is a term correcting for differences in intracellular and extracellular conductivity. Reprinted from Holland et al.<sup>76</sup> with permission.

This theory is also applicable for understanding some of the changes within the depolarization phase (QRS complex), which will be later highlighted.

### Association between amount of ST changes and clinical outcome

Several studies have evaluated the association between MaR and final IS (as estimated by single photon emission computed tomography (SPECT) or Selvester QRS score<sup>77</sup>) with various ST-segment measures, such as single-lead maximum ST-elevation, number of leads with ST-elevation, sum of ST-elevation among leads and sum of total ST-deviation<sup>78-84</sup>, however with conflicting results.

However, in larger cohorts various ST-segment measures have been found to predict clinical outcome after AMI<sup>85-87</sup>. In a multivariate analysis from the GUSTO-I database of 41,021 patients, the sum of absolute ST-segment deviation (both elevation and depression) of  $\geq 1.9$  mm was predictive of 30-day mortality after thrombolytic therapy<sup>85</sup>, with an odds ratio of 1.53. In a DANAMI-2 substudy Sejersten et al. showed how the sum of ST-segment deviation predicted 30-day mortality after either thrombolytic or pPCI treatment<sup>86</sup>. From the GISSI-1 trial of 8,731 patients the number of leads with ST-segment elevation related both to short- and long-term mortality<sup>87</sup> after thrombolytic therapy.

Also, spontaneous ST-segment resolution (STR), before reperfusion therapy has been shown to predict optimal outcome in STEMI patients<sup>88, 89</sup>. Furthermore, it has been shown that post-revascularization STR of acute STEMI predicts lower mortality rate, with level of single lead, maximum ST elevation being the strongest predictor<sup>90, 91</sup>.

One problem with using the sum of ST changes or the number of leads with ST elevation in various scores is that the 12-lead ECG does not represent all myocardial regions equally. Thus, similar size of MaR in different parts of the heart will not be equally represented by the ECG in terms of ST-segment deviation among the 12 leads. Furthermore, attenuation and augmentation effects might arise due to ischemia in opposing regions.

To summarize:

- Transmural ischemia can be detected by ST-segment elevation criteria on the standard 12-lead ECG.
- ST-segment elevation provides information on the location of ischemia, thus helping to identify the infarction related artery (IRA).
- Overall, there seems to be somewhat conflicting results regarding the correlation between ST-segment evaluation and MaR and IS as determined by SPECT or QRS scoring. However, larger studies support the association between ST-segment measures and clinical outcome after AMI, although most results are after thrombolytic rather than pPCI treatment.

- It has not been clarified whether ST-segment evaluation provides any information about the severity of ischemia.

Myocardial ischemia and evolving infarction, however, also affects the *depolarization phase* of the ECG. Some changes in the early portion of the QRS complex (Q waves) have mostly been considered to represent already necrotic areas, but other, potentially reversible changes, especially in the later parts of the QRS complex may also appear during severe ischemia. These are not as well understood and usually not considered for clinical decision-making. This is the focus of this thesis and will be further elaborated on in the following sections.

## 1.3 Depolarization changes during ischemia

If the electrical forces during ventricular depolarization suddenly change in magnitude or direction due to regional ischemia, the overall balance of the activation wavefront will change.

Within the ischemic region several different factors may contribute to changes in the depolarization phase, which can be visualized in the QRS complex:

- Local, direct effects of the changes of the AP, such as decreased resting membrane potential, slower AP upstroke, lower amplitude and shorter duration.
- Ischemia-induced changes in the overall conductivity due to extracellular hyperkalemia, intra- and extracellular volume effects, changes in the properties of the gap junctions as well as possible changes of LV filling pressure etc.
- Substantially delayed regional activation due to severe ischemia affecting also the Purkinje cells.

Thus the overall explanation for QRS changes in the ischemic myocardium is complex and multifactorial. Some of these effects are well correlated to and secondary to the injury current and ST-segment deviation, whereas others are related more to other, secondary effects of ischemia.

The solid angle theory<sup>76</sup>, as already described and illustrated in Figure 1.8 can serve as a model to explain some of the above mentioned factors that may affect also the R-wave amplitude level observed in a certain anatomically oriented ECG lead. The higher the conductivity factor (K), the greater R-wave amplitude will be registered on the surface ECG lead. Conductivity is affected by acute myocardial ischemia by several factors, such as changes in volume of intra- and extra-cellular space, acidosis, effects on gap-junctions etc. Overall this results in an increase in the conductivity factor, thus an increase of the R-wave amplitude.

## Severe ischemia and slow conduction

Although several factors may contribute to QRS changes during acute myocardial ischemia, an important pathophysiologic distinction could be made between these and QRS changes due to *severe* ischemia with significant effect on conduction through the ischemic area. In unprotected myocardium without well-developed collaterals or metabolic preconditioning, the response to sudden coronary occlusion is severe ischemia with rapid progress of myocardial necrosis over time. The most severe ischemia is within the subendocardial layer, but can extend throughout the myocardial wall over time.

During severe ischemia, the fast-conducting under normal circumstances, and ischemia-resistant Purkinje cell network, is also affected. This significantly slows conduction of the activation wavefront locally through the ischemic region<sup>64-66</sup>. Due to delayed activation, electrical forces heading in other directions at the instant of this area's normal depolarization will be unopposed, whereas the later activation within the ischemic region causes the later QRS waveforms to deviate toward this region. The most important QRS changes due to this primary effect on delayed regional depolarization will thus appear in the terminal part of the QRS waveform and may prolong the overall QRS duration.

### 1.3.1 Standard, 12-lead ECG

Depending on the lead distribution and the location of the affected myocardial region the following can be seen on the standard 12-lead ECG:

- Augmentation of the R wave in leads with qR configuration overlying the ischemic region.
- Decrease or total loss of the S wave in leads with an rS configuration (typically anteroseptal leads) overlying the ischemic zone.
- Increase of the overall QRS duration if the ischemic area is large.

#### 1.3.1.1 QRS amplitude changes

Several experimental animal studies have reported reversible QRS-amplitude changes, such as increased R waves and decreased S waves during transient ischemia due to coronary occlusion. These QRS amplitude changes have been shown to correlate to delayed regional depolarization evaluated by simultaneous registration of the conduction velocity<sup>92-96</sup>. In humans such changes were first described by Rakita et al. in patients with Prinzmetal's angina, due to short episodes of coronary vasospasm<sup>97</sup>. They described almost instant augmentation of the R wave in leads overlying the ischemic region during Holter monitoring, followed by rapid normalization to baseline levels. Later these findings have been

confirmed in studies performed during short (most often 0.5-2 minutes) episodes of elective PCI-induced transmural ischemia<sup>98-103</sup>.

In the early setting of acute MI some studies have characterized changes mostly in the terminal QRS amplitudes as well as findings of potential reversibility of Q waves<sup>104-107</sup>.

A practical limitation to the evaluation of QRS changes during acute MI, as compared to ST-segment evaluation, is an absent “isoelectric baseline”. Due to most often gradual changes of the QRS complex an earlier ECG recording in a pain-free situation under normal conditions are thus needed to make accurate comparisons as regards the ischemia-induced QRS changes. Furthermore, significant differences of electrode position, as well as changes of body position may alter the QRS morphology.

### *1.3.1.2 The Sclarovsky-Birnbaum ischemia grading*

The Sclarovsky-Birnbaum ischemia grading (S-B grading) system grades ischemia based on characteristics of the ECG in patients with STEMI (Figure 1.9). It is a “snapshot” grading system with no comparison to baseline ECGs. It defines three grades of ischemia with increasing severity as proposed by Sclarovsky and Birnbaum in the early 1990s<sup>108, 109</sup>:

- Grade 1 (G1): Tall T waves with no ST elevation.
- Grade 2 (G2): ST elevation of  $\geq 1$  mV in  $\geq 2$  adjacent leads without distortion of the terminal portion of the QRS complex.
- Grade 3 (G3): ST elevation of  $\geq 1$  mV in  $\geq 2$  adjacent leads with terminal QRS distortion.

Terminal QRS distortion is related to the previously mentioned characteristics of more severe ischemia, thus increased R waves and diminished S waves directed towards the electrodes overlying the ischemic region. Since grade 1 is a very brief and early phase in acute MI, it is seldom seen clinically. To make the dichotomized distinction between grade 2 and 3 without a previous baseline, two different grade 3 criteria were proposed depending on the terminal QRS configuration of the ECG leads with ST elevation:

1. Complete loss of S waves in typical leads with rS configuration, such as V1-V3.
2. ST-J point to R-wave amplitude ratio of greater than 0.5 in all other leads (with qR configuration).

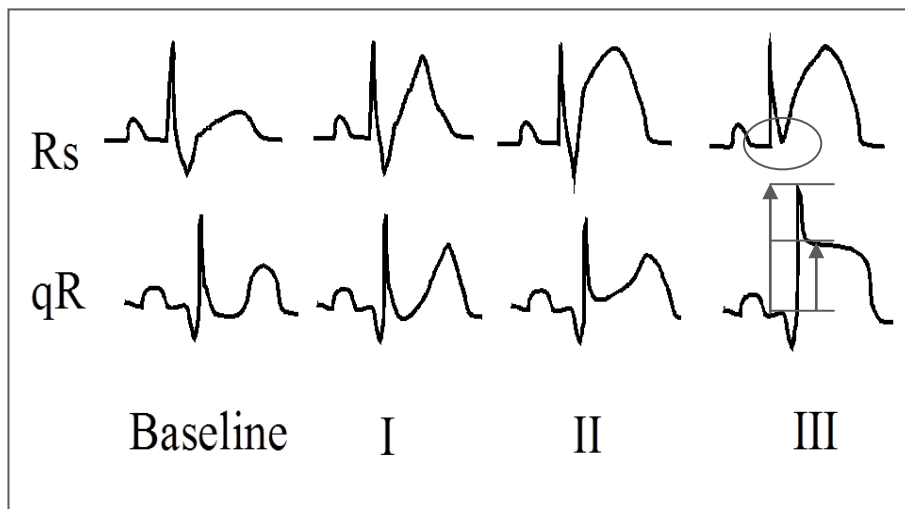


FIGURE 1.9. Criteria for the Sclarovsky-Birnbaum severity ischemia grading. The denotations I, II and III correspond to ischemia grade 1, 2 and 3, respectively. Loss of S wave in leads with Rs configuration and ST-J elevation larger than 50% of the R-wave height-Grade 3-is highlighted by circle and arrows, respectively. Adapted from Birnbaum et al.<sup>110</sup> with permission.

Prior studies have shown G3 to predict higher mortality (short, medium and long term) than G2 on admission ECG in patients treated either by thrombolysis<sup>109, 111, 112</sup> or pPCI<sup>113-115</sup>. Furthermore, G3 has been associated with larger infarct size, as estimated by cardiac biochemical marker release<sup>55-57, 115-118</sup>, Selvester QRS scoring<sup>118</sup>, SPECT<sup>56, 119-121</sup> and magnetic resonance imaging (MRI)<sup>117</sup>. Birnbaum et al.<sup>56</sup> reported significantly larger infarct size by pre-discharge SPECT in patients with G3 compared to G2, after thrombolytic therapy. The other studies evaluating ischemia grades by SPECT or MRI were after pPCI, however with small sample size<sup>117, 119-121</sup>.

Despite the numerous studies mentioned above, ischemia grading has not been routinely incorporated into clinical risk management of STEMI. Some questions still remain unanswered.

The pathophysiological mechanisms for differentiation between G2 ischemia and supposedly more severe G3 ischemia are still unclear.

Reversible QRS changes have been observed in animal experiments, in Prinzmetal's angina, during elective PCI and in the initial phase of acute MI compared to baseline (as reported above). However, it is still unclear whether the ECG characteristics in the S-B ischemia grading involving "QRS distortion" imply



that myocardial salvage is possible after reperfusion therapy administered hours after symptom onset in the STEMI situation.

One key question is whether G3 changes in STEMI reflect severely ischemic myocardium with salvage potential after reperfusion or is a sign of large, already mostly irreversible infarcted myocardium without significant salvage potential.

A consistent finding in previous ischemia grading studies has been similar time intervals from symptom onset to treatment in patients with or without “terminal QRS distortion”. Furthermore, comparable pre-treatment MaR between the grades have been seen in the limited information from SPECT or MRI<sup>117,119,120</sup> studies, with one exception, were only patients with anterior MI were included and in which also more severe ischemia by SPECT was noted for G3<sup>121</sup>. All prior studies showed patients with G3 to have a larger final infarct size as compared to patients with G2. From these results G3 has thus been assumed to be a sign of more severe ischemia in less protected myocardium, thus more prone to rapid infarct development. Further larger studies are needed with cardiac imaging data as the gold standard for MaR and IS.

In the vast majority of previous studies only the admission ECG, close in time to the subsequent reperfusion treatment, has been considered. If the hypothesis regarding severity of ischemia and rapid infarct evolution in G3 is correct, very early identification of G3 in the pre-hospital phase is necessary in order to make a difference in treatment strategy, for example. Also, the dynamic behavior of ischemia grading between the pre-hospital ECG and ECG just prior to pPCI would be of interest to explore.

Another key factor regarding the S-B ischemia grading system is that the two separate G3 criteria may represent different pathophysiological stages along the acute MI process. The G3 criterion based on the ratio between ST-J and R-wave amplitude could be due to severe ischemia with still augmented R waves and high ST-segment elevation. However as severe ischemia within the MaR gradually progresses into larger degree of necrosis, the R-wave amplitude as well as ST-segment elevation gradually decline, thus the ratio may theoretically be unchanged although the myocardium at risk has gone further into an irreversible infarction process. The loss of the S-wave criterion, on the other hand, may be a more reliable sign of severe ischemia and not an already necrotic area since an MI within the anterior region itself is not affecting the terminal part of the QRS complex by reduction or loss of the S wave<sup>77</sup>. This ischemia grading will be further elaborated on in *Study IV* of this thesis.

### *1.3.1.3 QRS prolongation*

Prolongation of the QRS complex has furthermore been described as a marker of more severe ischemia with slow conduction, both in animal and human studies during PCI and acute MI<sup>54, 98, 100, 107, 122</sup>.

In a large cohort of 17,073 STEMI patients (HERO-2-trial substudies), Wong et al. reported an independent, positive relationship between QRS duration on the admission ECG and 30-day mortality for anterior infarct location. This was observed in patients presenting with, or developing RBBB, within 60 minutes after thrombolysis<sup>123</sup>, as well as, in a second study, in patients without RBBB, but with an intraventricular conduction delay<sup>124</sup>. After adjustments for confounding clinical and electrocardiographic factors (such as ST-segment elevation level and presence of Q waves), a 30-40% relative increase in 30-day mortality risk per 20 ms QRS prolongation was shown. This was, however, found only in patients with anterior infarct location, but not in inferior location.

In the clinical situation, prolongation of the QRS duration is, however, difficult to determine correctly, since ST elevation commonly obscures the delineation between the end of depolarization and the beginning of repolarization.

### *1.3.1.4 QRS changes and myocardial infarction*

According to the sequence of ventricular depolarization described above, an evolving and later manifest MI comprised of necrotic, electrically inactive cells, will affect the wave front differently depending on the size and location of the infarcted area in relation to the exploring ECG electrode.

The balanced, smooth and homogenous ventricular vector is now affected by an inactive, electrically silent area. In contrast to the previously described ischemia/severe ischemia with injury current and delayed, regional activation, changing the vector towards the ischemic area, an infarcted region moves the vector away from the area. Thus, the electrode overlying the infarcted area will not register any signals from the necrotic area, but displays a new resultant at each time interval produced by unopposed signals from the opposite wall.

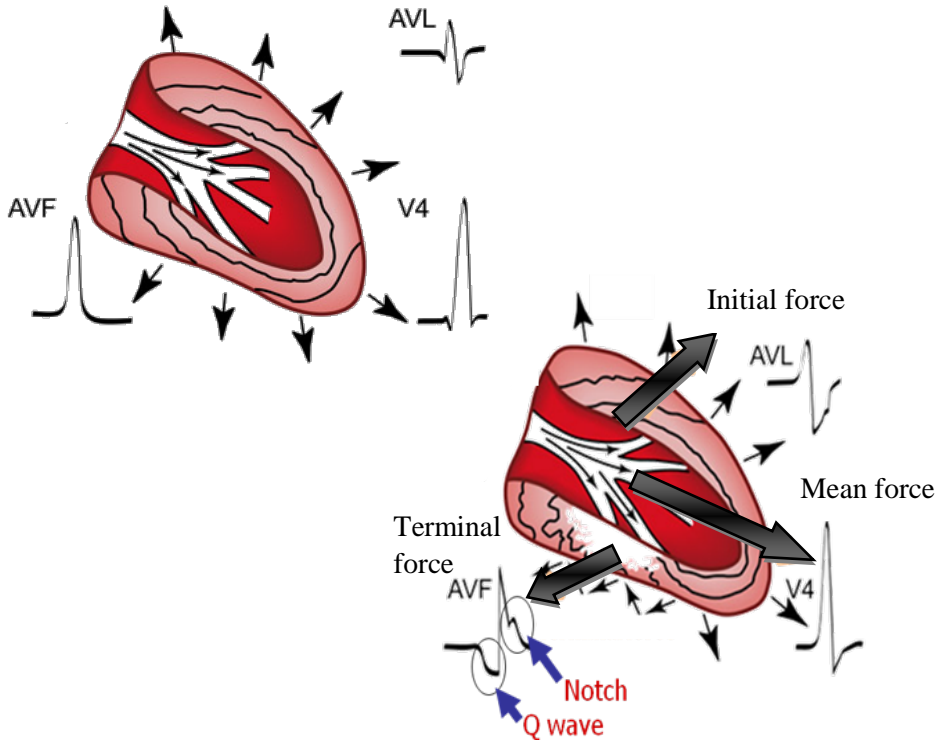


FIGURE 1.10 Rapid, balanced, synchronous conduction by the specialized ventricular conduction system (upper illustration) results in the normal symmetrical activation of both inferior and anterosuperior walls. In the lower picture, loss of inferior forces due to an inferior MI, while still normal anterosuperior forces, produce an imbalance and inferior Q waves (exemplified by lead aVF). Asynchronous, delayed activation of the subepicardial layers overlying the infarct blocks normal endo- to epicardial activation and may also produce a notched R wave in the MI region. Adjusted from Boineau<sup>125</sup>, with permission.

The changes seen in the QRS complex are related to the timing at which the necrotic area would normally be activated during depolarization.

Thus a Q wave will be the result in an early activated area, where the overlying electrode normally registers a positive initial deflection, but is now “seeing” more of a negative, opposite force in respect to its position initially in the depolarization phase. However due to the location, size and spatial relationship to the exploring electrodes, an MI can result in different changes in the QRS complex, including notches, or fragmentation of the QRS complex, R-wave changes, variations in the R-wave and S-wave ratio etc., as illustrated in Figures 1.10 and 1.11.

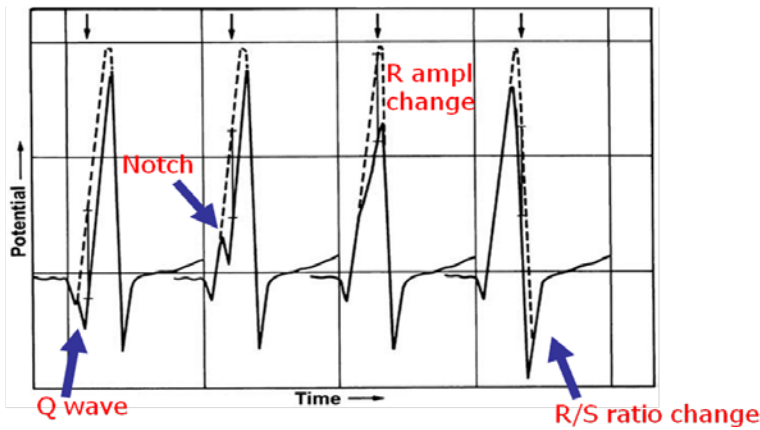


FIGURE 1.11 Simulated and observed effects of small, apical posterolateral infarcts. The four panels represent the effects of a small infarct (15x20x5 mm) placed (or found) at various levels of the apical posterolateral segment of the Selvester-Solomon fine grid (1 mm<sup>3</sup>) forward simulation of the human heart and its electrical field. Lead V6 is shown, and the dotted line in each case represents normal activation without infarct. The lesion was located in the apical endocardium in the first panel and moved outward 2 mm and more basal in each of the following panels. The arrows across the top represent the time when the activation front passed the center of the infarct in each case. It is important to note, as represented by the vertical bar between the solid line of the waveform of the infarct ECG and the normal dotted line, that in each of these waveforms, the basic finding is the lost R wave. In the first panel, the early loss of the R wave is a Q wave; in the second, it is a notched R wave, etc. The larger the posterolateral infarct, the smaller the R wave in lead V6 and the broader the Q and S waves. Adapted from Selvester<sup>126</sup> with permission.

Previously, Q waves were considered an irreversible sign of transmural infarct. However, it has been found that a Q wave that appears early during the infarct process can be a transient finding<sup>127-129</sup>, and it can also indicate a large subendocardial extent of the infarction<sup>130, 131</sup>.

### 1.3.1.5 Selvester QRS score

Based on the normal sequence of ventricular depolarization and how it is affected by local loss of electromotive force at various locations due to an MI, Selvester et al., by meticulous computer simulations<sup>132</sup>, developed a scoring system for both detecting and quantifying a previous MI by QRS analysis of the 12-lead standard ECG<sup>77</sup>. The practical application of the system was evaluated in humans in the 1980s by Wagner et al. including validation by correlation to post-mortem

findings at different infarct locations<sup>133-136</sup>. In the present 50-criteria/31-point QRS score, each point corresponds to 3% infarction of the LV myocardium. The score has been further evaluated for predicting clinical prognosis after AMI<sup>137,138</sup>, as well as correlation to infarct size determined by SPECT and MRI<sup>131,139,140</sup>.

In addition to infarct quantification, screening criteria for detection of old MIs using a subset of the criteria have been developed<sup>141</sup>. The three criteria are: 1.) Inferior MI location: in lead aVF- Q wave greater than or equal to 30 ms, 2.) Anterior MI location: In lead V2- any Q wave or R wave less than or equal to 0.1 mV and 10 ms and 3.) Posterior MI location: In lead V1- R wave greater than or equal to 40 ms. Sensitivities of 84% and 77% were found for detection of single inferior and anterior infarct locations, respectively, by using these screening criteria. The rate of false identification of MI in normal subjects was 5%<sup>141</sup>. This method was used in *Study I* and will be further described in the Methods section.

### 1.3.2 High frequency QRS analysis based on the 12-lead ECG system

#### High frequency QRS components (HF-QRS)

In the standard ECG, by convention, only frequencies in the range 0.05-150 Hz are considered. It has been found that the signal also contains high-frequency components, in particular within the depolarization phase.

Analysis of HF-QRS (frequencies >150Hz) thus offers the possibility of visualizing changes during depolarization in the ischemic myocardial tissue not seen in the standard ECG. These HF-components have very low amplitude compared to the standard ECG ( $\mu\text{V}$  compared to mV).

To extract the HF-QRS, first high resolution ECG recordings both in sampling frequency and amplitude resolution are needed. In general, a sampling rate twice the highest frequency to be evaluated is needed in order to avoid distortion of the signal. Mostly HF-QRS components within the frequency range 150-250Hz has been studied. In the HF-QRS related studies in this thesis (*Studies I* and *II*), a sampling frequency of 1000 Hz and amplitude resolution of 0.6 $\mu\text{V}$  were used.

The signal then needs to be averaged in order to reduce the noise level, thus increasing the signal-to-noise ratio. Subsequently, the signal-averaged QRS complexes are filtered in order to retrieve the specific HF-QRS components within a certain frequency band (most often 150-250 Hz). The most common way to quantify HF-QRS is by calculation of RMS values, by which the average amplitude of the HF-signal within the entire QRS complex is determined.

The pathophysiological basis of HF-QRS changes during ischemia is still not fully understood, but considered to be related to changes of the conduction velocity between the myocardial cells and/or the specialized conduction system<sup>142,143</sup>.

Earlier studies have shown a decrease of the HF-QRS during acute myocardial ischemia from coronary occlusion in animals,<sup>144-146</sup> and during short elective PCI in humans<sup>147-150</sup>. Furthermore, an increase of the HF-QRS has been observed during successful reperfusion by thrombolytic therapy of an acute myocardial infarction<sup>151,152</sup>. It has been reported that changes of HF-QRS is more sensitive than ST-segment deviation for detecting acute coronary artery occlusion<sup>149</sup>. None of these prior studies have, however, quantified the ischemia during coronary occlusion, or described the relationship between changes in HF-QRS and the extent (MaR) and severity of the ischemia as indicated by SPECT images.

Furthermore, studies of the levels of HF-QRS in the later, chronic phase after an acute MI comparing subgroups of individuals with and without prior MI have shown conflicting results. Both decrease and increase of HF-QRS after infarction have been reported in different bandwidths, in small samples and only in few ECG leads<sup>153-155</sup>.

Further understanding of how HF-QRS correlate to acute ischemia and their levels during situations with healed myocardial infarcts is needed.

HF-QRS analysis offers a unique possibility to evaluate information that perhaps could not be retrieved from a regular 12-lead ECG. However, it needs technically advanced methods and longer ECG recording for optimal signal-to-noise ratio.

### 1.3.3 QRS slope analysis based on 12-lead ECG system

Hypothesizing that changes in the myocardial conduction velocity could be estimated with less advanced methods than the high resolution, signal-averaged, filtered and noise sensitive HF-QRS method, Pueyo et al. in 2008 proposed a method for evaluation of depolarization changes by analyzing the slopes of the QRS complex: upward slope between Q and R waves (US) and downward slope between R and S waves (DS)<sup>156</sup>. During coronary artery occlusion by PCI, the QRS slopes became considerably less steep than in the control situation, in particular for the DS, as a combined result of both changes of the QRS amplitudes and duration. Furthermore, the QRS slope indices showed ischemia-induced alterations of twice the magnitude of that for HF-QRS analysis and was proposed to be a more robust method of measuring dynamic depolarization changes without requirements of signal averaging and much less noise dependent<sup>156</sup>.

To make it more robust in clinical situations, further development of this methodology is needed as well as more understanding of its clinical applicability, why we addressed these aspects to *Study III* in this thesis, as well as in *Technical Supplementary Study*<sup>157</sup> and in a pig experimental MI study<sup>158</sup>.

### *1.3.4 QRS evaluation by vectorcardiography (VCG)*

In addition to the clinically most appreciated standard 12-lead ECG system applied throughout this thesis, evaluation of QRS changes can also be performed using other lead configurations and ways to represent the magnitude and direction of the electrical activation of the myocardium, such as vectorcardiography (VCG). By this method a 3-dimensional view of the electrical activation sequence is produced by the orthogonal leads X (representing the left-right axis), Y (representing the caudal-cranial axis) and Z (representing the posterior-anterior axis). By combining pairs of these, three orthogonal planes are obtained (XY-frontal plane; XZ-transverse plane and YZ-sagittal plane). At every instant throughout the cell cycle a vector with a specific magnitude and direction is plotted in space, by which a “VCG loop” is constructed. The shape, area and direction of the rotation of the loop is then analyzed. Both animal and human studies have shown QRS changes by this method to detect acute myocardial ischemia as well correlate with MaR and IS<sup>159-162</sup>. Dellborg et al. furthermore tested its feasibility and clinical application of QRS monitoring in patients during unstable angina as well in acute MI after thrombolytic therapy<sup>163-165</sup>. It is beyond the scope of this thesis to additionally explore the VCG method. However, this approach has added further evidence to the value of including depolarization changes to the overall evaluation of the ECG in acute myocardial ischemia.

## 1.4 Myocardial Single Photon Emission Computed Tomography (SPECT)

SPECT is the most commonly used myocardial perfusion imaging (MPI) technique, by which a radioactive tracer, injected intravenously and distributed throughout the myocardium in proportion to coronary blood flow, is visualized by subsequent gamma camera analysis. The nuclear activity measured at the image acquisition reflects the myocardial perfusion at the time of injection. The technique allows estimation of myocardial blood flow both at rest and during exercise. For years it has been widely used clinically in the setting of stress test as a mean of detecting stable, stress induced IHD as well as estimating the size and location of the ischemia.

It can also be used in the acute setting of IHD as an adjunctive tool to differentiate unstable angina and NSTEMI from non-cardiac symptoms<sup>166</sup>.

### 1.4.1 Radioactive tracers: Tc-99m Sestamibi

Imaging of coronary perfusion is dependent on the physical properties of the radioactive tracer by its delivery to the heart as well as the uptake and retention by the myocardial cells. The optimal tracer has the following characteristics:

- High first-pass uptake by the myocardium.
- Linear relationship between uptake and perfusion.
- An uptake independent of metabolic status of the cell.
- Stable retention within the cells throughout the completed imaging procedure.

Technetium-99m labeled tracers preferably used today were developed in the late 1980s<sup>167</sup> as to better meet the favorable characteristics above as compared to previous agents. In addition technetium-99m has both higher photon energy and a shorter half-life, resulting in improved image resolution. Studies included in this thesis utilized the Tc99m-labeled compound <sup>99m</sup>Tc-sestamibi (Cardiolite<sup>TM</sup>).

Sestamibi is a lipophilic monovalent cation (thus positively charged). This characteristic enables it to passively cross the myocardial cell membrane into the plasma and be accumulated in the mitochondria by the negative membrane potential<sup>168</sup>. Unlike previous agents (Thallium), this agent does not need help from the Na<sup>+</sup>-K<sup>+</sup>-ATPase pump in order to cross the cell membrane<sup>169</sup>. The myocardial distribution is proportional to the blood flow up to 2-3 times the resting flow levels. However, animal models have indicated a higher cell uptake relative to the blood flow at very low levels of perfusion, thus slightly underestimating the perfusion defect<sup>170</sup>.



Sestamibi is stable within the myocardial cells undergoing only minimal redistribution. A clearance of less than 15% during a four hour period has been reported<sup>170</sup>. This makes it suitable for situations where the time interval from intravenous administration to acquisition of the tomographic imaging by the gamma camera is prolonged.

### 1.4.2 Tomographic imaging acquisition

Subsequent to administration of the radionuclide agent the images are acquired by a gamma camera. Basically, when the gamma radiation emitted by the tracer hits the camera the photon energy (when interacting with a sodium iodine crystal) produces a scintillation effect, or flash of light. This is registered by photomultiplier tubes, then amplified, and the energy and spatial location of the photon are recorded. A lead collimator is positioned in the front of the detector of the camera, so only photons that hit the detector at a 90 degree angle are registered. Usually two detectors are used, set at 90 degree angles to each other. The detectors rotate around the patient and acquire at least 30 projections over a 180-degree arc. The set of planar images is subsequently reconstructed and processed by filtered back projection, iterative reconstruction and low-pass filtering to compensate for various degrees of technical artifacts, attenuation of signals, as well as to enhance the image resolution and reduce noise.

This results in a large set of transaxial images perpendicular to the long axis of the patient's body. These images are then oriented correctly according to the heart, as to present vertical- and horizontal long-axis planes, as well as short-axis plane. From the short-axis slices polar plots, or bull's eye images, can be constructed, which cover all left ventricular myocardium.

These images can be either manually or automatically analyzed with regard to the location, extent (MaR) and severity of the myocardial perfusion defects (see specific methods section for *Studies II-IV*).

Perfusion myocardial scintigraphy by <sup>99m</sup>Tc-sestamibi has proved to be a reliable method of detecting and quantifying MaR as well as final IS and salvage after reperfusion therapy in studies with acute myocardial infarction<sup>171-176</sup>. It has also been used for assessment of MaR and severity in studies of reversible ischemia induced by elective PCI<sup>177,178</sup>. Christian et al. have shown the association between <sup>99m</sup>Tc-sestamibi SPECT estimation of severity and collateral flow in animals as well as in acute MI in humans<sup>172,179</sup>.

## 2 Aims of the thesis

The overall objectives of this thesis were to increase the understanding of depolarization changes during myocardial ischemia and to evaluate whether these changes have possible clinical implications in patients with acute myocardial ischemia. Based on the 12-lead ECG, different methods for evaluation of depolarization were applied in ischemic situations produced by controlled, prolonged PCI on humans and in clinical STEMI situations. Comparisons were made with conventional ECG parameters as well as non-electrocardiographic quantitative measures such as SPECT.

The specific aims for each study were:

### *Study I*

To compare HF-QRS in patients with and without standard ECG changes indicative of a previous MI.

### *Study II*

To test the ability of HF-QRS changes versus conventional ST-segment measurements to detect and quantify the extent and severity of myocardial ischemia, produced by acute coronary occlusion.

### *Study III*

To investigate whether the potentially more readily available (compared with HF-QRS), QRS-slopes are associated with the extent and severity of myocardial ischemia produced by temporary occlusion of a coronary artery, and test their performance against conventional ECG measures.

### *Study IV*

To study whether the Sclarovsky-Birnbaum ischemia grade on the pre-hospital ECG and its changes during transport to a PCI lab are associated with infarct size and myocardial salvage after pPCI.



## 3 Materials and methods

### 3.1 Study populations

Patients from three populations were studied. The *STAFF III* protocol was designed in order to study ECG changes during total coronary occlusion by prolonged balloon PCI as a model for the first 5 minutes of an acute MI. Quantification of ischemia was by SPECT imaging. The *STRESS* protocol was designed to evaluate ECG changes during ischemia evoked by a bicycle stress test and quantified by SPECT. However, only control ECG recordings before the stress test were used in this thesis. ST-monitoring in AMI patients (*MONAMI*) database includes three randomized trial populations of STEMI patients assigned by the pre-hospital ECG to receive pPCI<sup>180-182</sup>. Acute (before pPCI) and 30-day SPECT imaging studies were performed to estimate MaR and IS.

#### 3.1.1 “*STAFF III*” population

This is a dataset collected by me in Charleston, WV, USA during 1995-96. It comprises a total of 102 consecutive patients referred for elective balloon PCI with prolonged occlusion (5 minutes; before the stent era) due to stable, stress induced angina pectoris. In each patient acquisition of continuous, high resolution 12-lead ECGs were performed. The first, as a control for 5 minutes before the procedure, then during the entire PCI as well as another control, for 5 minutes at rest, after the procedure. In a subset of patients (n=40) additional acquisition of SPECT images during the procedure (tracer injection during occlusion) as well as a second, control SPECT imaging with a new tracer injection and imaging procedure the day after the procedure were performed, in order to quantify the amount of ischemia during balloon occlusion. All patients were clinically stable between the two SPECT studies.

In *Studies II* and *III*, only patients from the *STAFF III* population with a complete set of scintigraphic images (during PCI and the day after the procedure) were eligible. Comparisons between pre-procedural control, and dynamic occlusion ECGs were performed and correlated to SPECT data.

In *Study II*, a subset of 21 patients was included. Since it is essential to have as noise-free data as possible while studying the low-amplitude HF-QRS signals, very strict criteria were applied regarding noise level in the ECG signal for each of the 12 leads. In *Study III*, 38 patients were included.

### 3.1.2 “STRESS” population

This data was collected at the Department of Clinical Physiology in Lund 1995-97. A total of 117 consecutive patients undergoing elective bicycle stress tests with myocardial SPECT due to suspect, stable angina pectoris were enrolled. Continuous 5-minutes, 12-lead, high resolution ECG at rest before and after the stress test were acquired, as well as a “stress recording” immediately after finishing the stress test.

None of the patients in the *STAFF III* or *STRESS* populations had any clinical or ECG evidence of an acute or recent MI.

In *Study I*, control recordings in patients from both *STAFF III* and *STRESS* were considered. A total of 154 patients were included in the study. Patients with confounding factors in their ECG or inadequate ECG signal quality were excluded.

### 3.1.3 “MONAMI” population

This is a database of 892 STEMI patients referred for pPCI to Skejby University Hospital, Aarhus, Denmark between 2004 and 2008<sup>180-182</sup>. An index, pre-hospital or local hospital, 12-lead ECG, as well as a pre-PCI ECG at the cath lab were recorded on each patient. Furthermore, continuous 12-lead ECG recordings during the pre-hospital phase up to 90 minutes post-pPCI were acquired. Multiple clinical parameters including basic characteristics, angiographic variables and cardiac biochemical marker (TnT) analyses were collected. In a subset of patients, acute SPECT imaging (tracer injection in the cath lab before pPCI) was performed to determine the MaR, and 30-day SPECT imaging was performed to estimate final IS.

In *Study IV*, a subpopulation of 401 patients with a first acute MI, no prior CABG, complete index and pre-PCI, 12-lead ECGs with good signal quality as well as 30-day SPECT imaging for estimation of final IS were included. Further exclusion criteria were QRS duration > 120 ms, LBBB or RBBB on index ECG, ventricular or ventricular paced rhythm, LVH in either of the two ECGs and inverted T waves in leads with maximal ST elevation on the index ECG.

## 3.2 Ethical considerations

The design and protocols for the “*STAFF III*” and “*STRESS*” studies were approved by the local ethics committee in Charleston, West Virginia, USA and at Lund University, Lund, Sweden, respectively. Patients in the “*MONAMI* database” where included in three separate clinical trials<sup>180-182</sup>, for which each protocol and design was approved by the ethics committee at Skejby University, Aarhus,

Denmark. Prior to enrolment all patients gave their written informed consent for participation in the studies.

## 3.3 ECG analysis and processing

### 3.3.1 ECG acquisition

#### Studies I, II and III

ECGs in both the “*STAFF III*” and “*STRESS*” populations were recorded using equipment provided by Siemens-Elema AB (Solna, Sweden). For the limb leads, Mason-Likar electrode configuration was used to minimize noise levels<sup>183</sup>. The precordial leads were obtained using the standard electrode placements. The signals were digitized at a sampling rate of 1000 Hz, with an amplitude resolution of 0.6  $\mu$ V.

The control recordings (*Study I*) were acquired continuously for 5 minutes while the patient rested in the supine position, before exercise testing (“*STRESS*” patients) or in the cath lab, before any catheter insertion (“*STAFF III*” patients). None of the patients had clinical evidence of acute myocardial ischemia during the ECG recording.

In the “*STAFF III*” patients, a second ECG recording was initiated approximately 1 minute before balloon inflation and then continued until approximately 4 minutes after the balloon was deflated. The coronary occlusion period was extracted for further signal processing (*Study II* and *III*). To enable accurate comparison of ECG variables between recordings, electrodes were either retained on the patient or removed, and their exact positions marked. If more than one balloon occlusion was performed during the procedure, only the first was considered, to avoid possible bias due to either persistent ischemia in the myocardium or ischemia-induced collateral recruitment and preconditioning within the area of a previous occlusion.

#### Study IV

The index ECGs denoted as “pre-hospital ECGs” were acquired in the ambulance, or at a local hospital, before transfer to the PCI-center. A Lifepak-12 emergency care monitor (Medtronic Emergency Response Systems, Redmond, WA, USA) with Mason-Likar electrode placement<sup>183</sup> was used for 12-lead ECG pre-hospital acquisition as well as for continuous ST-segment monitoring. On arrival at the cath lab, patients had radiolucent carbon fiber lead wire electrodes mounted (Ambu Blue Sensor QR electrodes, Ambu A/S, Ballerup, Denmark) enabling both recording of the pre-PCI ECG and also ST monitoring during and after the PCI

procedure. The same monitor defibrillator (LIFEPAK 12) was used during and after pPCI. The analog ECG signals were digitized at a sampling rate of 500 Hz for processing by the GE/Marquette Medical Systems 12SL (Waukesha, WI, USA). Every 30 second, the built-in ST monitoring software automatically generated a median QRST complex for each of the 12 leads based on a 10-second interval of ECG data. From each of these median QRST complexes, the level of ST deviation at STM ( $J + \frac{1}{16}$  of the average R-R interval), was stored. In the event of at least 0.1 mV change in STM for at least 2.5 minutes, the software automatically stored a complete 12-lead ECG waveform. ST monitoring was terminated 90 minutes after pPCI. All 12-lead ECGs and continuous ST-monitoring data were transferred to a personal computer and stored for subsequent analysis.

### 3.3.2 *Standard 12-lead ECG analysis*

#### Study II

All ST-segment analyses in *Study II* were performed automatically with software developed by the Signal Processing Group, Department of Applied Electronics, Lund University, Sweden and additionally, manually checked by visual inspection of ECG print-outs. To make the comparison between standard ST-segment deviation and the HF-QRS, these two measurements were made at the same instant during both the control and at the end of the dynamic PCI recordings. The ST-segment measurements were made in each lead at the ST-J point + 60 ms, using the PR interval as the isoelectric level. The rationale for choosing ST-J point +60 ms was to avoid possible incorrect measurement of the ST segment, which is more likely at the J point because of the higher risk for its misdelineation. Maximal, single-lead ST elevation ( $\Delta$ ST elevation between PCI recording and control) was determined for each patient, as well as the calculation of the sum of  $\Delta$ ST deviation (both elevation and depression) among all 12 leads.

STEMI criteria from the 2000 ESC/ACC consensus document<sup>184</sup> were used as an indication of coronary occlusion in this PCI model (except from using ST-J+60 ms instead of ST-J): Absolute ST elevation in 2 or more contiguous leads with cut points of 0.2 mV or higher in leads V1, V2, or V3, and 0.1 mV in other leads (contiguity in the frontal plane is defined by the lead sequence aVL, I, -aVR, II, aVF, and III).

#### Study III

##### **ST-segment analysis**

ST-segment measurements were made automatically with software developed by the Communications Technology Group of Aragón Institute for Engineering

Research (I3A), University of Zaragoza and CIBER-BBN, Spain (including additional manual check of ECG print-outs), in each lead at the ST-J point, using the PR interval as the isoelectric level. Absolute ST-deviation  $\Delta ST_{PCI}$  at the end of the PCI recording relative to the ST level at rest was determined for each lead. In addition, maximal, single-lead ST elevation as well as the sum of ST elevation among all leads at the end of the PCI recording were determined for each patient.

### **Standard QRS analysis**

*R- and S-wave amplitudes* were automatically measured (by the Zaragoza, Spain software) using the PR interval as the isoelectric level. Deltas of R- and S-wave amplitudes were determined in each lead at the end of the PCI recording as compared to baseline.

The *QRS duration* was determined by taking a global measurement from the standard 12 leads. In each beat, the earliest QRS onset and the latest QRS offset among the 12 leads were selected as the beginning and end, respectively, of the depolarization phase taken as the longest temporal projection for the electrical activity of the depolarization. In addition, a multi-lead detection rule<sup>185</sup> was applied to reduce the risk of erroneous estimation, for example, due to large simultaneous ST segment deviation or noise, as explained in detail in *Study III*.

### **Study IV**

For inclusion in *Study IV* current STEMI criteria<sup>15</sup> had to be met by the index, pre-hospital ECG: ST elevation at the J-point in  $\geq 2$  contiguous leads of  $\geq 0.1$  mV in all leads other than V2 and V3, where cut points are  $\geq 0.2$  mV for men and  $\geq 0.15$  mV for women. These limits were manually checked.

The commercially available CodeStat Suite software (Medtronic Emergency Response System Inc, Redmond, WA, USA) was used for analysis of continuous ST monitoring data and 12-lead ECGs. Maximal ST elevation in any lead in the pre-hospital and pre-PCI ECGs were defined. Maximal cumulated ST elevation was determined by summation of the maximal pre-PCI ST elevation in each lead representing anterior ischemia (requiring  $\geq 0.2$  mV in leads V1-V3, and  $\geq 0.1$  mV in leads I, aVL, V4-V6) and in each lead representing non-anterior ischemia ( $\geq 0.1$  mV required in II, III, aVF, V5-V6), respectively. In patients with non-anterior ischemia who also had lateral (formerly labeled “posterior”) ischemia, ST depression in leads V1-V4 of  $\geq 0.1$  mV were added to the maximal cumulated ST elevation. Spontaneous ST resolution from pre-hospital to the pre-PCI ECG was defined as: ST resolution to  $< 0.1$  mV in leads I, II, III, aVL, aVF, V4-V6 and  $< 0.2$  mV in V1-V3.

Post-procedural ST resolution (STR) was determined in the lead with the maximum pre-interventional ST elevation. Relative ST resolution by at least 70% within 90 minutes after the first PCI was determined, as well as the time to reach



this threshold. Furthermore, absolute single-lead ST elevation was determined at 30 minutes after first PCI.

Presence of Q waves were determined in pre-hospital and pre-PCI ECGs, respectively. The Q wave definition applied was the criteria from “The third universal definition of AMI” document in 2012<sup>15</sup>, as described in detail in *Study IV*.

### **3.3.2.1 Selvester QRS scoring (Study I)**

In *Study I*, the Selvester QRS scoring system<sup>77</sup> was used to determine the presence, location and size of previous MIs as indicated by the standard 12-lead ECG. The scoring system is displayed in Figure 3.1.

Scoring was performed by two independent investigators (M.R. and G.W.) blinded to other data. Any differences were identified and adjudicated.

To be considered as indicating a previous MI, the ECG had to either:

1. Meet the Anderson screening criteria set from the complete Selvester QRS scoring system<sup>141</sup> for one or more MI locations:
  - a. Inferior location: In lead aVF- Q wave  $\geq 30$  ms.
  - b. Anterior location: In lead V2- Any Q wave, or R wave  $\leq 0.1$  mV and  $\leq 10$  ms.
  - c. Posterior location: In lead V1- R wave  $\geq 40$  ms.
- or,*
2. Achieve  $\geq 4$  points from non-screening criteria, with  $\geq 2$  of these points awarded in other leads than V4-V6<sup>186</sup>.

The location of the MI was indicated by the presence of either a screening criterion, or at least 2 points from non-screening criteria. Patients meeting criteria for both inferior and posterior location were regarded as inferior. The size of the MI was determined according to the Selvester QRS scoring system as illustrated in Figure 3.1. “No MI” was defined as neither any of the Anderson screening criteria in any available cycles, nor  $>2$  points from non-screening criteria.

FIGURE 3.1 The 50-criteria, 31 point Selvester QRS scoring system. Criteria for each lead are shown. If 2 or more criteria are met within the same box, only the one presenting the highest point is considered. Below each lead maximum lead score is shown within parenthesis. Each point corresponds to 3% of the LV myocardium. In gray circles Anderson screening criteria are marked, whereas arrows depict the respective MI location.

Lead	Criteria	Pts.
I	$Q \geq 30$ ms	1
[2]	$R/Q \leq 1$	1
	$R \leq 0.2$ mV	1
II	$Q \geq 40$ ms	2
[2]	$Q \geq 30$ ms	1
aVL	$Q \geq 30$ ms	1
[2]	$R/Q \leq 1$	1
aVF	$Q \geq 50$ ms	3
[5]	$Q \geq 40$ ms	2
	$Q \geq 30$ ms	1
	$R/Q \leq 1$	2
	$R/Q \leq 2$	1
V1(ant)	Any Q	1
[1]		
(post)	$R/S \geq 1$	1
[4]	$R \geq 50$ ms	2
	$R \geq 1.0$ mV	2
	$R \geq 40$ ms	1
	$R \geq 0.6$ mV	1
	$Q$ and $S \leq 0.3$ mV	1
V2(ant)	Any Q	1
[1]	$R \leq 0.1$ mV	1
	$R \leq 10$ ms	1
	$R \leq 0.1$ mV	1
(post)	$R/S \geq 1.5$	1
[4]	$R \geq 60$ ms	2
	$R \geq 2.0$ mV	2
	$R \geq 50$ ms	1
	$R \geq 1.5$ mV	1
	$Q$ and $S \leq 0.4$ mV	1
V3	Any Q	1
[1]	$R \leq 20$ ms	1
	$R \leq 0.2$ mV	1
V4	$Q \geq 20$ ms	1
[3]	$R/Q \leq 0.5$	2
	$R/S \leq 0.5$	2
	$R/Q \leq 1$	1
	$R/S \leq 1$	1
	$R \leq 0.7$ mV	1
V5	$Q \geq 30$ ms	1
[3]	$R/Q \leq 1$	2
	$R/S \leq 1$	2
	$R/Q \leq 2$	1
	$R/S \leq 2$	1
	$R \leq 0.7$ mV	1
V6	$Q \geq 30$ ms	1
[3]	$R/Q \leq 1$	2
	$R/S \leq 1$	2
	$R/Q \leq 3$	1
	$R/S \leq 3$	1
	$R \leq 0.6$ mV	1
Total score:		

Inferior location

Posterior location

Anterior location

### 3.3.2.2 Sclarovsky-Birnbaum ischemia grading (Study IV)

In *Study IV*, the pre-hospital and pre-PCI ECGs from each patient were separately evaluated by two experienced cardiologists (M.R. and Y.B.) blinded to all clinical patient data. Any disagreement was resolved in a second round by consensus.

Grade 3 was defined as  $\geq 2$  adjacent leads with ST elevation and either:

1. Complete loss of S waves in leads V1 to V3 (typical leads with baseline rS configuration), *or*
2. ST-J point to R-wave amplitude ratio of greater than 0.5 in other leads with baseline qR configuration.

Only ECG leads meeting the STEMI threshold<sup>187</sup> accompanied by positive T waves in leads with the largest ST-elevation were considered in the grading. Patients who met the STEMI criteria<sup>187</sup> but not the above grade 3 criteria were classified as grade 2. Patients were furthermore divided into five subgroups according to pattern of temporal behavior of the ischemia grade between the pre-hospital and pre-PCI ECGs as described in detail in *Study IV*.

### 3.3.3 QRS slope analysis (Study III)

In *Study III*, analysis of QRS slopes was performed. This method was first described by Pueyo et al. in 2008<sup>156</sup>, and further developed by our group, as described in detail in *Supplementary Technical Study*<sup>157</sup>.

#### Preprocessing

Prior to further analysis the ECG signals were preprocessed by:

- QRS detection.
- Normal beat selection.
- Baseline drift attenuation via cubic spline interpolation.
- Wave delineation using a wavelet-based technique, as previously described<sup>156, 157</sup>.

To reduce and compensate for low-frequency noise such as respiration modulations of the depolarization phase, a normalization procedure was applied to all the ECG signals before evaluation of the indices<sup>157</sup>.

#### QRS slope analysis

Three QRS slopes were determined in each beat, as shown in Figure 3.2:

1. US: the upward slope of the R wave.
2. DS: the downward slope of the R wave.

3. TS: the upward, terminal slope of the S wave (only in leads V1-V3).

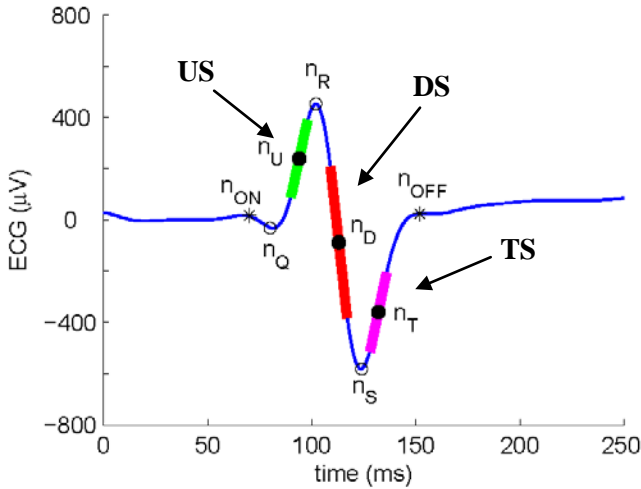


FIGURE 3.2 Beat example showing the delineation marks used to evaluate the QRS slopes.  $n_{ON}$  indicates QRS onset.  $n_{Q,R,S}$  indicate time locations for the peaks of these waves, whereas  $n_U$ ,  $n_D$ , and  $n_T$  represent maximum derivatives of the slopes. Final US, DS and TS are shown by arrows.

The successive steps of slope analysis are as follows:

1. Time locations for Q-, R-, and S-wave peaks are determined by delineation and denoted by  $n_Q$ ,  $n_R$ , and  $n_S$ . Beats for which no R-wave peak was present were rejected from the analysis. A Q- and S-wave peak were identified as corresponding to the lowest signal amplitude in the time window of 2 ms after QRS onset to 2 ms before the R-wave peak, and 2 ms after R-wave peak to 2 ms before the QRS offset, respectively.
2. Time instants for the maximum absolute derivative of the slopes between the Q- and R-wave peaks and between the R- and S-wave peaks,  $n_U$  and  $n_D$ , respectively, are determined.
3. A line is fitted in the least squares sense to the ECG signal, in a window of 8 ms centered around the time of each of the maximum absolute derivatives  $n_U$  and  $n_D$ , so as to generate a slope for that particular part of the QRS complex.

In leads V1 to V3 with a typical S-wave peak below baseline, a third slope (TS-slope) was measured by fitting a line to the ECG signal in a window centered around the maximal derivative  $nT$  of the ECG between the S-wave peak  $nS$  and the end of the QRS complex  $n_{OFF}$ .

If the S wave disappeared during ischemia evolution in the involved leads (V1-V3), the TS slope measurement was not evaluated for successive beats after that time instant.

One example of the evolution of the US, DS, and TS changes is shown in Figure 3.3, as well as representative beats at the beginning and end of the PCI procedure, respectively.

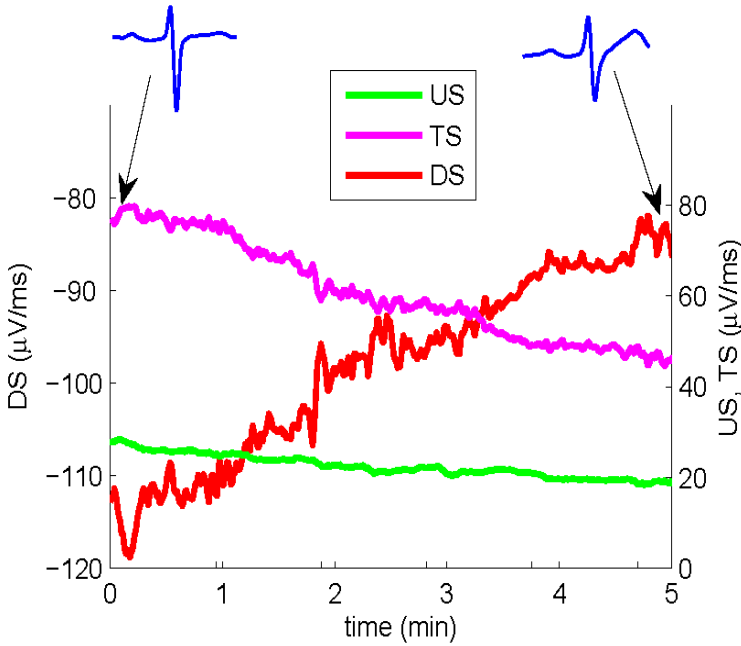


FIGURE 3.3 Temporal evolution of the US, DS, and TS for a particular ECG recording during the PCI procedure. Initial and final beats of the recording are additionally plotted to show how they link to the corresponding slope measurements

### Calculation of the QRS slope changes during PCI

The slope changes were computed for each of the 12 leads, at the end of the PCI procedure in the following manner, as illustrated in Figure 3.4:

1. The dynamic QRS slope measures for all beats from the onset of occlusion until the end were blockwise averaged in subsets of 8 beats.
2. Then, a line was fitted over these averaged values in a least square sense.

3. Subsequently, the change was defined as the product of the slope  $\ell$  of the resulting fitted line and the total duration of the PCI process<sup>156</sup>. This fitting strategy was used to reduce the effect of possible outlier measurements on the slope changes.

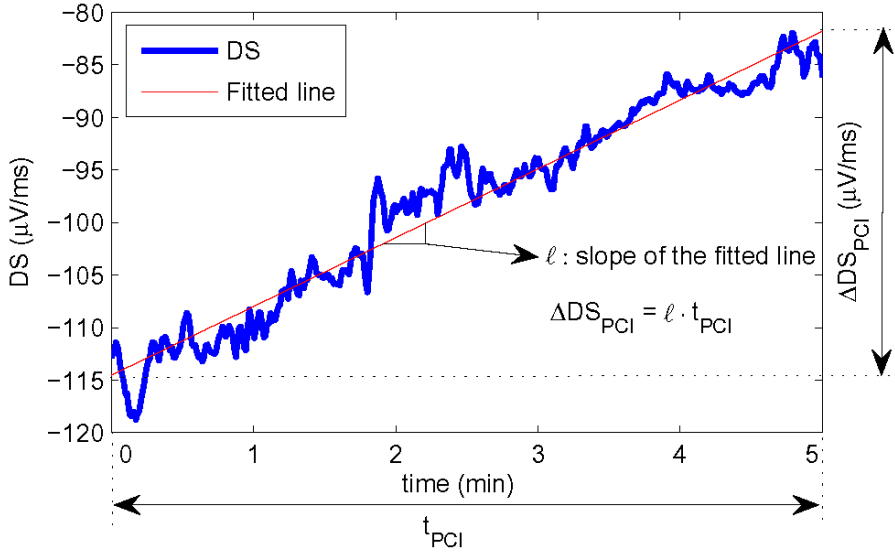


FIGURE 3.4 Representation of the strategy by which a line is fitted to the averaged DS values during the PCI procedure in a least square sense to reduce the effect of possible outlier measurements on the DS change computation.

Among all 12 leads, maximal positive delta of the DS deflection (positive change: DS slope getting less steep) and maximal negative change of the US deflection (negative change: US slope getting less steep) were determined for each patient. The sum of all positive deltas of the DS deflection and negative deltas of the US deflection, respectively among the 12 leads were calculated to quantify the changes.

### 3.3.4 High-Frequency QRS (HF-QRS) analysis (Studies I, II)

In *Studies I* and *II*, the HF-QRS methodology was applied for evaluation of depolarization changes due to chronic MI and acute ischemia, respectively. In contrast to the QRS slope analysis, HF-QRS evaluation is based on very low amplitude (in  $\mu\text{V}$ ) evaluation. Since much noise in the ECG signal lies within this high-frequency interval, it is of the outmost importance to achieve as high a signal-to-noise ratio as possible, thus exclude the noise and keep the HF-QRS

components subjected to analysis. Several steps are needed to accomplish this: a) ECG acquisition with proximal lead placement (Mason-Likar), so as to reduce noise from skeletal muscle; b) longer ECG recordings than usual to perform adequate signal-averaging; c) proper signal processing techniques, including preprocessing, noise reduction and filtering procedures. The high-resolution recordings were processed off-line using software for ECG analysis developed by the Signal Processing Group, Department of Applied Electronics, Lund University, Sweden.

### 3.3.4.1 Preprocessing

To avoid smearing of the signal during the averaging process each QRS complex needs to be as perfectly aligned as possible, to average the same point in the cardiac cycle, beat by beat. In addition, only normal beats should be selected, thus excluding beats with other morphologies.

This is achieved by template cross-correlation<sup>149, 188, 189</sup>. The template represents the predominant QRS morphology and is continuously adjusted by averaging 10 incoming beats at the time, where only beats that match the template morphologically well throughout the recording are included. The correlation coefficient was set to 0.97, which is the level used in previous studies<sup>149, 189, 190</sup>. Every incoming beat that did not match the template was discarded. Thus only beats with a cross-correlation coefficient higher than 0.97 were accepted for averaging.

### 3.3.4.2 Signal averaging-noise reduction

For the control recording (*Studies I and II*), conventional blockwise averaging was applied<sup>149</sup>. Trend samples of the signal-averaged ECG were obtained every 2 seconds.

The PCI recording (*Study II*) was expected to be subject to considerably larger dynamic changes compared to the control ECG, and therefore a different averaging technique had to be applied. For this reason, an exponentially updated beat average was used<sup>149, 188</sup>, which makes it possible to track the morphologic changes while still providing sufficient noise reduction. For both recordings, the noise level was calculated in each lead and expressed as a root-mean-square (RMS) value in an interval of 100 milliseconds, starting 100 milliseconds after the QRS offset. To avoid any bias in the HF-QRS analysis due to noise, only very low noise levels were accepted for each lead after signal averaging. Only patients with a noise level less than or equal to 0.75  $\mu\text{V}$  for each of the 12 individual leads were included in *Study II*. Furthermore, when comparing HF-QRS between the control and PCI recordings, only beats with similar noise level (within 0.35  $\mu\text{V}$ ) were

manually selected to avoid potential bias due to different noise levels. These cut-off levels have been applied previously<sup>149</sup>.

### 3.3.4.3 Band-pass filtering

The 12-lead signal averaged ECGs in the recordings were analyzed using a Butterworth filter at the frequency interval of 150 to 250 Hz (in *Study I* additional, separate filtering at the frequency interval 80 to 300 Hz was performed). Filtering was done in a forward/backward fashion<sup>191</sup>. This approach was used to provide sharper edges of the bandpass filter and to ensure linear phase of the filtering process and thus minimal distortion. An example of a signal-averaged ECG before and after filtering is illustrated in Figure 3.5. The QRS onset and offset were automatically determined from the signal averaged ECG in the standard frequency range before the filtering process<sup>145</sup>.

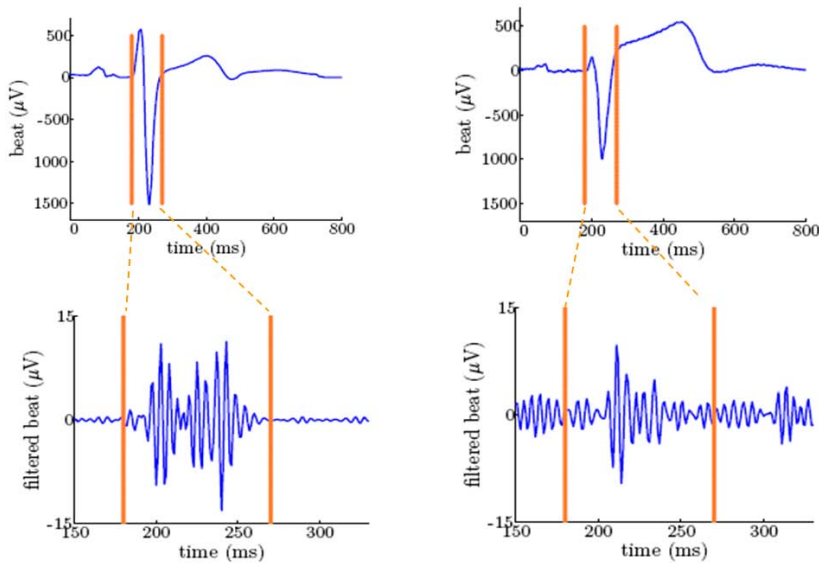


FIGURE 3.5 Signal-averaged ECGs at control (left panels) and during PCI (right panels) in the standard range (upper panel) and in the high-frequency range (lower panel). Vertical lines indicate the QRS duration as determined in the standard frequency range.

### 3.3.4.4 HF-QRS quantification

The HF-QRS in each of the 12 leads were expressed as RMS values in microvolts (Figure 3.6), which is the most common means of quantifying the high-frequency content within the QRS complex.



$$RMS = \sqrt{\frac{\sum_{i=1}^n (A_i)^2}{n}}$$

FIGURE 3.6 The RMS formula, where n is the number of measurements and  $A_i$ ,  $i=1, \dots, n$ , are the measured amplitudes within the entire QRS complex.

The difference in RMS values (in microvolts) between the control and the end of the PCI recording was calculated in each lead. To be considered as significant, either an absolute decrease in RMS value of more than 0.6  $\mu$ V or a relative decrease of more than 20% in any lead had to be met, which have been the criteria used in previous studies<sup>149, 151</sup>. The maximal HF-QRS reduction in any lead was determined for each patient both as an absolute (in microvolts) and as a relative value ( $\Delta$ RMS/baseline RMSx100). The sum of significant HF-QRS reduction among the 12 leads was calculated for each patient both as an absolute (in microvolts) and relative value (summed significant  $\Delta$ RMS/ summed baseline RMSx100).

## 3.4 Myocardial SPECT perfusion imaging

In *Studies II, III* and *IV*, SPECT imaging was used as the gold standard for myocardial ischemia and/or final infarct size (IS) and salvage. The  $^{99m}\text{Tc}$ -sestamibi tracer was used in all studies. Two protocols were used. An important distinction between them was the methodology regarding quantification of the perfusion defects. In *Studies II* and *III* totally reversible ischemia was studied and the patient was his/her own reference. The control image the day after the procedure was compared with the occlusion image during elective PCI<sup>178</sup>. In *Study IV*, on the other hand, a commercial analysis program was applied (see below), by means of which the images were compared to a large reference database<sup>182,192</sup>.

### 3.4.1 *Studies II and III*

#### 3.4.1.1 Acquisition

##### Occlusion study

As soon as coronary occlusion was confirmed by coronary angiography, approximately 30 mCi (1100 MBq) of  $^{99m}\text{Tc}$ -sestamibi was injected intravenously

in each patient. The scintigraphic SPECT images were obtained within 3 hours after completion of the PCI.

A single-head rotating gamma camera (Elscent, Haifa, Israel) was used. Acquisitions were made with a high-resolution collimator in a  $64 \times 64$  matrix, 6.9 mm pixel size, using 30 projections (25 seconds per projection) over  $180^\circ$  (from  $45^\circ$  right anterior oblique to  $45^\circ$  left posterior oblique). With the use of filtered back projection with a Butterworth filter, transverse sections were reconstructed, without attenuation correction. Short-axis sections were reconstructed for further analysis<sup>178</sup>.

### Control study

For the control study, another injection of 30 mCi (1100 MBq)  $^{99m}\text{Tc}$ -sestamibi was administered approximately 24 hours after the PCI and the images were obtained 2 to 3 hours later with the same gamma camera and acquisition protocol as for the PCI study. All patients were clinically stable between the 2 examinations.

#### 3.4.1.2 Image analysis

The Cedars-Sinai and Emory quantitative analysis program (CEqual, ADAC Laboratories, Milpitas, CA, USA)<sup>193</sup> was used for making volume-weighted bull's eye plots from the short-axis sections. Any loss of perfusion during the occlusion study compared to the control study was determined by an automatic procedure by comparing the bull's eye plot of the 2 studies for each patient<sup>178</sup>. The control image was used as a valuable means of obtaining information on preexisting perfusion defects and of quantifying the amount of balloon-induced changes. Two measures of myocardial ischemia were determined: extent and severity.

#### Extent of myocardial ischemia

Reduction of perfusion by 25% or more in the occlusion study compared to the control study was used as the threshold for indicating significantly hypoperfused myocardium<sup>178</sup>. This area in the bull's eye plot was delineated, resulting in an "extent map," representing all added slices (or volume) of the left ventricular myocardium, expressed as a percentage of the left ventricle (LV), and defining the extent of ischemia. In the thesis this measure is referred to either as "extent", or "myocardium at risk" (MaR).

#### Severity of myocardial ischemia

The total pixel count difference between the control and occlusion study within the delineated hypoperfused area in the "extent map" was calculated. This local

perfusion loss (severity) was expressed as a percentage of the total pixel count in the control situation within the same area<sup>178</sup>.

The extent and severity of ischemia were calculated for each patient. For the purpose of detection of ischemia, extent values were used as the gold standard. For correlation with ischemia, both extent and severity were used. All nuclear data analyses were performed at the Department of Clinical Physiology, Lund University, Sweden, blinded to the ECG data.

### *3.4.2 Study IV*

#### *3.4.2.1 Acquisition*

##### *Acute SPECT before pPCI for extent (MaR)*

After admittance to the catheterization laboratory, prior to initiation of the pPCI procedure, 700 MBq ( $\pm 10\%$ ) <sup>99m</sup>Tc-sestamibi was injected intravenously in each patient. The SPECT images were obtained within 8h of injection of the radionuclide, on a dual-headed rotating gamma camera with high-resolution, parallel-hole collimators (ADAC Laboratories, Forte, Milpitas, CA, USA).

##### *SPECT at 30 days after pPCI for final IS*

The same protocol was used, but imaging was started 60 minutes after tracer injection. To ensure equal count statistics, acquisition time varied between 25 and 60 seconds per projection, depending on the time elapsed from tracer injection<sup>182</sup>. Images were gated at 8 frames per cardiac cycle with no scatter or attenuation correction.

#### *3.4.2.2 Image analysis*

Imaging data were analyzed independently by 2 experienced nuclear cardiology readers (S.S.N. and A.K.K.), blinded to clinical data, using the commercially available automatic program Quantitative Perfusion SPECT (Cedars-Sinai Medical Center, Los Angeles, CA, USA)<sup>192</sup>. In case of failure of the automatic quantification algorithm, methods to mask extracardiac activity and/or define the valve plane and apex of the left ventricle, were used<sup>182</sup>. MaR and IS were determined as the area of the left ventricle containing counts lower than a mean normal limit for pixels according to the rest database<sup>192</sup>. If the difference in defect size between the 2 readers exceeded 3%, a consensus reading was obtained<sup>182</sup>. In patients with data for both MaR and IS, myocardial salvage was calculated as:  $(\text{MaR} - \text{IS}) / \text{MaR} \times 100$ .

### 3.5 Statistical methods

In *Study I*, data is expressed as mean $\pm$ 1 SD, unless otherwise specified. Comparisons of HF-QRS and age between the different groups of patients were performed with the Student t-test. The Fischer exact test was used to examine differences in proportions of sex in the patients groups. Statistical significance was defined as  $p<0.05$ .

In *Study II*, results are presented as mean  $\pm$ 1 SD. As small numbers of subjects and clear evidence for normal distribution could not be guaranteed, nonparametric tests were performed. Comparison among groups was made using the Mann-Whitney U test. Spearman's rank correlation coefficient ( $r$ ) was used for correlation analysis. McNemar's test was used testing significance between proportions. Statistical significance was defined as  $p<0.05$ . All statistical analyses were performed by SPSS version 16.0 for Windows (SPSS, Inc, Chicago, IL, USA).

In *Study III*, results are presented as mean  $\pm$ 1 SD. Due to the small number of patients in the study, nonparametric tests were used. Spearman's rank correlation coefficient ( $r$ ) was used for correlation analysis. Mann-Whitney U test was used for comparison between groups. Multiple linear regression analysis was used to evaluate additional values of assorted QRS changes to ST changes in predicting the extent and severity of ischemia. All these variables were considered continuous. All statistical tests were 2-sided, and significance was defined as  $p<0.05$ . The statistical analysis was performed by SPSS, version 15.0, for Windows (SPSS, Chicago, IL, USA).

In *Study IV*, Continuous variables are presented as medians (25<sup>th</sup>-75<sup>th</sup> percentiles; valid cases). Categorical data is presented as percentage (number/valid cases). For continuous variables the Student t- test and Mann-Whitney U test were used for comparisons between groups. Chi-square test or Fishers exact test was used as appropriate for categorical variables. Kruskal-Wallis test was applied for comparisons among more than two groups. All statistical tests were 2-sided, and significance was defined as  $p<0.05$ . Univariable linear regression was performed to evaluate the association between various covariates and IS, including basic characteristics as well as ECG parameters as appropriate. All variables with  $p<0.2$  in the univariable analysis were included in the initial multivariable regression analysis model. The variable with the highest p-value was then eliminated in each step, until a final multivariable model was achieved including only variables with  $p<0.05$ . In the multivariable analysis of the pre-hospital dynamic subgroups, group *STR* was used as the reference. The statistical analysis was performed by SPSS, version 19.0, for Windows (SPSS, Chicago, IL, USA).



## 4 Results and Discussion

### 4.1 Results

#### 4.1.1 HF-QRS in patients with and without old MI (Study I)

With a larger population than in prior studies and with a complete set of 12 leads of high resolution ECG recordings, the HF-QRS levels among patients with and without previous MI were compared. In addition, the HF-QRS values were evaluated separately in two frequency bands (150-250 Hz and 80-300Hz). In both frequency bands the inter-individual variation in the summed HF-QRS in patients without MI as well as in those with different MI locations (anterior, inferior and posterior) was large. In the 80-300 Hz frequency band the HF-QRS values were approximately three-fold higher than the 150-250 Hz due to contribution of low frequencies.

No significant differences were seen among subgroups in the summed HF-QRS of all 12 leads, mean HF-QRS in each individual lead or in the pattern of lead distribution of the HF-QRS (Figure 4.1). The same was seen for both frequency bands.

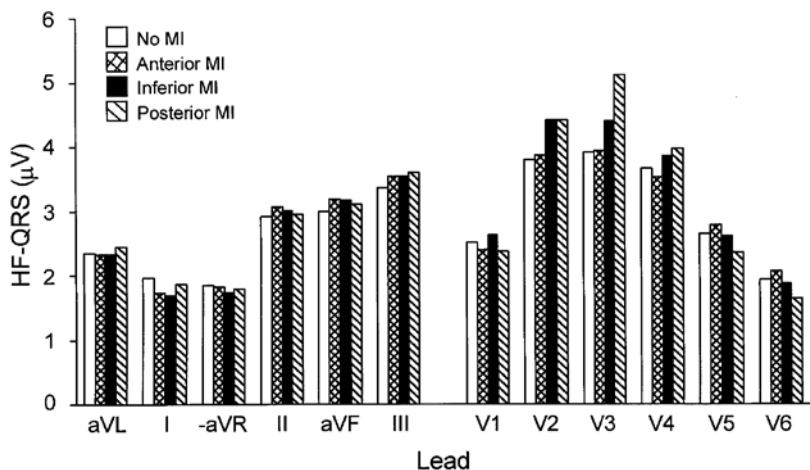


FIGURE 4.1 Mean HF-QRS (150-250 Hz frequency band) in the 12 standard leads among patients without previous MI and those with anterior, inferior, or posterior MI, respectively. There were no significant differences among groups (p-values ranging from 0.08 to 0.94).

Not even the patients with the greatest standard-QRS changes of previous MI (larger MI by Selvester QRS score) could be differentiated from those with no changes from previous MI on the standard ECG. Nor could the selected healthy subjects be differentiated within the no-MI group, as shown in Figure 4.2.

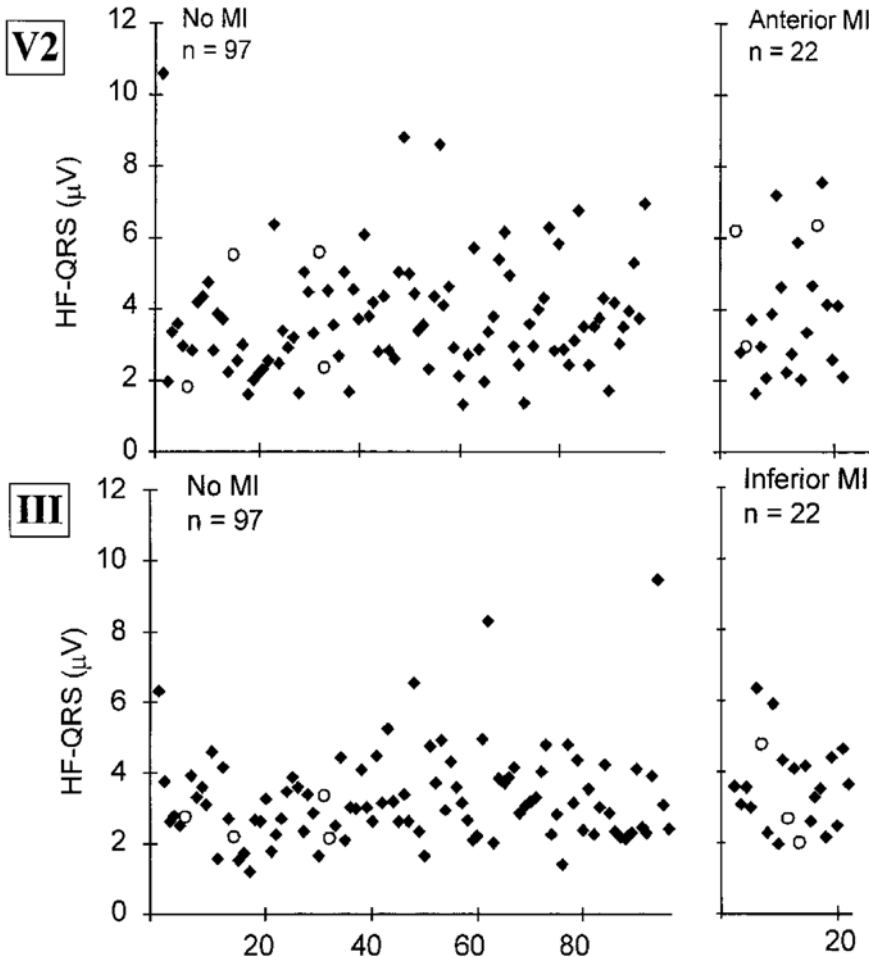


FIGURE 4.2 The HF-QRS (150-250 Hz frequency band) in each individual patient without old MI and with old anterior MI (upper panel) and inferior MI (lower panel). The circles within the no MI group indicate those 4 patients who had no signs of ischemic heart disease. The circles within the anterior and inferior MI groups indicate the 3 patients within the respective group with the largest infarct size (as indicated by the highest Selvester QRS scores). Upper panel anterior MI as exemplified by lead V2; lower panel, inferior MI as exemplified by lead III. Number of patients are on the x-axis.

### 4.1.2 HF-QRS to quantify acute ischemia (Study II)

#### Detection of ischemia by HF-QRS and STEMI criteria

Sixteen (76%) of 21 subjects met the HF-QRS reduction criteria, which was significantly higher than the 38% (8/21) meeting the STEMI criteria ( $p=0.008$ ) as shown in Figure 4.3. Five (24%) of the 21 patients did not meet the HF-QRS criteria, all showing small extents of ischemia (mean,  $6\pm6\%$  of the LV myocardium; range, 0.1-15%).

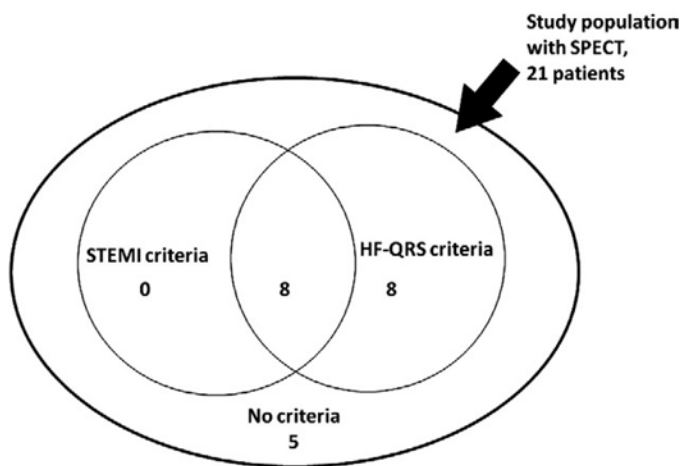


FIGURE 4.3 Venn diagram showing the distribution and overlap of patients meeting the HF-QRS and STEMI criteria.

#### Correlation between HF-QRS reduction and ischemia

We found that the amount of HF-QRS reduction correlated significantly with both the extent and severity of ischemia quantified by SPECT imaging. The highest correlation coefficient was shown for maximal, relative HF-QRS reduction in any lead ( $r=0.59$ ,  $p=0.005$  and  $r=0.69$ ,  $p=0.001$ , respectively) as illustrated in Figure 4.4. Table 4.1 summarizes Spearman's rank correlation coefficients between different HF-QRS measures and ischemia by SPECT (extent and severity). In general, the correlation coefficients were higher for severity than extent. All HF-QRS parameters showed significant correlation with ischemia except from maximal HF-QRS reduction in any lead, by which there was no correlation to the extent of ischemia.



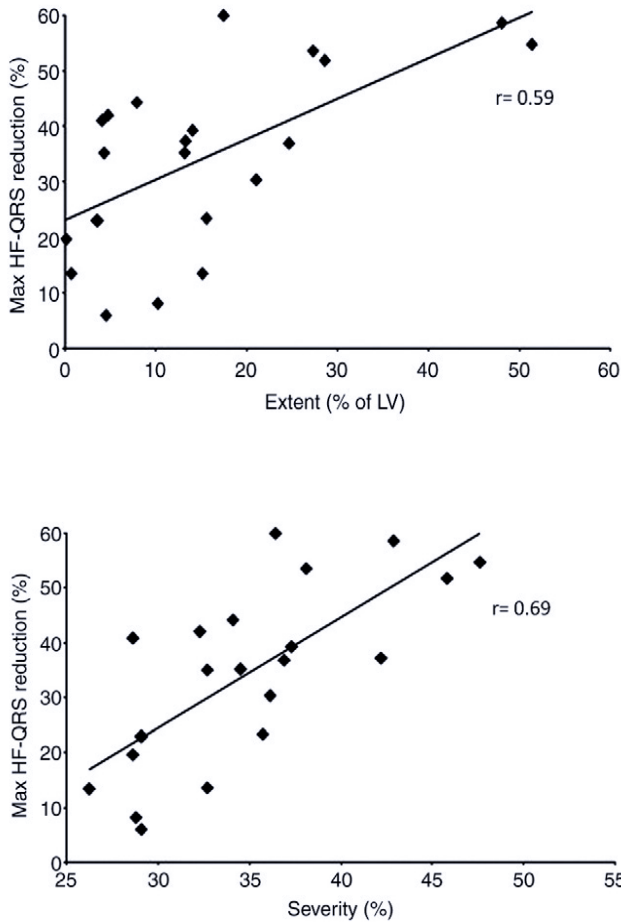


FIGURE 4.4 Spearman's rank correlation between maximal HF-QRS reduction (%) in any lead and extent (upper panel) and severity (lower panel) of ischemia by SPECT.

### Correlation between ST- segment deviation and ischemia

Also, a significant correlation between both maximum single-lead ST-segment elevation as well as sum of ST-segment deviation and ischemia was found (Table 4.1), but with lower correlation coefficients than for the HF-QRS measures.

	<b>Extent of ischemia</b>		<b>Severity of ischemia</b>	
	r	(p-value)	r	(p-value)
<b>HF-QRS parameters:</b>				
Relative changes:				
Max HF-QRS reduction in any lead (%)	0.59	(p=0.005)	0.69	(p=0.001)
Sum of HF-QRS reduction in 12 leads (%)	0.54	(p=0.012)	0.66	(p=0.001)
Absolute changes:				
Max HF-QRS reduction in any lead (μV)	0.40	(p=NS)	0.55	(p=0.01)
Sum of HF-QRS reduction in 12 leads (μV)	0.53	(p=0.014)	0.64	(p=0.002)
<b>ST-segment parameters:</b>				
Max ST elevation in any lead (mV)	0.49	(p=0.023)	0.57	(p=0.007)
Sum of ST deviation in 12 leads (mV)	0.45	(p=0.04)	0.61	(p=0.003)

TABLE 4.1 Correlations (Spearman's rank correlation coefficients) between relative HF-QRS reduction (maximal and sum among 12 leads), absolute HF-QRS reduction (maximal and sum among 12 leads), maximal ST elevation in any lead, and sum of ST-segment deviation among 12 leads and the amount of myocardial ischemia (extent and severity). NS= non-significant. Adapted from *Study II*.

### 4.1.3 QRS slope analysis to quantify acute ischemia (Study III)

By the introduction of QRS slopes in 2008 by Pueyo et al.<sup>156</sup> we learnt that this method proposes a potentially more readily available marker of ventricular depolarization distortion, as compared with HF-QRS. This method was further developed by our group as described in detail in *Supplementary Technical Study*<sup>157</sup>, becoming more robust, showing very low intra-individual variation in a control situation. Furthermore, we introduced a calculation for the most terminal slope for leads with an S wave (TS). In the same ischemia model as in *Study III* (during elective PCI) but in a larger study population, we showed that changes of the DS among the 12 standard ECG leads are generally more pronounced than US changes regardless of the coronary vessel occluded and that this measure performs equally to TS (in applicable leads V1- V3 during anterior ischemia). In previous studies, changes of the QRS slopes have not been correlated to the actual amount of ischemia or compared with other conventional ECG indices of ischemia, which were the aims of *Study III*.

Among patients in *Study III*, mean PCI occlusion time was  $4.9 \pm 0.9$  (range 2.4-7.3) min. As shown in Figure 4.5, the ischemia induced changes of DS were more pronounced than US in anterior leads (V1-V6) for LAD occlusions. The same was seen for RCA occlusions, as exemplified in leads II, aVF and III. There were no significant differences between the amount of change in TS and DS for LAD occlusions for the applicable leads V1-V3.

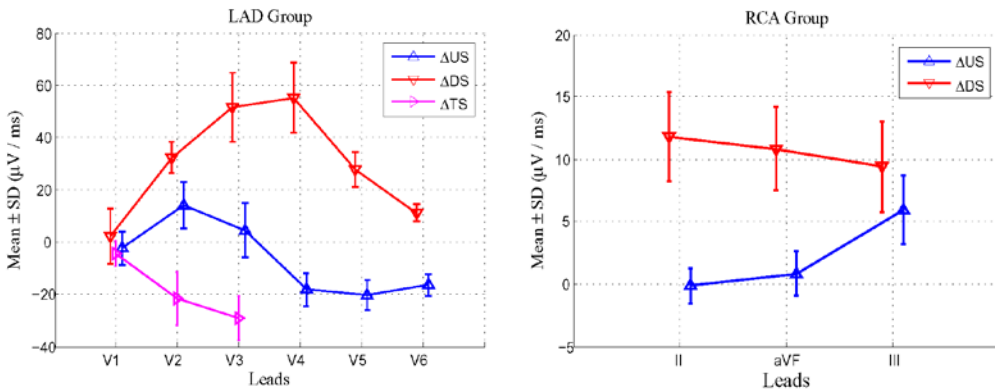


FIGURE 4.5 Mean $\pm$ SD of QRS slope changes for LAD (leads V1-V6) and RCA occlusions (leads II, aVF, and III). Changes in TS are shown only for leads V1 to V3 in the LAD group.

## Correlation between ECG measures and SPECT

Table 4.2 demonstrates the quantitative distribution of the depolarization changes as estimated by conventional parameters (R-wave amplitude changes and QRS-duration changes) as well as QRS slopes (R-wave up-slope, US as well as R-wave down-slope, DS). Furthermore the correlation between these respective changes and extent and severity of ischemia by SPECT are shown. QRS-slope changes correlated significantly with ischemia (for DS:  $r=0.71$ ,  $p<0.0001$  for extent, and  $r=0.73$ ,  $p<0.0001$  for severity). The best correlation between conventional electrocardiogram parameters and ischemia was for the sum of R-wave amplitude change ( $r=0.63$ ,  $p<0.0001$ ;  $r=0.60$ ,  $p<0.0001$ ).

TABLE 4.2 Quantitative distribution of the depolarization changes: (A) DS change, (B) US change, (C) R-wave amplitude change, and (D) QRS-duration change, as well as their correlation to extent and severity of ischemia (Spearman's rank correlation).

QRS parameter	Mean $\pm$ SD (range)	Extent (% of LV)		Severity (%)	
		<i>r</i>	<i>P</i>	<i>r</i>	<i>P</i>
(A) $\Delta$ DS ( $\mu$ V/ms)					
Max pos DS change	35 $\pm$ 28 (3-125)	0.60	<.0001	0.58	.0001
Sum pos DS change	116 $\pm$ 97 (8-125)	0.71	<.0001	0.73	<.0001
Sum tot DS change	154 $\pm$ 114 (17-552)	0.62	<.0001	0.62	<.0001
(B) $\Delta$ US ( $\mu$ V/ms)					
Max neg US change	15 $\pm$ 13 (0.9-54)	0.50	.0015	0.47	.0032
Sum neg US change	60 $\pm$ 60 (1-295)	0.62	<.0001	0.55	.0004
Sum total US change	92 $\pm$ 74 (16-319)	0.39	.0155	0.33	.0390
(C) $\Delta$ R wave ( $\mu$ V)					
Sum Ra increase	701 $\pm$ 862 (39-3291)	0.41	.0110	0.46	.0040
Sum Ra decrease	871 $\pm$ 811 (79-3668)	0.52	.0010	0.45	.0040
Sum tot Ra change	1574 $\pm$ 1377 (190-6291)	0.63	<.0001	0.60	<.0001
(D) $\Delta$ QRS (ms)					
QRS widening (n = 24)	8.4 $\pm$ 6.6 (0-23)	0.17	NS	0.30	NS
QRS narrowing (n = 14)	4.0 $\pm$ 5.0 (0.3-17.1)	0.39	NS	0.28	NS

Abbreviations: LV=left ventricle; Ra= R-wave amplitude; max= maximum; pos=positive; neg= negative; tot= total.

There was also a significant correlation between the maximal ST elevation in any lead and extent and severity of ischemia:  $r=0.73$  ( $p<0.0001$ ) for both ischemia measures. The corresponding correlations for summed ST elevation among all leads were  $r=0.67$  ( $p<0.0001$ ) and  $r=0.73$  ( $p<0.0001$ ) for extent and severity, respectively.

By multiple linear regression analysis, US and DS change provided the largest increase above and beyond that of the ST segment (Table 4.3) regarding explanation of the dependent variable (extent and severity). Regarding the extent of ischemia, the portion of the dependent variable explained by the independent variables,  $R^2$ , increased by 12.9% after adding US and by 12.2% after adding DS. A combination of the 2 increased the prediction of extent by 14.5%. The corresponding values for the severity of ischemia were 4.0%, 7.1%, and 7.1%, respectively. The additive effect of R-wave amplitude change was lower.

Predictor variables	Dependent variable extent of ischemia (% of LV), $R^2$ ( $P$ )	Dependent variable severity of ischemia (% of LV), $R^2$ ( $P$ )
ST	0.593 (<.0001)	0.665 (<.0001)
ST, US	0.722 (<.0001), $\uparrow$ 12.9%	0.705 (<.0001), $\uparrow$ 4.0%
ST, DS	0.715 (<.0001), $\uparrow$ 12.2%	0.736 (<.0001), $\uparrow$ 7.1%
ST, DS, US	0.738 (<.0001), $\uparrow$ 14.5%	0.736 (<.0001), $\uparrow$ 7.1%
ST, Ra sum neg	0.688 (<.0001), $\uparrow$ 9.5%	0.693 (<.0001), $\uparrow$ 2.8%
ST, Ra sum pos	0.593 (<.0001), $\uparrow$ 0.0%	0.669 (<.0001), $\uparrow$ 0.4%
ST, Ra sum tot	0.644 (<.0001), $\uparrow$ 5.1%	0.673 (<.0001), $\uparrow$ 0.8%

TABLE 4.3 Multiple regression analysis. Prediction of extent and severity of ischemia by adding  $\Delta$  of QRS slope (US and/or DS in  $\mu\text{V}/\text{ms}$ ) or  $\Delta$ R-wave amplitude changes ( $\mu\text{V}$ ) to  $\Delta$ sum of ST elevation (mV). Ra=R-wave amplitude; Ra sum neg/pos=sum of the decrease/increase of Ra among all leads; Ra sum tot=sum of all changes in Ra among all leads; LV=left ventricle; arrows=increase of the explanation of the dependent variable by the added independent variable/s.

#### 4.1.4 Ischemia severity grading in STEMI patients (Study IV)

Temporal behavior of the ischemia grades between the pre-hospital and pre-PCI ECGs

Slightly more than half the patients – 53% (211/401) – were stable with a persistent ischemia grade between pre-hospital and pre-PCI ECGs. Temporal changes of ischemia grades from pre-hospital to pre-PCI ECG are displayed in Figure 4.6.

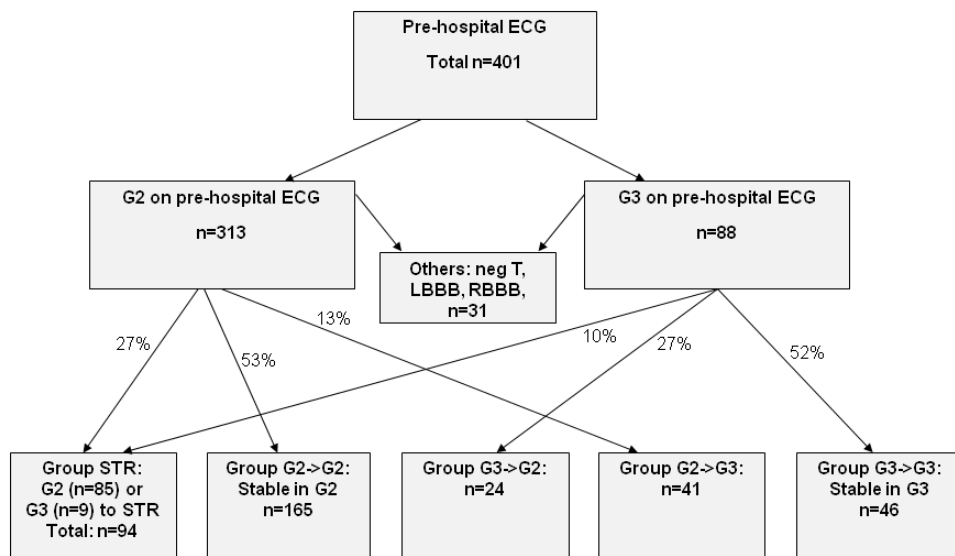


FIGURE 4.6 Overview of the initial stratification of patients into ischemia grade 2 or 3 on their pre-hospital ECG and their temporal changes between pre-hospital and pre-PCI ECG at the PCI center. Five subgroups of temporal behavior (lower panel) were defined.

#### Final IS by SPECT

##### Comparison between G3 and G2 on pre-hospital ECG

By first considering only the ischemia grading performed on the pre-hospital ECG and correlating G3 vs. G2 with final infarct size after pPCI, it was found that patients with G3 on the pre-hospital ECG had significantly larger IS as compared to G2 (Table 4.4). Time from symptom onset to pre-hospital ECG and to balloon was similar between these two groups, as was MaR (however in a subpopulation).

By linear regression analysis, G3 was independently associated with IS ( $B=3.8$ ;  $p=0.006$ ) as shown in Table 4.5. By including the presence of Q waves on the pre-hospital ECG in the initial model (otherwise the same modelling procedure), G3 remained independently associated with IS;  $B=3.31$ ;  $p=0.016$  (not shown in the Table).

TABLE 4.4 Findings regarding time intervals from symptom onset to the two ECGs and treatment; coronary angiography; SPECT and biochemical marker (TnT) in patients without and with terminal QRS distortion (G2 and G3, respectively) on initial, pre-hospital ECG. Modified from *Study IV*.

	<b>Grade 2 (n=313)</b>	<b>Grade 3 (n=88)</b>	<b>p -value</b>
<b>-Time intervals, symptom onset to:</b>			
Pre-hospital ECG (min)	87 (50-175)	106 (47-197)	0.81
Pre-PCI ECG (min)	186 (137-274)	194 (130-282)	0.72
First balloon (min)	195 (146-289;n=297)	199 (137-286;n=84)	0.68
<b>-Coronary angiography findings:</b>			
TIMI 0-1 pre-PCI	64% (197)	69% (60)	0.41
TIMI 3 post-PCI	89% (272)	86% (74)	0.52
<b>-SPECT findings:</b>			
MaR (% of LV)*	27(16-40;n=210)	31(20-43;n=55)	0.14
Infarct size (IS) (% of LV)	6(1-18)	11(3-26)	0.005
-Max Troponin T (µg/L)	4.5(1.7-8.2)	6.8(3.2-11.2)	0.003

\*MaR data was available for 265 patients. PCI=percutaneous coronary intervention;TIMI=thrombolysis in myocardial infarction; SPECT=single-photon emission computed tomography; MaR=myocardium at risk.

TABLE 4.5 Final model of multivariable linear regression analysis with IS as dependent variable, including co-variables at the time of pre-hospital ECG. Adjusted from *Study IV*.

<b>Independent predictors of IS</b>			
<b>Initial phase, pre-hospital ECG</b>	<b>B</b>	<b>t</b>	<b>p-value</b>
Age (years)	0.12	2.48	0.013
Grade 3 on pre-hospital ECG	3.80	2.74	0.006
Max, pre-hospital, single lead ST elevation (mV) <sup>1</sup>	4.48	1.97	0.049
Men	3.51	2.75	0.006
Anterior infarct location	6.16	4.98	<0.001

<sup>1</sup> See the Methods section for definition of parameters. B= unstandardized regression coefficient.

## Relationship between final infarct size and ischemia grade transition during transport to the PCI center

Overall, final IS differed significantly among the subgroups, with the largest IS in group *G3->G3*, and the smallest in group *STR* (Table 4.6). In a linear multivariate analysis with group *STR* as reference, groups *G2->G2*, *G2->G3* and *G3->G3* were independently associated with increasing IS ( $B=4.4$ ;  $p=0.004$ ,  $B=5.4$ ;  $p=0.01$  and  $B=10.2$ ;  $p<0.001$ , respectively), but group *G3->G2* was not ( $B=3.8$ ;  $p=0.133$ ), as seen in Table 4.7. Other variables in the final regression model associated with IS are shown in Table 4.7.

TABLE 4.6 Findings by time to treatment, coronary angiography, SPECT and biochemical markers in subgroups based on ischemia grade transition between pre-hospital and pre-PCI ECGs. Modified from *Study IV*.

	Group STR G2 or G3 to STR n=94	Group G2->G2 n=165	Group G3->G2 n=24	Group G2->G3 n=41	Group G3->G3 n=46	p- value
Symptom onset-to-balloon time (min)*	194 (148-280); n=86	196 (146-301); n=159	204 (124-297); n=22	192 (136-271); n=40	197 (141-286); n=44	0.99
-Coronary angiography:						
TIMI 0-1 pre-PCI	24%	79%	67%	85%	87%	<0.001; 0.19 <sup>1</sup>
TIMI 2-3 pre-PCI	76%	21%	33%	15%	13%	
TIMI 3 post-PCI	93%	88%	92%	88%	78%	0.11
Infarct related artery:						
RCA	39%	42%	54%	49%	56%	0.47
LAD	48%	47%	37%	41%	28%	
LCX	13%	11%	8%	10%	15%	
-SPECT findings:						
MaR (% of LV)†	17 (5-30); n=55	28 (19-42); n=109	28 (16-32.5); n=12	36 (30-45); n=23	40 (29-46); n=28	<0.001; 0.007 <sup>1</sup>
Infarct Size (% of LV)	2 (0-6)	10 (2-20)	7 (2-17)	11 (5-21)	19 (7-30)	<0.001; 0.034 <sup>1</sup>
Salvage (%)†	83 (50-100); n=55	58 (36-89); n=109	75 (39-88); n=12	63 (40-85); n=23	46 (35-70); n=28	0.041; 0.29 <sup>1</sup>
Max Troponin T (µg/L)	1.5 (0.4-4.7)	4.9 (2.3-8.9)	4.4 (2.5-7.1)	8.2 (5.4-9.8)	8.6 (5.7-12.1)	<0.001

Categorical data are presented as percentage of valid cases, and continuous data as median (25<sup>th</sup>-75<sup>th</sup> percentiles). n=valid cases as specified. \*Time to balloon was not available for 19 patients. †MaR and Salvage were available for 227 patients.<sup>1</sup>Comparison only among other groups than *Group STR* (Kruskal-Wallis). LAD=left anterior descending artery; RCA=right coronary artery; LCX=left circumflex coronary artery; other abbreviations, see Table 4.4.



TABLE 4.7 The final model of multivariable linear regression analysis with IS as dependent variable, including co-variables at admission including subgroups based on the pattern of ischemia grade behavior between pre-hospital and pre-PCI ECGs (Group *STR* as reference). Adjusted from *Study IV*.

Independent predictors of IS			
Admission phase including temporal ECG dynamics	<i>B</i>	<i>t</i>	p-value
Men	3.90	3.19	0.002
Anterior infarct location	6.45	5.90	<0.001
Pre-PCI TIMI 0-1	4.22	3.13	0.002
Symptom-to-balloon time (min)	0.016	4.50	<0.001
Sum of ST elevation on admission ECG <sup>1</sup>	1.55	2.74	0.006
ECG group (group <i>STR</i> =reference): 1			
G2->G2	4.44	2.90	0.004
G3->G2	3.79	1.51	0.133 <sup>2</sup>
G2->G3	5.41	2.48	0.014
G3->G3	10.17	4.58	<0.001

<sup>1</sup> See the Methods section for definition of parameters. <sup>2</sup> Group G3->G2 was not significantly, independently associated with final infarct size. *B*= unstandardized regression coefficient; other abbreviations, see previous tables.

## Salvage by SPECT

In the subgroup of 245 patients with both acute and 30-day SPECT data available (thus enabling to determine salvage), there was no significant overall difference in salvage between patients classified as G2 and G3 on their pre-hospital ECG; 63% (37-91) vs. 55% (36-81), *p*=0.21, as demonstrated in Table 4.8. Regarding the temporal subgroups, salvage was lowest in group G3->G3 and highest in group *STR*; 46%(35-70) vs. 83%(50-100), respectively, *p*=0.003 (Table 4.6).

Patients were divided into early- and late-treatment groups, with the cut-off set at 2.5 hours, corresponding to the 25<sup>th</sup> percentile of symptom-to-balloon time (Table 4.8). Among patients treated beyond 2.5 hours, those with G3 on the pre-hospital ECG were associated with lower salvage than G2; 48%(35-78) vs. 62% (40-87); *p*=0.04, whereas salvage was similar between the ischemia grades when treated early. Time intervals from symptom onset to pre-hospital ECG, as well as to balloon, were similar between G3 and G2 in both early- and late-treatment groups.

TABLE 4.8 Complete SPECT data as well as time from symptom onset to initial ECG and balloon. Comparison of patients with G2 or G3 on initial, pre-hospital ECG, stratified according to time to treatment.

	Total, n=245			Early <2.5 hours, n=58			Late ≥2.5 hours, n=187		
	G2 (n=195)	G3 (n=50)	P	G2 (n=43)	G3 (n=15)	p	G2 (n=152)	G3 (n=35)	p
SPECT findings:									
Salvage (%)	63 (37-91)	55 (36-81)	0.21	75 (36-96)	72 (49-96)	0.64	62 (40-87)	48 (35-78)	0.042
IS (% of LV )	7 (1-18)	11 (3-25)	0.047	4 (1-13)	3 (1-14)	0.90	8 (2-20)	16 (5-29)	0.015
MaR (% of LV )	28 (17-40)	33 (23-43)	0.062	25 (17-38)	28 (23-38)	0.65	28(16-41)	38(22-45)	0.040
Symptom onset to:									
Pre-hosp ECG (min)	95 (51-148)	111 (41-157)	0.37	39 (22-50)	25 (18-44)	0.42	118 (79-208)	129 (101-202)	0.83
Balloon (min)	204 (161-296)	199 (143-283)	0.79	112 ( 93-131)	119 (105-137)	0.47	235 (194-323)	237 (192- 312)	0.45

Data presented as median (25<sup>th</sup>-75<sup>th</sup> percentiles).SPECT= single-photon emission computed tomography; IS=infarct size; LV=left ventricle; MaR= myocardium at risk.

## 4.2 Discussion

### 4.2.1 *General clinical considerations*

Despite more sensitive cardiac biochemical markers and fast technical development of myocardial imaging (SPECT and MRI), the ECG remains the only readily available diagnostic tool for initial evaluation of patients with suspected acute MI. Along with generally improved reperfusion strategies by pPCI and developing algorithms for early pre-hospital evaluation and transport of patients to distant PCI centers, more individualized evaluation may possibly further improve acute management. This could, for example involve the selection of patients with a high risk for rapid infarct evolution that could benefit from receiving specific “upstream” treatment before pPCI, such as pharmacological agents or mechanical pre-conditioning therapy, hypothermia or specific peri- or post-PCI myocardial protection. Selected patients could perhaps also benefit from an immediate thrombolytic reperfusion strategy if transport time to the PCI center exceeds a certain limit. A key question is then if additional clinically relevant information can be retrieved from the depolarization phase of the ECG that can add to the present ST-segment evaluation (STEMI criteria), hence providing individual information about the severity within the MaR and risk of rapid progression of irreversible infarction. Basic understanding of these depolarization changes as well as proper ways to measure and quantify them are crucial for clinical application.

In this thesis different QRS analysis methods based on the 12-lead ECG system were evaluated in a model of the first 5 minutes of total coronary occlusion as to simulate the first few minutes of an acute MI. Furthermore, we evaluated the dichotomized ischemia severity grading system, with and without “terminal QRS distortion” in addition to STEMI criteria in a large patient cohort and related these ECG patterns to final IS, MaR and salvage.

### 4.2.2 *Depolarization changes in relation to extent (MaR) and severity of ischemia by SPECT*

The prolonged elective balloon PCI procedure, used in clinical practice at the inclusion site at the time (before the stent era), offered a unique model for studying ECG changes during the first 5 minutes of acute ischemia. SPECT data were acquired for quantification of the reversible ischemia regarding its extent (MaR) and severity.

#### HF-QRS analysis

In earlier studies HF-QRS content was shown to decrease due to ischemia<sup>144-150</sup>, and increase at successful reperfusion by thrombolytic therapy of an acute

MI<sup>151,152</sup>. None of these prior studies have, however, quantified the amount of ischemia during coronary occlusion, or described the relationship between changes in HF-QRS and the extent and severity of the ischemia as indicated by SPECT.

In *Study II*, we have described, for the first time, a significant correlation between the amount of HF-QRS reduction during the PCI procedure and the extent (MaR) as well as severity of ischemia. This was shown for both maximum HF-QRS reduction in any lead and for summed HF-QRS reduction among all leads. Relative as well as absolute changes were evaluated, showing similar results, except for the maximal absolute HF-QRS reduction in any lead. The reason may be the notably large inter-individual variation of HF-QRS, and when having low individual values the range in absolute terms is more limited in the correlation analysis compared to relative changes. Strict noise criteria were applied for inclusion in order to have as clean data as possible, which considerably reduced the sample size in *Study II*.

The common explanation for the changes seen by the HF-QRS analysis method relates to the change in conduction velocity in the myocardial cells and/or conduction fibers<sup>147-151,189</sup>. In a canine model, Watanabe et al.<sup>142</sup> have shown that reduction of HF-QRS correlates linearly with local conduction delay induced by local administration of sodium channel blockers. By a simulated reduction of conduction velocity in a 3-dimensional heart model, Abboud et al.<sup>143</sup> suggested that a decreased number of terminal branches in the activation process would cause more synchronized activation in the myocardium leading to reduction of the HF-QRS. A study by Trägårdh et al.<sup>194</sup> showed HF-QRS to be significantly lower in patients with a bundle branch block than in healthy subjects.

The changes in HF-QRS seen during acute ischemia might well be due to changed properties of the cellular ion channels, gap junctions, and other basic elements of signal propagation within the myocardium. The question remains, however, whether HF-QRS changes reflect certain very high-frequency pathophysiologic alterations within the conduction system or the myocardium itself, or are merely secondary to changes of the overall QRS slopes, due to this local slowing of conduction through the ischemic region<sup>156</sup>.

In severe ischemia depolarization changes are usually confined to the later part of the QRS complex. The RMS quantification method used by our group gives an overall measure of the total high-frequency content within the QRS complex. Other ways to express the HF-QRS content have been suggested by Abboud et al. using a more morphologic evaluation<sup>148</sup> by reduced amplitude zones (RAZ), as determined by locally minima or maxima in the HF-QRS signal. Later, this method was further developed by Schlegel et al. at the National Aeronautics and Space Administration<sup>195</sup>. These morphological methods are thus categorical and do not provide a continuous measure such as RMS. In 2011 Magrans et al. evaluated HF-QRS changes expressed as RMS values early vs. late during the QRS complex

(using our *STAFF III* dataset) and found RMS changes in the later part to be more sensitive to ischemia. However, no correlation to SPECT was performed<sup>196</sup>.

Schlegel et al. have developed a real-time HF-QRS analysis<sup>195</sup> with immediately available results after the ECG recording as compared to the off-line version used in *Study I* and *II*. Still the analysis method is sensitive to noise and as such less suitable in a busy clinical environment.

## QRS-slope analysis

In *Study III*, more readily available (compared with HF-QRS) markers of ventricular depolarization distortion based on calculation of up- and downslopes of the QRS complex were evaluated. These measures combine information from overall QRS duration as well as amplitudes of the R and S waves. This analysis was first introduced by Pueyo et al.<sup>156</sup>, while further development of the methodology was performed by our group as described in *Supplementary Technical Study*<sup>157</sup>.

In *Study III* we found that changes of QRS-slopes correlated significantly with SPECT measurements of ischemia, both in terms of MaR and severity. The correlation seems comparable to the one found for HF-QRS in *Study II*. Being less sensitive to noise as compared to HF-QRS analysis, the QRS slope method allowed more patients to be included in *Study III* as compared to *Study II*.

In *Study III*, in addition to QRS-slopes, conventional QRS-parameters such as R-wave amplitude and QRS duration were evaluated separately in relation to the SPECT findings. The correlation coefficients when comparing the sum of R-wave amplitude change in the overall population and the measures of ischemia were similar to those found for the sum of R wave down-slope (DS) change.

However, using regression analysis, the value of R-wave amplitude change appeared to be lower than for QRS-slope changes as to explain the dependent variables MaR and severity.

## QRS duration

No significant correlation between QRS prolongation and MaR or severity by SPECT was observed in *Study III*. This was in contrast to prior experimental findings in animals, where QRS prolongation was associated with more severe ischemia (as measured by microspheres) during ischemia, as well as less salvage at post-mortem findings<sup>54, 122, 197</sup>.

In *Study III*, QRS prolongation was observed in 63% of the patients, whereas others showed a slight shortening during the ischemic period. Prolongation was in general more pronounced than shortening. QRS duration is, however, difficult to determine correctly, because ST elevation commonly obscures the delineation between the end of the depolarization and the beginning of repolarization.

The QRS slope methodology thus offers a more robust way to express the QRS changes as compared to the HF-QRS method, taking into consideration both changes of duration and amplitude changes of the depolarization phase.

## QRS amplitudes

It was beyond the scope of *Study III* to also report in detail on the specific R-, and S-wave amplitude changes during the PCI procedure, although they both contribute to the QRS slope changes besides the effect of the QRS duration. In general terms the US is related to R-wave amplitude and overall QRS duration, whereas the DS is related to the terminal portion of the QRS complex, incorporating variations in both R-wave amplitude and S-wave amplitude (when present), as well as possible passive effect of the ST-segment shift itself. In the correlation analysis with both MaR and severity we found higher correlation coefficients regarding changes in DS than US, thus suggesting changes of more terminal portion of the depolarization may be more relevantly associated with these SPECT measures.

In *Study III*, both increase and decrease of the R-wave amplitudes were seen among the 12 leads during the PCI procedure. By *post hoc* analysis (non-published data) of the patients with occlusion of RCA (n=21), increased R waves were observed in leads II, aVF and III by 10/21(48%), 11/21(62%) and 16/21 (76%), respectively. No relationship was seen between number of leads with R-wave amplitude augmentation and SPECT findings.

Among patients with LAD occlusion (n=8), reduction or total loss of S waves during the PCI procedure in leads V1, V2 and V3 were seen in 6/8(75%), 7/8(87%) and 7/8 (87%), respectively. The only patient with LAD occlusion that showed no reduction of the S wave amplitude had the lowest amount of ischemia by SPECT (MaR 15% of the LV, and severity by 33%) and no significant ST-segment elevation. The remaining 7 patients with various degree of either S-wave reduction or total loss of S wave had a median (25<sup>th</sup>-75<sup>th</sup> percentile) MaR of 47%(40-51) of the LV myocardium and a severity score of 48%(43-53). The one patient with total loss of S waves in leads V1 through V3 had the largest MaR and highest severity score among all patients in *Study III* (MaR: 65% of the LV myocardium and 62% severity).

## Feasibility of QRS evaluation in the clinical setting of acute ischemia

In the ambition to mimic the first minutes of an acute MI, the elective PCI model used in this thesis is unique because of its long duration of coronary occlusion, that is not possible to repeat after the introduction of stents. However, it is still far from the actual acute MI-situation with vulnerable plaque rupture and thrombotic occlusion of the coronary artery. It is, however, reasonable to think that during the balloon occlusion significant transmural ischemia with various amounts of MaR

and severity was developed, with effects on both the repolarization and depolarization phases, sufficient to test these novel ECG methods for quantification of the QRS changes.

In clinical evaluation of the severity of acute ischemia using information within the depolarization phase in addition to the conventional ST-segment analysis, robust and fairly noise resistant methods are needed. Basic understanding of how different QRS variables react during coronary occlusion and how they relate to the extent and severity of ischemia are important. Analysis of QRS changes from a single, “snap-shot” ECG is more complex as compared to ST-segment evaluation, due to the lack of an “isoelectric baseline”. This makes the slope method to be most clinically applicable in a monitoring situation where the patient is its own control. With expanding digital databases with patient’s prior ECGs readily available, however, more baseline information is becoming available, in which slope measurements could be included as a standard.

To further test the feasibility of the QRS-slope method as to monitor longer periods of acute myocardial ischemia and evolving infarction, it was applied in an experimental, acute MI study in pigs<sup>158</sup>. We found the method suitable in this setting of 40 minutes LAD occlusion to track the dynamic changes of the QRS slopes in the standard 12 lead ECG.

In several studies Dellborg and colleagues evaluated a vectorcardiographic (VCG) method for its feasibility and clinical application of QRS (and ST-segment) monitoring in patients during unstable angina as well in acute MI after thrombolytic therapy<sup>163-165</sup>. However the VCG method did not gain broad clinical acceptance, and thus is seldom used today.

In the pig experimental study<sup>158</sup> we also added analysis of VCG in order to be able to compare with the QRS slopes and prior studies using the vectorial approach. There were clear similarities between the dynamics of the vector-based QRS max parameter and Ra and up-slope of the R wave (US) during the occlusion period. However, it was not within the scope of this thesis to additionally explore the VCG-based representation of depolarization changes.

More studies are needed to apply the QRS-slope method in STEMI patients to evaluate dynamic changes relating to the depolarization due to ischemia and infarct evolution.

### 4.2.3 Ischemia grades and “terminal QRS distortion” in relation to MaR, severity and evolving infarct in acute STEMI

#### General, clinical considerations

In *Study IV*, we evaluated the clinical value of early, pre-hospital ischemia grading during STEMI as a means of identifying patients with possible severe ischemia, prone to rapid infarct evolution and large final IS.

The ischemia grading system was developed by Birnbaum et al.<sup>109</sup> as a means of predicting final infarct size in patients presenting with an acute MI. The grading is based on assessment of the T wave, ST-segment and the terminal part of the QRS complex. Thus, it categorizes the gradually increasing severity during acute MI, as dependent on the degree of myocardial protection, into three grades. The most severe, third grade (G3) includes “terminal QRS distortion” in addition to significant ST-segment elevation. By this categorical ischemia-grading method no baseline ECG is needed, thus providing a “snap-shot” stratification of patients with acute MI.

The “distortion” of the terminal portion of the QRS complex due to severe ischemia includes disappearance of the S waves in leads V1 to V3 (typical leads with baseline rS configuration) and augmentation of the R wave in other leads. The S-wave criterion is easy to recognize without a previous, baseline ECG. However, proper identification of increasing R-wave amplitude in leads with a typical qR configuration needs either continuous ECG monitoring of the patient or an earlier baseline ECG recording for comparison. The grade 3 criterion for these leads was *a priori* set to an ST-J point-to-R-wave amplitude ratio above 0.5. By performing the grading only on leads with positive T waves increases the probability of making the evaluation early in the infarction evolution process, before R-waves decrease due to infarction development.

In several studies patients with G3 at their admission ECG have been associated with larger IS as compared to patients with G2 when final IS has been estimated by cardiac biochemical marker release<sup>55,56,112,115-117,198</sup> and Selvester QRS scoring<sup>118</sup>. In four previous studies with similar results, final IS was quantified by SPECT imaging<sup>56, 119-121</sup>. In two of these, Birnbaum et al. have reported G3 to predict larger IS by pre-discharge SPECT after thrombolytic therapy: one in a large AMI cohort (n=378)<sup>56</sup>, the other in a smaller population (n=49)<sup>120</sup>. In the other two studies using pPCI as the reperfusion strategy Billgren et al.<sup>119</sup> found larger IS by SPECT in patients with G3 as compared to G2 in a small sample (n=79) including only 15 patients with G3, whereas similar results were found by<sup>121</sup>, (n=46).

Uncertainty remains as to whether G3 represents severe ischemia more prone to fast progression of necrosis, or is merely a sign of large MaR that has already reached a high degree of irreversible infarct development. The second G3 criteria



based on the ratio between ST-J and R-wave amplitude could be due to severe ischemia with still augmented R waves and high ST-segment elevation. As severe ischemia within the MaR gradually progresses into a larger degree of necrosis, the R-wave amplitude as well as ST-segment elevation gradually decline. Although patients with negative T-waves are excluded from the ischemia grading, it is theoretically plausible however, that gradual decline of R-wave amplitude and ST-segment level due to infarct progression may either keep their relative ratio stable, or make it change due to relatively more pronounced R-wave as compared to ST-segment attenuation. Then this G3 criterion still is met, despite the MaR being far into the irreversible infarction process.

### Association between grade 3 ischemia on ECG and MaR and severity by SPECT

One major reason to justify the theory of G3 as a sign of more severe ischemia than G2 has been similar time to treatment and larger infarct size despite supposedly comparable MaR. There are, however some conflicting results regarding the latter. Only a few studies have evaluated MaR by myocardial perfusion imaging, all with small sample sizes (ranging between 37 and 79 patients). Two of three studies using SPECT<sup>119,120</sup> showed no difference in MaR. Yang et al.<sup>121</sup>, however, found larger MaR in patients with G3 as compared to patients with G2 by studying only anterior MIs (n=46 patients).

In agreement with previous results, we found time from symptom onset to ECG and treatment in *Study IV* similar between patients with G3 as compared to patients with G2. We found MaR to be similar for patients with G3 and G2 on the pre-hospital ECG, but differed significantly between the temporal groups regarding the type of dynamic change of ischemia grade from pre-hospital ECG to admission, pre-PCI ECG.

No significant difference was, however observed in MaR between patients with G3 (by pooling groups G3->G3 and G2->G3) as compared to patients with G2 (by pooling groups G2->G2 and G3->G2) when considering grading separately only of the *admission ECG* at the PCI center (as performed in previous studies).

MaR was, however present only in a subgroup of *Study IV*, and used as a means of evaluating our secondary aim of the study, salvage. Nevertheless it represents a significantly larger cohort than in prior studies, and as such lends some more support regarding previous findings of similar MaR between the ischemia grades.

In contrast to *Study II* and *III*, no severity measure by SPECT was applied in the STEMI population in *Study IV*. In the situation with ongoing myocardial infarction with various degrees of already necrotic areas within the MaR, such evaluation is more difficult to interpret compared to the totally reversible, PCI-induced ischemia in *Studies II-III*. This imaging modality cannot differentiate between viable myocardium and myocardium already infarcted. Nevertheless, residual flow

during MI can be quantified by  $^{99m}\text{Tc}$ -sestamibi SPECT as shown by Christian et al.<sup>82,173,179,199</sup>. In addition, Yang et al.<sup>121</sup> also evaluated residual perfusion by SPECT within the MaR as a measure of severity, and found significantly lower values in patients with G3 as compared to those with G2 at the admission ECG. Contrary to this finding, residual perfusion was similar between the two grades in the study by Billgren et al.<sup>119</sup>.

### Pre-hospital, temporal behavior of ischemia grades - association to IS and salvage

In the vast majority of previous studies only the admission ECG, just prior to reperfusion therapy has been used to grade patients into G3 or G2 ischemia. If G3 reflects more severe ischemia with rapid infarct progression, early identification of patients with this ischemia grade would be of importance. Furthermore, insight into the temporal behavior of the grades before reperfusion therapy is a missing link in the exploration and general understanding of ischemia grades.

Being the first we thus, in *Study IV*, deliberately evaluated the clinical value of pre-hospital ischemia grading and explored their temporal behavior between the index, pre-hospital ECG to the pre-PCI ECG just prior to reperfusion therapy by pPCI.

In agreement with earlier reports<sup>55,56,112,115-120,198</sup>, we found grade 3 on admission, pre-PCI ECG to be associated with larger IS. The new findings by *Study IV*, that grade 3 ischemia also, already on the pre-hospital ECG predicts larger final IS as compared to grade 2, independent of ST-segment elevation and presence of Q waves, is an important step towards possible clinical utilization of this simple electrocardiographic “snap-shot” evaluation. Furthermore, the pattern of temporal behavior during the pre-hospital phase also predicted IS, whereby development and persistence of G3 ischemia grade (groups G2->G3 and G3->G3) appeared to be the strongest predictors of larger IS. This prediction was stronger than the prediction for the sum of ST elevation.

As the secondary aim of *Study IV*, salvage after pPCI was compared between ischemia grades in the subgroup of patients who had pre-PCI SPECT performed in addition to the 30-day SPECT. We found overall salvage for patients with G3 and G2 on the pre-hospital ECG to be similar, although it differed within the dynamic groups, with the highest salvage being in group STR, and the lowest – in group G3->G3. By dividing patients into early- and late-treatment groups, with the cut-off set at 2.5 hours, we found interesting differences between the two grades. Among patients treated beyond 2.5 hours, those with G3 on the pre-hospital ECG were associated with lower salvage than patients with G2, whereas salvage was similar between the ischemia grades when treated early. Time intervals from symptom onset to pre-hospital ECG, as well as to balloon, were similar between patients with the two ischemia grades in both early and late-treatment groups. This

finding on the association between time to treatment and salvage may further support the theory that G3 is a sign of more severe ischemia as compared to G2, with equal salvage potential for the two grades if treated early, but lower for G3 patients than G2 patients if treated late. This corresponds to findings by Birnbaum et al.<sup>111</sup> and Sejersten et al.<sup>113</sup>, with worse outcome for patients with G3 than for patients with G2 when treated later than 2 and 3 hours, respectively.

This secondary evaluation of subpopulations with small samples should be considered as hypothesis generating. Larger samples with SPECT-verified salvage would be needed to further test this hypothesis.

Additional studies are needed to identify ECG patterns that differentiate severe ischemia from established necrosis in the myocardium during STEMI.

### Additional aspects of the present S-B ischemia grading system

In *Study IV*, we sought to further evaluate and increase the understanding of the Sclarovsky-Birnbaum (S-B) ischemia grading with its predefined, conventional grade 3 criteria applied in previous studies.

In theory, the two different grade 3 criteria - absence of S waves in leads V1-V3, and ST-J point to R-wave amplitude ratio of  $>0.5$  in other leads, may reflect different pathophysiologic phases along the ischemia/infarction process. Furthermore, the transition between the severity grades is gradual and continuous, so the dichotomized grading by total loss of S waves and the *a priori* ST-J/R-wave amplitude ratio cut-off at 0.5 may not be the most optimal. Further studies are needed both to evaluate potential pathophysiologic differences between the two present grade 3 criteria, as well as test a more gradual scale for a severity measure.

In the present study, by *post-hoc* analysis of patients with anterior MI location, we found one half of patients with anterior G3 on the pre-hospital ECG to meet either loss of S wave, or ST-J point/R-wave amplitude criteria. There were no significant differences between these groups as regards MaR, final IS and severity. Further separating them into the patterns of ischemia-grade changes between pre-hospital ECG and pre-PCI ECG (i.e.  $G3 \rightarrow G2$  or  $G3 \rightarrow G3$ ), there were no difference between them either regarding MaR, IS or salvage according to the specific grade 3 criterion met. However, these subgroup analyses were done on small number of patients, and larger sample sizes are needed to further elucidate whether there are significant differences between these ischemia grade 3 criteria.

#### 4.2.4 Depolarization changes by HF-QRS and standard ECG in relation to prior MI

Clinically, a general concept has been that depolarization changes in the early part of the QRS complex by Q waves reflect a prior, transmural MI<sup>200</sup>. However, an infarct may result in various depolarization changes depending on its location, size

within the LV myocardium and degree of transmural. An old MI located in the posterolateral wall of the left ventricle, for example, cannot, due its later representation during the depolarization wavefront, produce Q waves, but rather gives rise to prominent R waves in anteroseptal leads V1-V2. The larger the area that produces no electrical forces due to a MI scar, the more effects will result on the overall QRS vector. Also the transmural factor has been challenged by newer techniques like MRI, thus confirming that subendocardial extent, rather than degree of transmural relates more strongly to the presence of Q waves<sup>130,131,201</sup>.

In *Study I*, the ability of HF-QRS to differentiate between patients with and without previous MI as defined by standard 12-lead ECG Selvester score was evaluated.

Early attempts to characterize depolarization changes in MI other than Q waves using more high-resolution ECG recordings have reported notches and slurs, or fragmentations, of the QRS complex<sup>202-205</sup>. These “high-frequency components” were shown to be increased in patients after infarct as compared to healthy individuals. More sophisticated methods, with use of signal averaging and digital filtering techniques, later made it possible to assess intra-QRS high-frequency energy in a more quantitative and more easily measured way. Goldberger et al. were first to report that MI increases the low-amplitude QRS notching, but diminishes the total, high-frequency QRS voltage in the frequency range of 80 to 300 Hz<sup>153, 206</sup>. Others found similar results in small sample sizes, few ECG leads and various frequency bands<sup>155,207,208</sup>, whereas opposite results were reported by Novak et al<sup>209</sup>.

In *Study I*, a considerably larger population than in previous studies was evaluated regarding the HF-QRS content in patients with and without standard QRS changes of a previous MI, by the Selvester QRS scoring system<sup>77</sup>. In addition, HF-QRS in a complete set of 12 leads was evaluated using two different bandwidths (80-300 Hz and 150-250 Hz). In contrast to previous findings, no significant differences were observed between the two groups of patients, regardless of frequency band studied. Nor were any significant differences observed regarding location or size of the MI.

There may be several reasons for the different results in *Study I* as compared to earlier studies. We included a much larger cohort of patients, however the no-MI group did not constitute healthy individuals, as did previous studies. Instead, they were admitted for either stress testing or elective PCI, thus presumably having a high prevalence of IHD. Although the *post hoc* defined healthy subgroup within our no-MI group could not be differentiated either from the remainder of the no-MI group, or from the MI-group, it was small, which hampers definitive conclusions. To investigate this further, a subsequent study from our group by Trägårdh et al. using, in part the same cohort (*STAFF III*) as in *Study I*, was

undertaken<sup>189</sup>. It showed that the HF-QRS, independent of age, sex and QRS duration, was significantly lower in patients with IHD as compared to a healthy control group. Thus, these results may infer that HF-QRS reduction by the IHD itself, as compared to healthy individuals is more important than the presence of MI or not among IHD patients.

In *Study I*, patients were allocated into the MI or no-MI group based on another, ECG based method. The Selvester QRS, screening criteria<sup>141, 186</sup> have shown high sensitivity and specificity for the detection of a previous MI. Nevertheless, other results may have been found by using a non-ECG based classification of prior MI, such as SPECT or MRI.

The findings in this study are important in the sense that an infarct within the myocardium does not change the electrophysiological basis of HF-QRS more than can be explained by changes only due to IHD in general. Notably, not even patients with the largest MIs within the anterior and inferior subgroups, (24-27% and 24-30% of the LV myocardium, respectively, as determined by Selvester QRS score) could be differentiated from the ones without prior MI. This may, however, in part be due to the large inter-individual variation of HF-QRS, within which absolute differences induced by a previous MI may be concealed.

Despite large inter-individual variation seen in HF-QRS, intra-individual variation has proven to be low<sup>210</sup>. For additional and deeper understanding of the effect of a prior MI as compared to supposedly more diffuse changes due to general IHD, an evaluation of HF-QRS in IHD patients before and after the MI is needed. After an acute MI, localized formation of a fibrous scar takes place, which replaces the necrotic myocardial cells. In contrast to the localized post-MI situation, in general IHD more diffuse, interstitial fibrosis by collagenous connective tissue surrounds and separates individual myocardial muscle fibers. Furthermore there is a reduction of myofibrillar content as well as the overall gap junctions<sup>211-213</sup>. All these processes alter the conduction through the myocardium, which may be related to the lower HF-QRS content in found by Trägårdh et al<sup>189</sup>.

Based on the findings from *Study I*, we could thus conclude that within a population of presumed high prevalence of IHD, no significant differences in HF-QRS (in the frequency bands 80-300Hz and 150-250Hz) could be seen between patients with or without standard QRS changes of an old MI. This finding further supported the design of *Study II*, in which a presumably uniform HF-QRS baseline for patients included in this study could be expected, regardless of a prior MI or not.

## 5 Conclusions

The major conclusions are as follows:

*Study I:* Analysis of HF-QRS cannot differentiate between patients with and without a previous MI.

*Study II:* HF-QRS analysis may provide valuable information for both detecting acute ischemia and quantifying myocardium at risk and its severity.

*Study III:* The QRS slopes and especially the downward slope between R- and S-waves correlate with ischemia and may have potential value in risk stratification in acute ischemia as an add-on to ST-T analysis.

*Study IV:* In STEMI patients, grade 3 ischemia at the pre-hospital stage is a dynamic ECG characteristic that predicts larger IS and rapid infarct evolution as compared to grade 2. Further studies are needed to determine whether grade 3 ischemia represents potentially reversible severe ischemia, or whether it represents already mostly irreversible, infarcted myocardium.

The studies in this thesis were supported by grants from American Heart Association, Durham, NC, USA; the Southern Healthcare Region, Lund; Blekinge Scientific Council, Karlskrona and Donation Funds at Skåne University Hospital, Lund, Sweden.

## 6 Acknowledgements

I would like to express my gratitude to all those who gave their support and encouragement during the work on this thesis. I greatly appreciate all your generous contributions. It could never have been accomplished without your help.

I particularly want to express my gratitude to:

**Pyotr Platonov**, my enthusiastic and brilliant supervisor. Thank you for offering and providing me with your supervision and for your faith in our ability to achieve this goal. For your positive energy and continuous willingness to provide support, despite all your other extensive scientific endeavors and commitments.

My co-supervisor **Olle Pahlm** for always being a great support to me. For your sharp and clear mind. For many years of friendship knowing you were always there by my side when help was needed, and for your quick and valuable editing of manuscripts and this thesis.

My co-supervisor **Galen Wagner** for being such a great research mentor. For your unconditional and enthusiastic support throughout the years. For all fruitful and great moments throughout our journeys discussing everything from electrocardiology to life in general.

My co-supervisor **Christian Juhl Terkelsen** for introducing me to larger scale clinical trials and allowing me access to data from the great STEMI database at Skejby. For always being helpful on the numerous occasions I came to Skejby and Copenhagen. For fruitful discussions of clinical research and statistical support.

**Jonas Pettersson** for introducing me to this research topic through the high-frequency ECG. For your positive personality, good advice and longstanding friendship.

**Stafford Warren** for being a role model of a warm and caring clinician, a great invasive cardiologist, and unsurpassed work capacity. For your outstanding support during my year in the US, and your unlimited hospitality. For good memories and strong friendship throughout the years.

**Esther Pueyo, Daniel Romero and Pablo Laguna**. For years of excellent collaboration between Lund and Zaragoza and for outstanding technical support. I hope our collaboration will continue as well as the collaboration between Lund and Zaragoza intensifies.

**Leif Sörnmo** for helping us in the field of signal processing and laying the ground for a fruitful collaboration between Lund and Zaragoza.

**Yochai Birnbaum** for excellent collaboration and for numerous of ECGs scored according to the S-B ischemia grading. I look forward to our next studies.



**Monica Magnusson** for providing immediate assistance whenever needed and being the best research secretary imaginable.

All people in **The STAFF Studies Symposium organization** for years of interesting, stimulating meetings around the world. For great discussions, collaboration and friendship. An extra and special thanks to **Kathy Shuping**, who together with Galen Wagner have been the driving forces.

**Colleagues at the Department of Cardiology, Lund** for always making me feel welcome in the clinic and for discussions regarding my thesis. For letting me share the scientific atmosphere of the Department.

**Colleagues during the years at the Department of Clinical Physiology, Lund:** Eva Persson, Henrik Engblom, Elin Trägårdh Johansson, Marcus Carlsson, Einar Heiberg, Martin Ugander, David Strauss, Håkan Arheden et al. for stimulating discussions regarding ischemic heart disease, ECG and cardiac imaging.

**All my colleagues at the Thoracic Center in Karlskrona.** Special thanks to my great supervisor and mentor in clinical cardiology, **Erik Ljungström** as well as **Sergej Scheel**, both sharing my interest in electrocardiology. To all other colleagues for not being too critical of my choice of doing a PhD thesis right in the middle of my clinical career. Particular thanks to our Department head, **Carl-Magnus Pripp** for allowing my part-time research; **Dan Westlin**, and above all **Malin Persson** for understanding my need for focus in order to finish the thesis.

**All my family and wonderful friends** for enriching my life, supporting me in every way and boosting my energy and wellbeing.

My dear father and step mother **Kent** and **Inge Ringborn**. For always believing in me, and although from a distance, giving your best support and care.

My beloved mother and father-in-law, **Kerstin** and **Uno Persson** who always are there for me and Helena, regardless for what matter. For your endless energy and total dedication to support us, which is totally amazing. For being such wonderful grandparents for William, Hugo and Ella, giving them so much love. What would we do without you?

My mother **Anita Ringborn** for simply being the most wonderful mother imaginable! For totally unconditional love and complete, unlimited support at any time, for any reason and for all our best. For being the greatest grandparent to William, Hugo and Ella. For endless times of baby-sitting when I was always too involved in many things.

Our three beautiful, loving children **William, Hugo** and **Ella** for love and being the best of our lives. I long for spending more time with you soon.

Finally, my beautiful, kind, supportive wife, best friend and soul mate **Helena**. For your endless patience with my long work-hours and sometimes (or mostly) distracted mind. I couldn't have done it without you, I'm sure you know that. I love you with all of my heart!

## 7 References

1. Lopez AD, Mathers CD, Ezzati M, Jamison DT, Murray CJ. Global and regional burden of disease and risk factors, 2001: systematic analysis of population health data. *Lancet* 2006;367(9524):1747-57.
2. Steg PG, James SK, Atar D, Badano LP, Lundqvist CB, Borger MA, et al. ESC Guidelines for the management of acute myocardial infarction in patients presenting with ST-segment elevation: The Task Force on the management of ST-segment elevation acute myocardial infarction of the European Society of Cardiology (ESC). *Eur Heart J* 2012;33(20):2569-619.
3. Nichols M TN, Scarborough P, Luengo-Fernandez R, Leal J, Gray A, Rayner M. European Cardiovascular Disease Statistics 2012. European Heart Network, Brussels, European Society of Cardiology, Sophia Antipolis. In: European Cardiovascular Disease Statistics 2012. European Heart Network, Brussels, European Society of Cardiology, Sophia Antipolis; 2012.
4. Lloyd-Jones D, Adams RJ, Brown TM, Carnethon M, Dai S, De Simone G, et al. Executive summary: heart disease and stroke statistics--2010 update: a report from the American Heart Association. *Circulation*;121(7):948-54.
5. Ford ES, Ajani UA, Croft JB, Critchley JA, Labarthe DR, Kottke TE, et al. Explaining the decrease in U.S. deaths from coronary disease, 1980-2000. *N Engl J Med* 2007;356(23):2388-98.
6. Levi F, Lucchini F, Negri E, La Vecchia C. Trends in mortality from cardiovascular and cerebrovascular diseases in Europe and other areas of the world. *Heart* 2002;88(2):119-24.
7. Fox CS, Coady S, Sorlie PD, D'Agostino RB, Sr., Pencina MJ, Vasan RS, et al. Increasing cardiovascular disease burden due to diabetes mellitus: the Framingham Heart Study. *Circulation* 2007;115(12):1544-50.
8. Libby P, Theroux P. Pathophysiology of coronary artery disease. *Circulation* 2005;111(25):3481-8.
9. Kolodgie FD, Burke AP, Farb A, Gold HK, Yuan J, Narula J, et al. The thin-cap fibroatheroma: a type of vulnerable plaque: the major precursor lesion to acute coronary syndromes. *Curr Opin Cardiol* 2001;16(5):285-92.
10. Shah PK. Mechanisms of plaque vulnerability and rupture. *J Am Coll Cardiol* 2003;41(4 Suppl S):15S-22S.
11. Stanley WC, Lopaschuk GD, Hall JL, McCormack JG. Regulation of myocardial carbohydrate metabolism under normal and ischaemic conditions. Potential for pharmacological interventions. *Cardiovasc Res* 1997;33(2):243-57.
12. Jennings RB, Ganote CE, Reimer KA. Ischemic tissue injury. *Am J Pathol* 1975;81(1):179-98.
13. Nomenclature and criteria for diagnosis of ischemic heart disease. Report of the Joint International Society and Federation of Cardiology/World Health Organization task force on standardization of clinical nomenclature. *Circulation* 1979;59(3):607-9.
14. Alpert JS, Thygesen K, Antman E, Bassand JP. Myocardial infarction redefined--a consensus document of The Joint European Society of Cardiology/American College of Cardiology Committee for the redefinition of myocardial infarction. *J Am Coll Cardiol* 2000;36(3):959-69.
15. Thygesen K, Alpert JS, Jaffe AS, Simoons ML, Chaitman BR, White HD. Third Universal Definition of Myocardial Infarction. *Circulation* 2012;126(16):2020-2035.

16. Anderson JL, Karagounis LA, Califf RM. Metaanalysis of five reported studies on the relation of early coronary patency grades with mortality and outcomes after acute myocardial infarction. *Am J Cardiol* 1996;78(1):1-8.
17. Gersh BJ, Stone GW, White HD, Holmes DR, Jr. Pharmacological facilitation of primary percutaneous coronary intervention for acute myocardial infarction: is the slope of the curve the shape of the future? *JAMA* 2005;293(8):979-86.
18. Huber K, De Caterina R, Kristensen SD, Verheugt FW, Montalescot G, Maestri LB, et al. Pre-hospital reperfusion therapy: a strategy to improve therapeutic outcome in patients with ST-elevation myocardial infarction. *Eur Heart J* 2005;26(19):2063-74.
19. Kushner FG, Hand M, Smith SC, Jr., King SB, 3rd, Anderson JL, Antman EM, et al. 2009 Focused Updates: ACC/AHA Guidelines for the Management of Patients With ST-Elevation Myocardial Infarction (Updating the 2004 Guideline and 2007 Focused Update) and ACC/AHA/SCAI Guidelines on Percutaneous Coronary Intervention (Updating the 2005 Guideline and 2007 Focused Update): a Report of the American College of Cardiology Foundation/American Heart Association Task Force on Practice Guidelines. *Catheter Cardiovasc Interv* 2009.
20. Antman EM, Hand M, Armstrong PW, Bates ER, Green LA, Halasyamani LK, et al. 2007 focused update of the ACC/AHA 2004 guidelines for the management of patients with ST-elevation myocardial infarction: a report of the American College of Cardiology/American Heart Association Task Force on Practice Guidelines. *J Am Coll Cardiol* 2008;51(2):210-47.
21. Levine GN, Bates ER, Blankenship JC, Bailey SR, Bittl JA, Cercek B, et al. 2011 ACCF/AHA/SCAI Guideline for Percutaneous Coronary Intervention: a report of the American College of Cardiology Foundation/American Heart Association Task Force on Practice Guidelines and the Society for Cardiovascular Angiography and Interventions. *Circulation*;124(23):e574-651.
22. Van de Werf F, Bax J, Betriu A, Blomstrom-Lundqvist C, Crea F, Falk V, et al. Management of acute myocardial infarction in patients presenting with persistent ST-segment elevation: the Task Force on the Management of ST-Segment Elevation Acute Myocardial Infarction of the European Society of Cardiology. *Eur Heart J* 2008;29(23):2909-45.
23. Fujita M, Ikemoto M, Kishishita M, Otani H, Nohara R, Tanaka T, et al. Elevated basic fibroblast growth factor in pericardial fluid of patients with unstable angina. *Circulation* 1996;94(4):610-3.
24. Fleisch M, Billinger M, Eberli FR, Garachemani AR, Meier B, Seiler C. Physiologically assessed coronary collateral flow and intracoronary growth factor concentrations in patients with 1- to 3-vessel coronary artery disease. *Circulation* 1999;100(19):1945-50.
25. Matsunaga T, Warltier DC, Weihrauch DW, Moniz M, Tessmer J, Chilian WM. Ischemia-induced coronary collateral growth is dependent on vascular endothelial growth factor and nitric oxide. *Circulation* 2000;102(25):3098-103.
26. Schaper W. Collateral vessel growth in the human heart. Role of fibroblast growth factor-2. *Circulation* 1996;94(4):600-1.
27. Lee CW, Park SW, Cho GY, Hong MK, Kim JJ, Kang DH, et al. Pressure-derived fractional collateral blood flow: a primary determinant of left ventricular recovery after reperfused acute myocardial infarction. *J Am Coll Cardiol* 2000;35(4):949-55.
28. Elsmann P, van 't Hof AW, de Boer MJ, Hoorntje JC, Suryapranata H, Dambrink JH, et al. Role of collateral circulation in the acute phase of ST-segment-elevation myocardial infarction treated with primary coronary intervention. *Eur Heart J* 2004;25(10):854-8.

29. Perez-Castellano N, Garcia EJ, Abeytua M, Soriano J, Serrano JA, Elizaga J, et al. Influence of collateral circulation on in-hospital death from anterior acute myocardial infarction. *J Am Coll Cardiol* 1998;31(3):512-8.
30. Murry CE, Jennings RB, Reimer KA. Preconditioning with ischemia: a delay of lethal cell injury in ischemic myocardium. *Circulation* 1986;74(5):1124-36.
31. Schott RJ, Rohmann S, Braun ER, Schaper W. Ischemic preconditioning reduces infarct size in swine myocardium. *Circ Res* 1990;66(4):1133-42.
32. Liu GS, Thornton J, Van Winkle DM, Stanley AW, Olsson RA, Downey JM. Protection against infarction afforded by preconditioning is mediated by A1 adenosine receptors in rabbit heart. *Circulation* 1991;84(1):350-6.
33. Schulz R, Rose J, Heusch G. Involvement of activation of ATP-dependent potassium channels in ischemic preconditioning in swine. *Am J Physiol* 1994;267(4 Pt 2):H1341-52.
34. Schulz R, Post H, Vahlhaus C, Heusch G. Ischemic preconditioning in pigs: a graded phenomenon: its relation to adenosine and bradykinin. *Circulation* 1998;98(10):1022-9.
35. Walker DM, Walker JM, Pugsley WB, Pattison CW, Yellon DM. Preconditioning in isolated superfused human muscle. *J Mol Cell Cardiol* 1995;27(6):1349-57.
36. Maybaum S, Ilan M, Mogilevsky J, Tzivoni D. Improvement in ischemic parameters during repeated exercise testing: a possible model for myocardial preconditioning. *Am J Cardiol* 1996;78(10):1087-91.
37. Bogaty P, Kingma JG, Jr., Robitaille NM, Plante S, Simard S, Charbonneau L, et al. Attenuation of myocardial ischemia with repeated exercise in subjects with chronic stable angina: relation to myocardial contractility, intensity of exercise and the adenosine triphosphate-sensitive potassium channel. *J Am Coll Cardiol* 1998;32(6):1665-71.
38. Lambiase PD, Edwards RJ, Cusack MR, Bucknall CA, Redwood SR, Marber MS. Exercise-induced ischemia initiates the second window of protection in humans independent of collateral recruitment. *J Am Coll Cardiol* 2003;41(7):1174-82.
39. Deutsch E, Berger M, Kussmaul WG, Hirshfeld JW, Jr., Herrmann HC, Laskey WK. Adaptation to ischemia during percutaneous transluminal coronary angioplasty. Clinical, hemodynamic, and metabolic features. *Circulation* 1990;82(6):2044-51.
40. Yellon DM, Alkhulaifi AM, Pugsley WB. Preconditioning the human myocardium. *Lancet* 1993;342(8866):276-7.
41. Murry CE, Richard VJ, Reimer KA, Jennings RB. Ischemic preconditioning slows energy metabolism and delays ultrastructural damage during a sustained ischemic episode. *Circ Res* 1990;66(4):913-31.
42. Jennings RB, Sebbag L, Schwartz LM, Crago MS, Reimer KA. Metabolism of preconditioned myocardium: effect of loss and reinstatement of cardioprotection. *J Mol Cell Cardiol* 2001;33(9):1571-88.
43. Soares PR, de Albuquerque CP, Chacko VP, Gerstenblith G, Weiss RG. Role of preischemic glycogen depletion in the improvement of postischemic metabolic and contractile recovery of ischemia-preconditioned rat hearts. *Circulation* 1997;96(3):975-83.
44. Baines CP, Goto M, Downey JM. Oxygen radicals released during ischemic preconditioning contribute to cardioprotection in the rabbit myocardium. *J Mol Cell Cardiol* 1997;29(1):207-16.
45. Cleveland JC, Jr., Meldrum DR, Cain BS, Banerjee A, Harken AH. Oral sulfonylurea hypoglycemic agents prevent ischemic preconditioning in human myocardium. Two paradoxes revisited. *Circulation* 1997;96(1):29-32.

46. Ottani F, Galvani M, Ferrini D, Sorbello F, Limonetti P, Pantoli D, et al. Prodromal angina limits infarct size. A role for ischemic preconditioning. *Circulation* 1995;91(2):291-7.
47. Kloner RA, Shook T, Przyklenk K, Davis VG, Junio L, Matthews RV, et al. Previous angina alters in-hospital outcome in TIMI 4. A clinical correlate to preconditioning? *Circulation* 1995;91(1):37-45.
48. Anzai T, Yoshikawa T, Asakura Y, Abe S, Akaishi M, Mitamura H, et al. Preinfarction angina as a major predictor of left ventricular function and long-term prognosis after a first Q wave myocardial infarction. *J Am Coll Cardiol* 1995;26(2):319-27.
49. Kloner RA, Shook T, Antman EM, Cannon CP, Przyklenk K, Yoo K, et al. Prospective temporal analysis of the onset of preinfarction angina versus outcome: an ancillary study in TIMI-9B. *Circulation* 1998;97(11):1042-5.
50. Ishihara M, Sato H, Tateishi H, Kawagoe T, Shimatani Y, Kurisu S, et al. Implications of prodromal angina pectoris in anterior wall acute myocardial infarction: acute angiographic findings and long-term prognosis. *J Am Coll Cardiol* 1997;30(4):970-5.
51. Leeser MA, Stoddard M, Ahmed M, Broadbent J, Bolli R. Preconditioning of human myocardium with adenosine during coronary angioplasty. *Circulation* 1997;95(11):2500-7.
52. Cribier A, Korsatz L, Koning R, Rath P, Gamra H, Stix G, et al. Improved myocardial ischemic response and enhanced collateral circulation with long repetitive coronary occlusion during angioplasty: a prospective study. *J Am Coll Cardiol* 1992;20(3):578-86.
53. Birnbaum Y, Hale SL, Kloner RA. Progressive decrease in the ST segment elevation during ischemic preconditioning: is it related to recruitment of collateral vessels? *J Mol Cell Cardiol* 1996;28(7):1493-9.
54. Floyd JS, Maynard C, Weston P, Johanson P, Jennings RB, Wagner GS. Effects of ischemic preconditioning and arterial collateral flow on ST-segment elevation and QRS complex prolongation in a canine model of acute coronary occlusion. *Journal of Electrocardiology* 2009;42(1):19-26.
55. Lee CW, Hong MK, Yang HS, Choi SW, Kim JJ, Park SW, et al. Determinants and prognostic implications of terminal QRS complex distortion in patients treated with primary angioplasty for acute myocardial infarction. *Am J Cardiol* 2001;88(3):210-3.
56. Birnbaum Y, Kloner RA, Sclarovsky S, Cannon CP, McCabe CH, Davis VG, et al. Distortion of the terminal portion of the QRS on the admission electrocardiogram in acute myocardial infarction and correlation with infarct size and long-term prognosis (Thrombolysis in Myocardial Infarction 4 Trial). *Am J Cardiol* 1996;78(4):396-403.
57. Garcia-Rubira JC, Nunez-Gil I, Garcia-Borbolla R, Manzano MC, Fernandez-Ortiz A, Cobos MA, et al. Distortion of the terminal portion of the QRS is associated with poor collateral flow before and poor myocardial perfusion after percutaneous revascularization for myocardial infarction. *Coron Artery Dis* 2008;19(6):389-93.
58. Celik T, Yuksel UC, Iyisoy A, Kilic S, Kardesoglu E, Bugan B, et al. The impact of preinfarction angina on electrocardiographic ischemia grades in patients with acute myocardial infarction treated with primary percutaneous coronary intervention. *Ann Noninvasive Electrocardiol* 2008;13(3):278-86.
59. Kleber AG, Janse MJ, van Capelle FJ, Durrer D. Mechanism and time course of S-T and T-Q segment changes during acute regional myocardial ischemia in the pig heart determined by extracellular and intracellular recordings. *Circ Res* 1978;42(5):603-13.

60. Kleber AG, Janse MJ, Wilms-Schopmann FJ, Wilde AA, Coronel R. Changes in conduction velocity during acute ischemia in ventricular myocardium of the isolated porcine heart. *Circulation* 1986;73(1):189-98.
61. Cascio WE, Johnson TA, Gettes LS. Electrophysiologic changes in ischemic ventricular myocardium: I. Influence of ionic, metabolic, and energetic changes. *J Cardiovasc Electrophysiol* 1995;6(11):1039-62.
62. Shaw RM, Rudy Y. Electrophysiologic effects of acute myocardial ischemia: a theoretical study of altered cell excitability and action potential duration. *Cardiovasc Res* 1997;35(2):256-72.
63. Vincent GM, Abildskov JA, Burgess MJ. Mechanisms of ischemic ST-segment displacement. Evaluation by direct current recordings. *Circulation* 1977;56(4 Pt 1):559-66.
64. Boineau JP, Blumenschein SD, Spach MS, Sabiston DC. Relationship between ventricular depolarization and electrocardiogram in myocardial infarction. *J Electrocardiol* 1968;1(2):233-40.
65. Dehaan RL. Differentiation of the atrioventricular conducting system of the heart. *Circulation* 1961;24:458-70.
66. Hackel DB, Wagner G, Ratliff NB, Cies A, Estes EH, Jr. Anatomic studies of the cardiac conducting system in acute myocardial infarction. *Am Heart J* 1972;83(1):77-81.
67. Durrer D, van Dam RT, Freud GE, Janse MJ, Meijler FL, Arzbaeher RC. Total excitation of the isolated human heart. *Circulation* 1970;41(6):899-912.
68. Solomon JC, Selvester RH. Simulation of measured activation sequence in the human heart. *Am Heart J* 1973;85(4):518-24.
69. Selvester RH, Solomon JC, Tolan GD. Fine grid computer simulation of QRS-T and criteria for the quantitation of regional ischemia. *J Electrocardiol* 1987;20 Suppl:1-8.
70. Selvester RH, Wagner NB, Wagner GS. Ventricular excitation during percutaneous transluminal angioplasty of the left anterior descending coronary artery. *Am J Cardiol* 1988;62(16):1116-21.
71. Selvester RH WG, Ideker RE., editor. Myocardial infarction. In: Macfarlane PW, Lawrie TDV, editors. *Comprehensive electrocardiology: theory and practice in health and disease*. New York: Pergamon press; 1989.
72. Hancock EW, Deal BJ, Mirvis DM, Okin P, Kligfield P, Gettes LS, et al. AHA/ACCF/HRS recommendations for the standardization and interpretation of the electrocardiogram: part V: electrocardiogram changes associated with cardiac chamber hypertrophy: a scientific statement from the American Heart Association Electrocardiography and Arrhythmias Committee, Council on Clinical Cardiology; the American College of Cardiology Foundation; and the Heart Rhythm Society. Endorsed by the International Society for Computerized Electrocardiology. *J Am Coll Cardiol* 2009;53(11):992-1002.
73. Pahlm-Webb U, Pahlm O, Sadanandan S, Selvester RH, Wagner GS. A new method for using the direction of ST-segment deviation to localize the site of acute coronary occlusion: the 24-view standard electrocardiogram. *Am J Med* 2002;113(1):75-8.
74. Strauss DG, Selvester RH. The QRS complex--a biomarker that "images" the heart: QRS scores to quantify myocardial scar in the presence of normal and abnormal ventricular conduction. *J Electrocardiol* 2009;42(1):85-96.
75. Dressler W, Roesler H. High T waves in the earliest stage of myocardial infarction. *Am Heart J* 1947;34(5):627-45.
76. Holland RP, Arnsdorf MF. Solid angle theory and the electrocardiogram: physiologic and quantitative interpretations. *Prog Cardiovasc Dis* 1977;19(6):431-57.

77. Selvester RH, Wagner GS, Hindman NB. The Selvester QRS scoring system for estimating myocardial infarct size. The development and application of the system. *Arch Intern Med* 1985;145(10):1877-81.
78. Persson E, Pettersson J, Ringborn M, Sornmo L, Warren SG, Wagner GS, et al. Comparison of ST-segment deviation to scintigraphically quantified myocardial ischemia during acute coronary occlusion induced by percutaneous transluminal coronary angioplasty. *Am J Cardiol* 2006;97(3):295-300.
79. Faraggi M, Steg PG, Francois D, Sarda L, Foulst JM, Daou D, et al. Residual area at risk after anterior myocardial infarction: are ST segment changes during coronary angioplasty a reliable indicator? A comparison with technetium 99m-labeled sestamibi single-photon emission computed tomography. *J Nucl Cardiol* 1997;4(1 Pt 1):11-7.
80. Aldrich HR, Wagner NB, Boswick J, Corsa AT, Jones MG, Grande P, et al. Use of initial ST-segment deviation for prediction of final electrocardiographic size of acute myocardial infarcts. *Am J Cardiol* 1988;61(10):749-53.
81. Clemmensen P, Grande P, Aldrich HR, Wagner GS. Evaluation of formulas for estimating the final size of acute myocardial infarcts from quantitative ST-segment elevation on the initial standard 12-lead ECG. *J Electrocardiol* 1991;24(1):77-83.
82. Christian TF, Gibbons RJ, Clements IP, Berger PB, Selvester RH, Wagner GS. Estimates of myocardium at risk and collateral flow in acute myocardial infarction using electrocardiographic indexes with comparison to radionuclide and angiographic measures. *J Am Coll Cardiol* 1995;26(2):388-93.
83. Clements IP, Kaufmann UP, Bailey KR, Pellikka PA, Behrenbeck T, Gibbons RJ. Electrocardiographic prediction of myocardial area at risk. *Mayo Clin Proc* 1991;66(10):985-90.
84. Birnbaum Y, Criger DA, Wagner GS, Strasberg B, Mager A, Gates K, et al. Prediction of the extent and severity of left ventricular dysfunction in anterior acute myocardial infarction by the admission electrocardiogram. *Am Heart J* 2001;141(6):915-24.
85. Hathaway WR, Peterson ED, Wagner GS, Granger CB, Zabel KM, Pieper KS, et al. Prognostic significance of the initial electrocardiogram in patients with acute myocardial infarction. GUSTO-I Investigators. Global Utilization of Streptokinase and t-PA for Occluded Coronary Arteries. *JAMA* 1998;279(5):387-91.
86. Sejersten M, Ripa RS, Maynard C, Wagner GS, Andersen HR, Grande P, et al. Usefulness of quantitative baseline ST-segment elevation for predicting outcomes after primary coronary angioplasty or fibrinolysis (results from the DANAMI-2 trial). *Am J Cardiol* 2006;97(5):611-6.
87. Mauri F, Franzosi MG, Maggioni AP, Santoro E, Santoro L. Clinical value of 12-lead electrocardiography to predict the long-term prognosis of GISSI-1 patients. *J Am Coll Cardiol* 2002;39(10):1594-600.
88. Terkelsen CJ, Kaltoft AK, Norgaard BL, Bottcher M, Lassen JF, Clausen K, et al. ST changes before and during primary percutaneous coronary intervention predict final infarct size in patients with ST elevation myocardial infarction. *J Electrocardiol* 2009;42(1):64-72.
89. Rimar D, Crystal E, Battler A, Gottlieb S, Freimark D, Hod H, et al. Improved prognosis of patients presenting with clinical markers of spontaneous reperfusion during acute myocardial infarction. *Heart* 2002;88(4):352-6.
90. Schroder K, Wegscheider K, Zeymer U, Tebbe U, Schroder R. Extent of ST-segment deviation in a single electrocardiogram lead 90 min after thrombolysis as a predictor of medium-term mortality in acute myocardial infarction. *Lancet* 2001;358(9292):1479-86.

91. Schroder K, Wegscheider K, Zeymer U, Neuhaus KL, Schroder R. Extent of ST-segment deviation in the single ECG lead of maximum deviation present 90 or 180 minutes after start of thrombolytic therapy best predicts outcome in acute myocardial infarction. *Z Kardiol* 2001;90(8):557-67.
92. Hamlin RL, Pipers FS, Hellerstein HK, Smith CR. QRS alterations immediately following production of left ventricular free-wall ischemia in dogs. *Am J Physiol* 1968;215(5):1032-40.
93. Holland RP, Brooks H. The QRS complex during myocardial ischemia. An experimental analysis in the porcine heart. *J Clin Invest* 1976;57(3):541-50.
94. Hamlin RL, Smith CR, Hellerstein HK, Pipers FS. Alterations in QRS during ischemia of the left ventricular free-wall in goats. *J Electrocardiol* 1969;2(3):223-8.
95. Barnhill JE, Wikswo JP, Jr., Dawson AK, Gundersen S, Robertson RM, Robertson D, et al. The QRS complex during transient myocardial ischemia: studies in patients with variant angina pectoris and in a canine preparation. *Circulation* 1985;71(5):901-11.
96. David D, Naito M, Michelson E, Watanabe Y, Chen CC, Morganroth J, et al. Intramyocardial conduction: a major determinant of R-wave amplitude during acute myocardial ischemia. *Circulation* 1982;65(1):161-7.
97. Rakita L, Borduas JL, Rothman S, Prinzmetal M. Studies on the mechanism of ventricular activity. XII. Early changes in the RS-T segment and QRS complex following acute coronary artery occlusion: experimental study and clinical applications. *Am Heart J* 1954;48(3):351-72.
98. Wagner NB, Sevilla DC, Krucoff MW, Lee KL, Pieper KS, Kent KK, et al. Transient alterations of the QRS complex and ST segment during percutaneous transluminal balloon angioplasty of the left anterior descending coronary artery. *Am J Cardiol* 1988;62(16):1038-42.
99. Wagner NB, Sevilla DC, Krucoff MW, Pieper KS, Lee KL, White RD, et al. Transient alterations of the QRS complex and ST segment during percutaneous transluminal balloon angioplasty of the right and left circumflex coronary arteries. *Am J Cardiol* 1989;63(17):1208-13.
100. Surawicz B, Orr CM, Hermiller JB, Bell KD, Pinto RP. QRS changes during percutaneous transluminal coronary angioplasty and their possible mechanisms. *J Am Coll Cardiol* 1997;30(2):452-8.
101. Kornreich F, MacLeod RS, Dzavik V, Selvester RH, Kornreich AM, Stoupel E, et al. QRST changes during and after percutaneous transluminal coronary angioplasty. *J Electrocardiol* 1994;27 Suppl:113-7.
102. Charlap S, Shani J, Schulhoff N, Herman B, Lichstein E. R- and S-wave amplitude changes with acute anterior transmural myocardial ischemia. Correlations with left ventricular filling pressures. *Chest* 1990;97(3):566-71.
103. Sinno MC, Kowalski M, Kenigsberg DN, Krishnan SC, Khanal S. R-wave amplitude changes measured by electrocardiography during early transmural ischemia. *J Electrocardiol* 2008;41(5):425-30.
104. Bateman TM, Czer LS, Gray RJ, Maddahi J, Raymond MJ, Geft IL, et al. Transient pathologic Q waves during acute ischemic events: an electrocardiographic correlate of stunned but viable myocardium. *Am Heart J* 1983;106(6):1421-6.
105. Barnhill JE, 3rd, Tendra M, Cade H, Campbell WB, Smith RF. Depolarization changes early in the course of myocardial infarction: significance of changes in the terminal portion of the QRS complex. *J Am Coll Cardiol* 1989;14(1):143-9.



106. Bashour TT, Kabbani SS, Brewster HP, Wald SH, Hanna ES, Cheng TO. Transient Q waves and reversible cardiac failure during myocardial ischemia: electrical and mechanical stunning of the heart. *Am Heart J* 1983;106(4 Pt 1):780-3.
107. Surawicz B. Reversible QRS changes during acute myocardial ischemia. *J Electrocardiol* 1998;31(3):209-20.
108. Sclarovsky S, Mager A, Kusniec J, Rechavia E, Sagie A, Bassevich R, et al. Electrocardiographic classification of acute myocardial ischemia. *Isr J Med Sci* 1990;26(9):525-31.
109. Birnbaum Y, Sclarovsky S, Blum A, Mager A, Gabbay U. Prognostic significance of the initial electrocardiographic pattern in a first acute anterior wall myocardial infarction. *Chest* 1993;103(6):1681-7.
110. Birnbaum Y, Sclarovsky S. The grades of ischemia on the presenting electrocardiogram of patients with ST elevation acute myocardial infarction. *J Electrocardiol* 2001;34 Suppl:17-26.
111. Birnbaum Y, Herz I, Sclarovsky S, Zlotikamien B, Chetrit A, Olmer L, et al. Prognostic significance of the admission electrocardiogram in acute myocardial infarction. *J Am Coll Cardiol* 1996;27(5):1128-32.
112. Garcia-Rubira JC, Perez-Leal I, Garcia-Martinez JT, Molano F, Hidalgo R, Gomez-Barrado JJ, et al. The initial electrocardiogram pattern is a strong predictor of outcome in acute myocardial infarction. *Int J Cardiol* 1995;51(3):301-5.
113. Sejersten M, Birnbaum Y, Ripa RS, Maynard C, Wagner GS, Clemmensen P. Influences of electrocardiographic ischaemia grades and symptom duration on outcomes in patients with acute myocardial infarction treated with thrombolysis versus primary percutaneous coronary intervention: results from the DANAMI-2 trial. *Heart* 2006;92(11):1577-82.
114. Birnbaum Y, Goodman S, Barr A, Gates KB, Barbash GI, Battler A, et al. Comparison of primary coronary angioplasty versus thrombolysis in patients with ST-segment elevation acute myocardial infarction and grade II and grade III myocardial ischemia on the enrollment electrocardiogram. *Am J Cardiol* 2001;88(8):842-7.
115. Postma S, Heestermaans T, Ten Berg JW, van Werkum JW, Suryapranata H, Birnbaum Y, et al. Predictors and outcome of grade 3 ischemia in patients with ST-segment elevation myocardial infarction undergoing primary percutaneous coronary intervention. *J Electrocardiol* 2011;44(5):516-22.
116. Wolak A, Yaroslavtsev S, Amit G, Birnbaum Y, Cafri C, Atar S, et al. Grade 3 ischemia on the admission electrocardiogram predicts failure of ST resolution and of adequate flow restoration after primary percutaneous coronary intervention for acute myocardial infarction. *Am Heart J* 2007;153(3):410-7.
117. Weaver JC, Rees D, Prasan AM, Ramsay DD, Binnekamp MF, McCrohon JA. Grade 3 ischemia on the admission electrocardiogram is associated with severe microvascular injury on cardiac magnetic resonance imaging after ST elevation myocardial infarction. *J Electrocardiol* 2011;44(1):49-57.
118. Birnbaum Y, Maynard C, Wolfe S, Mager A, Strasberg B, Rechavia E, et al. Terminal QRS distortion on admission is better than ST-segment measurements in predicting final infarct size and assessing the Potential effect of thrombolytic therapy in anterior wall acute myocardial infarction. *Am J Cardiol* 1999;84(5):530-4.
119. Billgren T, Maynard C, Christian TF, Rahman MA, Saeed M, Hammill SC, et al. Grade 3 ischemia on the admission electrocardiogram predicts rapid progression of necrosis over time and less myocardial salvage by primary angioplasty. *J Electrocardiol* 2005;38(3):187-94.

120. Birnbaum Y, Mahaffey KW, Criger DA, Gates KB, Barbash GI, Barbagelata A, et al. Grade III ischemia on presentation with acute myocardial infarction predicts rapid progression of necrosis and less myocardial salvage with thrombolysis. *Cardiology* 2002;97(3):166-74.
121. Yang HS, Lee CW, Hong MK, Moon DH, Kim YH, Lee SG, et al. Terminal QRS complex distortion on the admission electrocardiogram in anterior acute myocardial infarction and association with residual flow and infarct size after primary angioplasty. *Korean J Intern Med* 2005;20(1):21-5.
122. Weston P, Johanson P, Schwartz LM, Maynard C, Jennings RB, Wagner GS. The value of both ST-segment and QRS complex changes during acute coronary occlusion for prediction of reperfusion-induced myocardial salvage in a canine model. *J Electrocardiol* 2007;40(1):18-25.
123. Wong CK, Gao W, Stewart RA, van Pelt N, French JK, Aylward PE, et al. Risk stratification of patients with acute anterior myocardial infarction and right bundle-branch block: importance of QRS duration and early ST-segment resolution after fibrinolytic therapy. *Circulation* 2006;114(8):783-9.
124. Wong CK, Gao W, Stewart RA, French JK, Aylward PE, White HD. Relationship of QRS duration at baseline and changes over 60 min after fibrinolysis to 30-day mortality with different locations of ST elevation myocardial infarction: results from the Hirulog and Early Reperfusion or Occlusion-2 trial. *Heart* 2009;95(4):276-82.
125. Boineau J, editor. *The ECG in multiple myocardial infarction and the progression of ischemic heart disease*. St Louis: CardioRhythm Inc.; 2004.
126. Selvester RH. The signal-averaged high-resolution ECG. *J Electrocardiol* 1995;28 Suppl:216-25.
127. Bar FW, Vermeer F, de Zwaan C, Ramentol M, Braat S, Simoons ML, et al. Value of admission electrocardiogram in predicting outcome of thrombolytic therapy in acute myocardial infarction. A randomized trial conducted by The Netherlands Interuniversity Cardiology Institute. *Am J Cardiol* 1987;59(1):6-13.
128. Rechavia E, Blum A, Mager A, Birnbaum Y, Strasberg B, Sclarovsky S. Electrocardiographic Q-waves inconstancy during thrombolysis in acute anterior wall myocardial infarction. *Cardiology* 1992;80(5-6):392-8.
129. Raitt MH, Maynard C, Wagner GS, Cerqueira MD, Selvester RH, Weaver WD. Appearance of abnormal Q waves early in the course of acute myocardial infarction: implications for efficacy of thrombolytic therapy. *J Am Coll Cardiol* 1995;25(5):1084-8.
130. Wu E, Judd RM, Vargas JD, Klocke FJ, Bonow RO, Kim RJ. Visualisation of presence, location, and transmural extent of healed Q-wave and non-Q-wave myocardial infarction. *Lancet* 2001;357(9249):21-8.
131. Engblom H, Hedstrom E, Heiberg E, Wagner GS, Pahlm O, Arheden H. Size and transmural extent of first-time reperfused myocardial infarction assessed by cardiac magnetic resonance can be estimated by 12-lead electrocardiogram. *Am Heart J* 2005;150(5):920.
132. Selvester RH, Solomon JC, Gillespie TL. Digital computer model of a total body electrocardiographic surface map. An adult male-torso simulation with lungs. *Circulation* 1968;38(4):684-90.
133. Ideker RE, Wagner GS, Ruth WK, Alonso DR, Bishop SP, Bloor CM, et al. Evaluation of a QRS scoring system for estimating myocardial infarct size. II. Correlation with quantitative anatomic findings for anterior infarcts. *Am J Cardiol* 1982;49(7):1604-14.

134. Roark SF, Ideker RE, Wagner GS, Alonso DR, Bishop SP, Bloor CM, et al. Evaluation of a QRS scoring system for estimating myocardial infarct size. III. Correlation with quantitative anatomic findings for inferior infarcts. *Am J Cardiol* 1983;51(3):382-9.
135. Wagner GS, Freye CJ, Palmeri ST, Roark SF, Stack NC, Ideker RE, et al. Evaluation of a QRS scoring system for estimating myocardial infarct size. I. Specificity and observer agreement. *Circulation* 1982;65(2):342-7.
136. Ward RM, White RD, Ideker RE, Hindman NB, Alonso DR, Bishop SP, et al. Evaluation of a QRS scoring system for estimating myocardial infarct size. IV. Correlation with quantitative anatomic findings for posterolateral infarcts. *Am J Cardiol* 1984;53(6):706-14.
137. Tjandrawidjaja MC, Fu Y, Westerhout CM, Wagner GS, Granger CB, Armstrong PW. Usefulness of the QRS score as a strong prognostic marker in patients discharged after undergoing primary percutaneous coronary intervention for ST-segment elevation myocardial infarction. *Am J Cardiol*;106(5):630-4.
138. Jones MG, Anderson KM, Wilson PW, Kannel WB, Wagner NB, Wagner GS. Prognostic use of a QRS scoring system after hospital discharge for initial acute myocardial infarction in the Framingham cohort. *Am J Cardiol* 1990;66(5):546-50.
139. De Sutter J, Van de Wiele C, Gheeraert P, De Buyzere M, Gevaert S, Taeymans Y, et al. The Selvester 32-point QRS score for evaluation of myocardial infarct size after primary coronary angioplasty. *Am J Cardiol* 1999;83(2):255-7, A5.
140. Engblom H, Wagner GS, Setser RM, Selvester RH, Billgren T, Kasper JM, et al. Quantitative clinical assessment of chronic anterior myocardial infarction with delayed enhancement magnetic resonance imaging and QRS scoring. *Am Heart J* 2003;146(2):359-66.
141. Anderson WD, Wagner NB, Lee KL, White RD, Yuschak J, Behar VS, et al. Evaluation of a QRS scoring system for estimating myocardial infarct size. VI: Identification of screening criteria for non-acute myocardial infarcts. *Am J Cardiol* 1988;61(10):729-33.
142. Watanabe T, Yamaki M, Tachibana H, Kubota I, Tomoike H. Decrease in the high frequency QRS components depending on the local conduction delay. *Jpn Circ J* 1998;62(11):844-8.
143. Abboud S, Berenfeld O, Sadeh D. Simulation of high-resolution QRS complex using a ventricular model with a fractal conduction system. Effects of ischemia on high-frequency QRS potentials. *Circ Res* 1991;68(6):1751-60.
144. Mor-Avi V, Abboud S, Akselrod S. Frequency content of the QRS notching in high-fidelity canine ECG. *Comput Biomed Res* 1989;22(1):18-25.
145. Abboud S, Cohen RJ, Sadeh D. A spectral analysis of the high frequency QRS potentials observed during acute myocardial ischemia in dogs. *Int J Cardiol* 1990;26(3):285-90.
146. Abboud S, Smith JM, Shargorodsky B, Laniado S, Sadeh D, Cohen RJ. High frequency electrocardiography of three orthogonal leads in dogs during a coronary artery occlusion. *Pacing Clin Electrophysiol* 1989;12(4 Pt 1):574-81.
147. Mor-Avi V, Shargorodsky B, Abboud S, Laniado S, Akselrod S. Effects of coronary occlusion on high-frequency content of the epicardial electrogram and body surface electrocardiogram. *Circulation* 1987;76(1):237-43.
148. Abboud S, Cohen RJ, Selwyn A, Ganz P, Sadeh D, Friedman PL. Detection of transient myocardial ischemia by computer analysis of standard and signal-averaged high-frequency electrocardiograms in patients undergoing percutaneous transluminal coronary angioplasty. *Circulation* 1987;76(3):585-96.

149. Pettersson J, Pahlm O, Carro E, Edenbrandt L, Ringborn M, Sornmo L, et al. Changes in high-frequency QRS components are more sensitive than ST-segment deviation for detecting acute coronary artery occlusion. *J Am Coll Cardiol* 2000;36(6):1827-34.
150. Pettersson J, Lander P, Pahlm O, Sornmo L, Warren SG, Wagner GS. Electrocardiographic changes during prolonged coronary artery occlusion in man: comparison of standard and high-frequency recordings. *Clin Physiol* 1998;18(3):179-86.
151. Aversano T, Rudikoff B, Washington A, Traill S, Coombs V, Raqueno J. High frequency QRS electrocardiography in the detection of reperfusion following thrombolytic therapy. *Clin Cardiol* 1994;17(4):175-82.
152. Pettersson J, Wagner GS, Sornmo L, Johansson ET, Ohlin H, Pahlm O. High-frequency electrocardiogram as a supplement to standard 12-lead ischemia monitoring during reperfusion therapy of acute inferior myocardial infarction. *J Electrocardiol* 2010;44(1):11-7.
153. Goldberger AL, Bhargava V, Froelicher V, Covell J. Effect of myocardial infarction on high-frequency QRS potentials. *Circulation* 1981;64(1):34-42.
154. Novak P, Li Z, Novak V, Hatala R. Time-frequency mapping of the QRS complex in normal subjects and in postmyocardial infarction patients. *J Electrocardiol* 1994;27(1):49-60.
155. Bhargava V, Goldberger A. Myocardial infarction diminishes both low and high frequency QRS potentials: power spectrum analysis of lead II. *J Electrocardiol* 1981;14(1):57-60.
156. Pueyo E, Sornmo L, Laguna P. QRS slopes for detection and characterization of myocardial ischemia. *IEEE Trans Biomed Eng* 2008;55(2 Pt 1):468-77.
157. Romero D, Ringborn M, Laguna P, Pahlm O, Pueyo E. Depolarization Changes During Acute Myocardial Ischemia by Evaluation of QRS Slopes: Standard Lead and Vectorial Approach. *IEEE Trans Biomed Eng* 2011;58(1):110-20.
158. Romero D, Ringborn M, Demidova M, Koul S, Laguna P, Platonov PG, et al. Characterization of ventricular depolarization and repolarization changes in a porcine model of myocardial infarction. *Physiol Meas* 2012;33(12):1975-91.
159. Grottum P, Mohr B, Kjekshus JK. Evolution of vectorcardiographic QRS changes during myocardial infarction in dogs and their relation to infarct size. *Cardiovasc Res* 1986;20(2):108-16.
160. Sederholm M, Grottum P, Erhardt L, Kjekshus J. Quantitative assessment of myocardial ischemia and necrosis by continuous vectorcardiography and measurement of creatine kinase release in patients. *Circulation* 1983;68(5):1006-12.
161. Naslund U, Haggmark S, Johansson G, Reiz S. Ischaemia and reperfusion induced transient QRS vector changes: relationship to size of the ischaemic territory. *Cardiovasc Res* 1993;27(2):327-33.
162. Dellborg M, Herlitz J, Risenfors M, Swedberg K. Electrocardiographic assessment of infarct size: comparison between QRS scoring of 12-lead electrocardiography and dynamic vectorcardiography. *Int J Cardiol* 1993;40(2):167-72.
163. Dellborg M, Malmberg K, Ryden L, Svensson AM, Swedberg K. Dynamic on-line vectorcardiography improves and simplifies in-hospital ischemia monitoring of patients with unstable angina. *J Am Coll Cardiol* 1995;26(6):1501-7.
164. Dellborg M, Riha M, Swedberg K. Dynamic QRS-complex and ST-segment monitoring in acute myocardial infarction during recombinant tissue-type plasminogen activator therapy. The TEAHAT Study Group. *Am J Cardiol* 1991;67(5):343-9.

165. Dellborg M, Topol EJ, Swedberg K. Dynamic QRS complex and ST segment vectorcardiographic monitoring can identify vessel patency in patients with acute myocardial infarction treated with reperfusion therapy. *Am Heart J* 1991;122(4 Pt 1):943-8.
166. Anderson JL, Adams CD, Antman EM, Bridges CR, Califf RM, Casey DE, Jr., et al. ACC/AHA 2007 guidelines for the management of patients with unstable angina/non ST-elevation myocardial infarction: a report of the American College of Cardiology/American Heart Association Task Force on Practice Guidelines (Writing Committee to Revise the 2002 Guidelines for the Management of Patients With Unstable Angina/Non ST-Elevation Myocardial Infarction): developed in collaboration with the American College of Emergency Physicians, the Society for Cardiovascular Angiography and Interventions, and the Society of Thoracic Surgeons: endorsed by the American Association of Cardiovascular and Pulmonary Rehabilitation and the Society for Academic Emergency Medicine. *Circulation* 2007;116(7):e148-304.
167. Wackers FJ, Berman DS, Maddahi J, Watson DD, Beller GA, Strauss HW, et al. Technetium-99m hexakis 2-methoxyisobutyl isonitrile: human biodistribution, dosimetry, safety, and preliminary comparison to thallium-201 for myocardial perfusion imaging. *J Nucl Med* 1989;30(3):301-11.
168. Piwnica-Worms D, Kronauge JF, Chiu ML. Uptake and retention of hexakis (2-methoxyisobutyl isonitrile) technetium(I) in cultured chick myocardial cells. Mitochondrial and plasma membrane potential dependence. *Circulation* 1990;82(5):1826-38.
169. Maublant JC, Moins N, Gachon P, Renoux M, Zhang Z, Veyre A. Uptake of technetium-99m-teboroxime in cultured myocardial cells: comparison with thallium-201 and technetium-99m-sestamibi. *J Nucl Med* 1993;34(2):255-9.
170. Glover DK, Okada RD. Myocardial kinetics of Tc-MIBI in canine myocardium after dipyridamole. *Circulation* 1990;81(2):628-37.
171. Gibbons RJ, Verani MS, Behrenbeck T, Pellikka PA, O'Connor MK, Mahmarian JJ, et al. Feasibility of tomographic 99mTc-hexakis-2-methoxy-2-methylpropyl-isonitrile imaging for the assessment of myocardial area at risk and the effect of treatment in acute myocardial infarction. *Circulation* 1989;80(5):1277-86.
172. Christian TF, Schwartz RS, Gibbons RJ. Determinants of infarct size in reperfusion therapy for acute myocardial infarction. *Circulation* 1992;86(1):81-90.
173. Clements IP, Christian TF, Higano ST, Gibbons RJ, Gersh BJ. Residual flow to the infarct zone as a determinant of infarct size after direct angioplasty. *Circulation* 1993;88(4 Pt 1):1527-33.
174. Bruce CJ, Christian TF, Schaer GL, Spaccavento LJ, Jolly MK, O'Connor MK, et al. Determinants of infarct size after thrombolytic treatment in acute myocardial infarction. *Am J Cardiol* 1999;83(12):1600-5.
175. Gibbons RJ, Miller TD, Christian TF. Infarct size measured by single photon emission computed tomographic imaging with (99m)Tc-sestamibi: A measure of the efficacy of therapy in acute myocardial infarction. *Circulation* 2000;101(1):101-8.
176. Carlsson M, Ubachs JF, Hedstrom E, Heiberg E, Jovinge S, Arheden H. Myocardium at risk after acute infarction in humans on cardiac magnetic resonance: quantitative assessment during follow-up and validation with single-photon emission computed tomography. *JACC Cardiovasc Imaging* 2009;2(5):569-76.
177. Haronian HL, Remetz MS, Sinusas AJ, Baron JM, Miller HI, Cleman MW, et al. Myocardial risk area defined by technetium-99m sestamibi imaging during percutaneous transluminal coronary angioplasty: comparison with coronary angiography. *J Am Coll Cardiol* 1993;22(4):1033-43.

178. Persson E, Palmer J, Pettersson J, Warren SG, Borges-Neto S, Wagner GS, et al. Quantification of myocardial hypoperfusion with 99m Tc-sestamibi in patients undergoing prolonged coronary artery balloon occlusion. *Nucl Med Commun* 2002;23(3):219-28.
179. Christian TF, O'Connor MK, Schwartz RS, Gibbons RJ, Ritman EL. Technetium-99m MIBI to assess coronary collateral flow during acute myocardial infarction in two closed-chest animal models. *J Nucl Med* 1997;38(12):1840-6.
180. Kaltoft A, Bottcher M, Nielsen SS, Hansen HH, Terkelsen C, Maeng M, et al. Routine thrombectomy in percutaneous coronary intervention for acute ST-segment-elevation myocardial infarction: a randomized, controlled trial. *Circulation* 2006;114(1):40-7.
181. Kelbaek H, Terkelsen CJ, Helqvist S, Lassen JF, Clemmensen P, Klovgaard L, et al. Randomized comparison of distal protection versus conventional treatment in primary percutaneous coronary intervention: the drug elution and distal protection in ST-elevation myocardial infarction (DEDICATION) trial. *J Am Coll Cardiol* 2008;51(9):899-905.
182. Botker HE, Kharbanda R, Schmidt MR, Bottcher M, Kaltoft AK, Terkelsen CJ, et al. Remote ischaemic conditioning before hospital admission, as a complement to angioplasty, and effect on myocardial salvage in patients with acute myocardial infarction: a randomised trial. *Lancet* 2010;375(9716):727-34.
183. Mason RE, Likar I. A new system of multiple-lead exercise electrocardiography. *Am Heart J* 1966;71(2):196-205.
184. Myocardial infarction redefined--a consensus document of The Joint European Society of Cardiology/American College of Cardiology Committee for the redefinition of myocardial infarction. *Eur Heart J* 2000;21(18):1502-13.
185. Laguna P, Jane R, Caminal P. Automatic detection of wave boundaries in multilead ECG signals: validation with the CSE database. *Comput Biomed Res* 1994;27(1):45-60.
186. Hindman NB, Schocken DD, Widmann M, Anderson WD, White RD, Leggett S, et al. Evaluation of a QRS scoring system for estimating myocardial infarct size. V. Specificity and method of application of the complete system. *Am J Cardiol* 1985;55(13 Pt 1):1485-90.
187. Thygesen K, Alpert JS, White HD, Jaffe AS, Apple FS, Galvani M, et al. Universal definition of myocardial infarction. *Circulation* 2007;116(22):2634-53.
188. Pahlm O, Sornmo L. Data processing of exercise ECG's. *IEEE Trans Biomed Eng* 1987;34(2):158-65.
189. Tragardh E, Pahlm O, Wagner GS, Pettersson J. Reduced high-frequency QRS components in patients with ischemic heart disease compared to normal subjects. *J Electrocardiol* 2004;37(3):157-62.
190. Pettersson J, Warren S, Mehta N, Lander P, Berbari EJ, Gates K, et al. Changes in high-frequency QRS components during prolonged coronary artery occlusion in humans. *J Electrocardiol* 1995;28 Suppl:225-7.
191. Proakis JG MD, editor. Digital signal processing – principles, algorithms and applications. Upper Saddle River (NJ): Prentice Hall; 1996.
192. Kaltoft A, Nielsen SS, Terkelsen CJ, Bottcher M, Lassen JF, Krusell LR, et al. Scintigraphic evaluation of routine filterwire distal protection in percutaneous coronary intervention for acute ST-segment elevation myocardial infarction: a randomized controlled trial. *J Nucl Cardiol* 2009;16(5):784-91.
193. Garcia EV, Cooke CD, Van Train KF, Folks R, Peifer J, DePuey EG, et al. Technical aspects of myocardial SPECT imaging with technetium-99m sestamibi. *Am J Cardiol* 1990;66(13):23E-31E.

194. Tragardh E, Pettersson J, Wagner GS, Pahlm O. Reduced high-frequency QRS components in electrocardiogram leads facing an area of the heart with intraventricular conduction delay due to bundle branch block. *J Electrocardiol* 2007;40(2):127-32.
195. Schlegel TT, Kulecz WB, DePalma JL, Feiveson AH, Wilson JS, Rahman MA, et al. Real-time 12-lead high-frequency QRS electrocardiography for enhanced detection of myocardial ischemia and coronary artery disease. *Mayo Clin Proc* 2004;79(3):339-50.
196. Magrans R, Gomis P, Voss A, Caminal P. Effect of acute myocardial ischemia on different high-frequency bandwidths and temporal regions of the QRS. *Conf Proc IEEE Eng Med Biol Soc*;2011:7083-6.
197. Wagner GS, Johanson P, Weston P, Floyd J, Jennings R. The supplementary effect of QRS changes on the inverse relationship between ST changes and salvage: testing the Sclarovsky/Birnbaum clinical method in the basic Jennings/Reimer model. *J Electrocardiol* 2003;36 Suppl:13-6.
198. Garcia-Rubira JC, Garcia-Borbolla R, Nunez-Gil I, Manzano MC, Garcia-Romero MM, Fernandez-Ortiz A, et al. Distortion of the terminal portion of the QRS is predictor of shock after primary percutaneous coronary intervention for acute myocardial infarction. *Int J Cardiol* 2008;130(2):241-5.
199. Chareonthaitawee P, Christian TF, O'Connor MK, Berger PB, Higano ST, O'Keefe JH, et al. Noninvasive prediction of residual blood flow within the risk area during acute myocardial infarction: a multicenter validation study of patients undergoing direct coronary angioplasty. *Am Heart J* 1997;134(4):639-46.
200. Prinzmetal M, Shaw CM, Jr., Maxwell MH, Flamm EJ, Goldman A, Kimura N, et al. Studies on the mechanism of ventricular activity. VI. The depolarization complex in pure subendocardial infarction; role of the subendocardial region in the normal electrocardiogram. *Am J Med* 1954;16(4):469-89.
201. Moon JC, De Arenaza DP, Elkington AG, Taneja AK, John AS, Wang D, et al. The pathologic basis of Q-wave and non-Q-wave myocardial infarction: a cardiovascular magnetic resonance study. *J Am Coll Cardiol* 2004;44(3):554-60.
202. Langner PH, Jr., Geselowitz DB, Mansure FT, Lauer JA. High-frequency components in the electrocardiograms of normal subjects and of patients with coronary heart disease. *Am Heart J* 1961;62:746-55.
203. Reynolds EW, Jr., Muller BF, Anderson GJ, Muller BT. High-frequency components in the electrocardiogram. A comparative study of normals and patients with myocardial disease. *Circulation* 1967;35(1):195-206.
204. Flowers NC, Horan LG, Thomas JR, Tolleson WJ. The anatomic basis for high-frequency components in the electrocardiogram. *Circulation* 1969;39(4):531-9.
205. Flowers NC, Horan LG, Tolleson WJ, Thomas JR. Localization of the site of myocardial scarring in man by high-frequency components. *Circulation* 1969;40(6):827-34.
206. Goldberger AL, Bhargava V, Froelicher V, Covell J, Mortara D. Effect of myocardial infarction on the peak amplitude of high frequency QRS potentials. *J Electrocardiol* 1980;13(4):367-71.
207. Talwar KK, Rao GS, Nayar U, Bhatia ML. Clinical significance of high frequency QRS potentials in myocardial infarction: analysis based on power spectrum of lead III. *Cardiovasc Res* 1989;23(1):60-3.

208. Berkalp B, Baykal E, Caglar N, Erol C, Akgun G, Gurel T. Analysis of high frequency QRS potentials observed during acute myocardial infarction. *Int J Cardiol* 1993;42(2):147-53.
209. Daluge SM, Purifoy DJ, Savina PM, St Clair MH, Parry NR, Dev IK, et al. 5-Chloro-2',3'-dideoxy-3'-fluorouridine (935U83), a selective anti-human immunodeficiency virus agent with an improved metabolic and toxicological profile. *Antimicrob Agents Chemother* 1994;38(7):1590-603.
210. Batdorf NJ, Feiveson AH, Schlegel TT. Month-to-month and year-to-year reproducibility of high frequency QRS ECG signals. *J Electrocardiol* 2004;37(4):289-96.
211. Anderson KR, Sutton MG, Lie JT. Histopathological types of cardiac fibrosis in myocardial disease. *J Pathol* 1979;128(2):79-85.
212. Vanoverschelde JL, Wijns W, Depre C, Essamri B, Heyndrickx GR, Borgers M, et al. Mechanisms of chronic regional postischemic dysfunction in humans. New insights from the study of noninfarcted collateral-dependent myocardium. *Circulation* 1993;87(5):1513-23.
213. Peters NS, Green CR, Poole-Wilson PA, Severs NJ. Reduced content of connexin43 gap junctions in ventricular myocardium from hypertrophied and ischemic human hearts. *Circulation* 1993;88(3):864-75.





# Studies I-IV

And Supplementary Technical Study